# Synthesis and biophysical characterization of oligonucleotides modified with O2'-alkylated RNA monomers featuring substituted pyrene moieties

Saswata Karmakar,[a] Tyler Horrocks,[a,b] Bradley C. Gibbons,[a,b] Dale C. Guenther,[a] Raymond Emehiser,[a] and Patrick J. Hrdlicka[a,*]

[a]Department of Chemistry, University of Idaho, Moscow, ID-83844, USA

[b]Department of Chemistry, Brigham Young University-Idaho, ID-83440, USA

## ELECTRONIC SUPPLEMENTARY INFORMATION

**General experimental section.** Analytical grade reagents and solvents were obtained from commercial sources and used without further purification. Petroleum ether of the distillation range 60-80 °C was used. Solvents were dried over activated molecular sieves: THF (3Å); $CH_2Cl_2$, 1,2-dichloroethane, *N,N'*-diisopropylethylamine and anhydrous DMSO (4Å). Water content of anhydrous solvents was checked on Karl-Fisher apparatus. Reactions were monitored by TLC using silica gel plates coated with a fluorescence indicator ($SiO_2$-60, F-254) that were visualized a) under UV light and/or b) by dipping in 5% conc. $H_2SO_4$ in absolute ethanol (v/v) followed by heating. Silica gel column chromatography was performed with Silica gel 60 (particle size 0.040–0.063 mm) using moderate pressure (pressure ball). Evaporation of solvents was carried out under reduced pressure at temperatures below 45 °C. Following column chromatography, appropriate fractions were pooled, evaporated and dried at high vacuum for at least 12h to afford the obtained products in high purity (>95%) as ascertained by 1D NMR techniques unless otherwise mentioned. Chemical shifts of $^{1}H$ NMR (500 MHz), $^{13}C$ NMR (125.6 MHz), and/or $^{31}P$ NMR (121.5 MHz) are reported relative to deuterated solvent or internal standard (80% phosphoric acid for $^{31}P$ NMR). Exchangeable (ex) protons were detected by disappearance of signals upon $D_2O$ addition. Assignments of NMR spectra are based on 2D spectra (COSY, HSQC and, in key instances, HMBC) and DEPT-spectra. Quaternary carbons are generally not assigned in $^{13}C$ NMR spectra but their presence was verified from HSQC and DEPT spectra (absence of signals). MALDI-HRMS spectra of compounds were recorded on a Waters Q-TOF Premiere mass spectrometer using 2,5-dihydroxybenzoic acid as a matrix and polyethylene glycol (PEG 600) as an internal calibration standard.

**Discussion – synthesis and characterization of 7NP-PyCH$_2$OH**. A reaction sequence entailing Friedel Crafts acylation of 4,5,9,10-tetrahydropyrene, reductive decarbonylation, aromatization, and regioselective Rieche formylation at the 1-position was expected to afford 7-NP-PyCHO, which upon reduction could afford the key label 7-NP-PyCH$_2$OH (Scheme S1). Two key literature findings motivated our approach: 1) 4,5,9,10-tetrahydropyrene is known to undergo regioselective Friedel-Crafts acylation at the 2-position[S1] (i.e., 7-position in the final label), and 2) Rieche formylations of pyrene are known to occur at the 1-position[S2]; the steric bulk of the 7-neopentyl group was expected to prevent formylations at the 6- or 8-positions. Indeed, we were able to proceed as planned and telescoped the first four steps to afford 7-NP-PyCHO in 27% overall yield, which was reduced to 7-NP-PyCHO in 99% yield. The 1,7-disubstituted nature of 7-NP-PyCHO (and the subsequent downstream products) was corroborated by NMR data. Briefly, H6 and H8 appear as two singlets at 8.0-8.1 ppm in the $^1$H NMR spectrum (establishing 7-substitution), while H2 and H3 appear as mutually coupling doublets ($J$ = 9.2 Hz) at ~8.4 ppm and ~8.2 ppm, respectively. H4/H5 and H9/H10 also appear as coupling doublets. Importantly, crosspeaks between the aldehyde proton (~10.76 ppm) and C2 (~131.3 ppm) and C10a (~131.1 ppm) are observed in the HMBC spectrum (establishing 1-substitution).

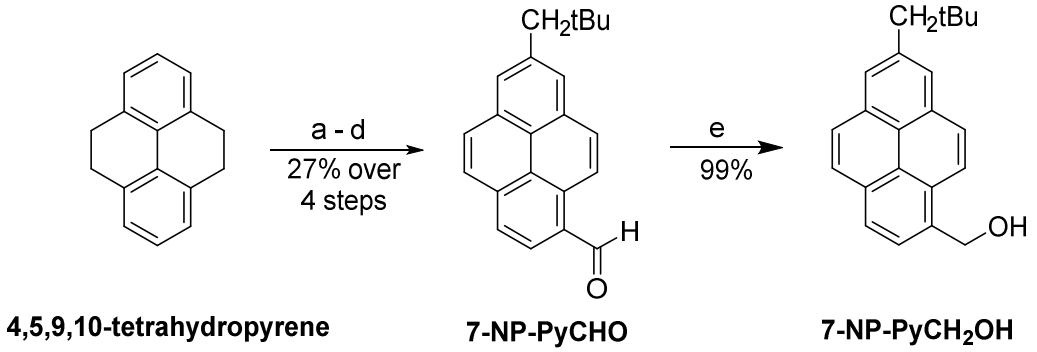


**Scheme S1**. Synthesis of 7NP-PyCH$_2$OH. Reagents and conditions: (a) $(CH_3)_3CCOCl$, $AlCl_3$, $CH_2Cl_2$, 0 °C to rt, 2.5 hours; (b) $CF_3CO_2H$, $Et_3SiH$, rt, 30 min; (c) DDQ, benzene, reflux, 4 hours; (d) $Cl_2CHOCH_3$, $TiCl_4$, $CH_2Cl_2$, 0 °C to rt, 3 hours; (e) $NaBH_4$, THF, rt, 14 hours. DDQ = 2,3-dichloro-5,6-dicyano-1,4-benzoquinone.

**7-*neo*-pentyl-1-pyrenecarboxaldehyde (7-NP-PyCHO)**. Anhydrous aluminium chloride (3.00 g, 22.6 mmol) from a brand-new bottle was added to an ice-cold solution of 4,5,9,10-tetrahydropyrene **1**[S3] (4.50 g, 22.6 mmol) in anhydrous $CH_2Cl_2$ (60 mL) under an argon atmosphere. Pivaloyl chloride (2.80 mL, 22.6 mmol) was added while maintaining the temperature at 0 °C. After ended addition, the reaction mixture was stirred at 0 °C for 30 min and then at room temperature for 2 h. At this point ice-cold water (80 mL) was added and the mixture extracted with $CH_2Cl_2$ (150 mL). The organic phase was evaporated to dryness to afford an off-white solid (~3.6 g), which was used in the next step without further purification.

To the crude product from the previous step was added triethylsilane (11.9 mL, 74.4 mmol) and trifluoroacetic acid (9.24 mL, 124 mmol) and the reaction mixture was stirred at room temperature for 30 min, at which point $CH_2Cl_2$ (80 mL) was added. The organic phase was washed with water (3 × 30 mL), evaporated to near dryness, and the resulting crude purified via

silica gel column chromatography (petroleum ether) to obtain a white solid (~3.0 g), which was used in the next step without further purification.

The crude product from the previous step was reacted with DDQ (8.13 g, 35.8 mmol) in refluxing benzene for 4h. Following cooling to room temperature, the reaction mixture was filtered through a celite pad and washed with benzene. The filtrate was diluted with additional benzene (200 mL) and washed with 10 % aq. NaOH (3 × 50 mL) and water (2 × 50 mL). The organic phase was evaporated to dryness and the resulting residue purified by silica gel column chromatography (petroleum ether) to furnish a white solid material (~2.6 g), which was used in the next step without further purification.

Titanium tetrachloride (2.01 mL, 17.8 mmol) was added dropwise over 1 h to an ice-cold solution of the crude product from the previous step and dichloromethyl methyl ether (1.10 mL, 12.2 mmol) in anhydrous $CH_2Cl_2$ (100 mL). After ended addition, the reaction mixture was stirred at room temperature for an additional 2 h at which point the mixture was slowly poured into ice-cold water, and extracted with $CH_2Cl_2$. The organic phase was evaporated to dryness and and the resulting residue was purified by silica gel column chromatography (1-2% EtOAc in petroleum ether, v/v) to afford **7-NP-PyCHO** (1.80 g, 27% over four steps) as a bright yellow solid material. $R_f$ = 0.6 (50%, $CH_2Cl_2$ in petroleum ether, v/v); MALDI-HRMS *m*/*z* 323.1398 ($[M+Na]^+$, $C_{22}H_{20}O{\cdot}Na^+$, Calc. 323.1406); $^1$H NMR ($CDCl_3$): $\delta$ 10.76 (s, 1H, CHO), 9.38 (d, 1H, $J$ = 9.3 Hz, H10), 8.38-8.39 (d, 1H, $J$ = 7.8 Hz, H2), 8.26 (d, 1H, $J$ = 9.3 Hz, H9), 8.19-8.21 (d, 1H, $J$ = 7.8 Hz, H3), 8.16-8.18 (d, 1H, $J$ = 8.8 Hz, H5), 8.03-8.07 (2s + d, 3H, $J$ = 8.8 Hz, H4, H6, H8), 2.95 (s, 2H, $CH_2(CH_3)_3$), 1.02 (s, 9H, $(CH_3)_3CH_2$); $^{13}$C NMR ($CDCl_3$) $\delta$ 193.3 (CHO), 138.8 (C7), 135.6 (C3a), 131.3 (C2), 131.1 (C10a), 131.0 (C9), 130.9 (C5), 130.7 (C5a), 130.2

(C8a), 129.5 (C6), 129.2 (C8), 127.6 (C5a1), 127.3 (C4), 124.9 (C1), 124.6 (C3), 123.1 (C10), 122.8 (C3a1), 50.9 ($CH_2(CH_3)_3$), 32.5, 29.7 (($CH_3)_3CH_2$).

**7-*neo*-Pentyl-1-pyrenemethanol (7-NP-PyCH$_2$OH).** $NaBH_4$ (0.27 g, 7.19 mmol) was added to a room temperature solution of **7-NP-PyCHO** (1.80 g, 5.99 mmol) in anhydrous THF (20 mL) and the reaction mixture was stirred for 14 h. The reaction mixture was then diluted with EtOAc (~100 mL), which was followed by a separation of layers. The organic phase was washed with 10% aq. $NaHCO_3$ (~50 mL) and brine (~50 mL) and evaporated to dryness. The resulting material was purified via silica gel column chromatography (1% MeOH in $CH_2Cl_2$, v/v) to afford compound **7-NP-PyCH$_2$OH** (1.79 g, 99%) as a pale yellow solid. $R_f$ = 0.5 (10%, MeOH in $CH_2Cl_2$, v/v); MALDI-HRMS *m*/*z* 325.1555 ($[M+Na]^+$, $C_{22}H_{22}O{\cdot}Na^+$, Calc. 325.1563); $^1$H NMR (DMSO-$d_6$): $\delta$ 8.33-8.36 (d, 1H, $J$ = 9.3 Hz, Ar), 8.22-8.24 (d, 1H, $J$ = 7.8 Hz, Ar), 8.16-8.19 (d, 1H, $J$ = 9.3 Hz, Ar), 8.07-8.13 (m, 3H, Ar), 8.05 (br s, 1H, Ar), 8.04 (br s, 1H, Ar), 5.47 (t, 1H, ex, $J$ = 5.7 Hz, OH), 5.24 (d, 2H, $J$ = 5.7 Hz, $CH_2OH$), 2.91 (s, 2H, $CH_2C(CH_3)_3$), 0.99 (s, 9H, $(CH_3)_3CCH_2$)); $^{13}$C NMR (DMSO-$d_6$) $\delta$ 137.3, 135.8, 130.3, 129.9, 129.7, 127.4, 127.3 (Py), 127.0 (Py), 126.9 (Py), 126.7 (Py), 125.2 (Py), 124.4 (Py), 123.9, 123.3 (Py), 122.5, 61.3 ($CH_2OH$), 49.7 ($CH_2C(CH_3)_3$), 31.8, 29.3 (($CH_3)_3CCH_2$).

**Discussion – synthesis and characterization of 7-tBu-1-OMe-5-PyCH$_2$OH**. A synthetic route to 7-*tert*-butyl-1-methoxypyrene - a late stage intermediate towards 7-tBu-1-OMe-5-PyCH$_2$OH - and its reactivity in electrophilic aromatic substitution reactions, was previously established in the literature.[S2] Rieche formylation of 7-*tert*-butyl-1-methoxypyrene, followed by reduction of the aldehyde afforded 7-tBu-1-OMe-5-PyCH$_2$OH as the only isolated regioisomer in 24% yield

over two steps. The 5-position is reactive due to the electron-donating character of the methoxy group.[S2] The substitution pattern for 7-tBu-1-OMe-5-PyCH$_2$OH was established by structural elucidation of downstream product **2Y**. Briefly, C2 – which is ortho to the methoxy group – appears at high field in the $^{13}$C NMR (~108.5 ppm) and correlates with H2 (~7.7 ppm) in the HSQC spectrum. The proton at the 2-position appears as a doublet ($J$ = 8.5 Hz) that couples with H3 at ~8.18 ppm, which excludes a 1,3-substitution pattern between the methoxy group and the (original) formyl group. H4 – correlating with C4 (~127.4 ppm) in HSQC, which in turn has a cross-peak with H3 in the HMBC spectrum – appears as a singlet in the $^1$H NMR spectrum (~8.06 ppm), thus establishing the 1,5,7-substitution pattern and 5-formylation. This assignment is further substantiated by a cross-peak in the HMBC spectrum between C4 and the protons of the OCH$_2$-linker at the 5-position (~5.30 ppm).

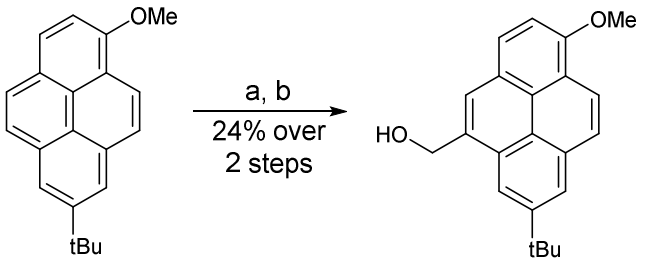


**7-tert-butyl-1-methoxypyrene** **7-tBu-1-OMe-5-PyCH$_2$OH**

**Scheme S2**. Synthesis of 7-tBu-1-OMe-5-PyCH$_2$OH. Reagents and conditions: (a) Cl$_2$CHOCH$_3$, TiCl$_4$, CH$_2$Cl$_2$, rt, 2h; (b) NaBH$_4$, THF, rt, 18 h.

**7-*tert*-butyl-1-methoxy-5-pyrenemethanol (7-tBu-1-OMe-5-PyCH$_2$OH)**. TiCl$_4$ (2.5 mL, 22.1 mmol) was added dropwise to an ice-cold solution of 7-*tert*-butyl-1-methoxypyrene[S2] (3.2 g, 11.1 mmol) and dichloromethyl methyl ether (1.6 mL, 17.7 mmol) in anhydrous CH$_2$Cl$_2$ (100

mL). After ended addition, the reaction mixture was warmed up to room temperature and stirred for 2 h, at which point it was carefully poured into ice-cold water. Following extraction with $CH_2Cl_2$ and evaporation of the organic phase to near dryness, the resulting material was purified by silica gel column chromatography (0-50% benzene in pet. ether, v/v) to afford a crude product (~2.5 g), which was used in the next step without further purification.

The crude product from the previous step was split up into a ~0.5 g and ~2.0 g batch, which were reacted separately in substantially similar fashion. Describing the latter, $NaBH_4$ (0.27 g, 7.00 mmol) was added in several portions to a solution of the crude product (~2.0 g) in THF (60 mL) and the reaction mixture was stirred at room temperature for ~18 h, at which point aq. $NaHCO_3$ and $CH_2Cl_2$ were added. The layers were separated, and the organic phase was washed with brine, evaporated to dryness, and the resulting crude subjected to silica gel column chromatography (0-5% EtOAc in pet. ether, v/v) to afford **7-tBu-1-OMe-5-PyCH$_2$OH** (0.84 g, 24% combined yield from 7-*tert*-butyl-1-methoxypyrene from the two batches). $R_f$ = 0.7 (2.5%, MeOH in $CH_2Cl_2$, v/v). MALDI-HRMS *m*/*z* 341.1535 ($[M+Na]^+$, $C_{22}H_{22}O_2{\cdot}Na^+$, Calc. 341.1517); $^1$H NMR (DMSO-$d_6$): $\delta$ 8.31-8.33 (m, 2H, Ar), 8.24-8.26 (br s, 1H, Ar), 8.20-8.23 (d, 1H, $J$ = 8.5 Hz, Ar), 8.10-8.13 (d, 1H, $J$ = 9.0 Hz, Ar), 8.07 (s, 1H, Ar), 7.68-7.71 (d, 1H, $J$ = 8.5 Hz, Ar), 5.40 (t, 1H, $J$ = 5.5 Hz, OH), 5.13 (d, 2H, $J$ = 5.5 Hz, $CH_2OH$), 4.14 (s, 3H, $CH_3O$), 1.55 (s, 9H, $C(CH_3)_3$); $^{13}$C NMR (DMSO-$d_6$) $\delta$ 153.0 (C), 148.6 (C), 134.2 (C), 131.1 (C), 129.4 (C), 126.7 (CH), 125.8 (CH), 124.5 (CH), 124.2 (C), 124.0 (C), 122.6 (C), 121.1 (CH), 120.3 (CH), 118.9 (C), 117.8 (CH), 108.5 (CH), 61.7 ($CH_2OH$), 56.1 ($CH_3O$), 35.1 (C), 31.6 ($CH_3$).

A trace amount of an unidentified impurity with the following signals in the $^{13}$C NMR spectrum was observed $\delta$: 126.8 (CH), 125.4 (CH), 125.1 (CH), 121.5 (CH), 117.0 (CH), 108.6 (CH). This impurity did not impede - and was removed during - the subsequent step.

**Table S1**. MALDI-MS of ONs modified with monomers **V** or **Y**.[a]

| ONs | Sequence | Calc. *m/z* [M+H] | Found *m/z* [M+H] |
|---|---|---|---|
| **V1** | 5'-G**V**G ATA TGC | 3039 | 3039 |
| **V2** | 5'-GTG A**V**A TGC | 2968 | 2968 |
| **V3** | 5'-GTG ATA **V**GC | 2967 | 2968 |
| **V4** | 3'-CAC **V**AT ACG | 3039 | 3039 |
| **V5** | 3'-CAC TA**V** ACG | 3039 | 3039 |
| | | | |
| **Y1** | 5'-G**Y**G ATA TGC | 3055 | 3056 |
| **Y2** | 5'-GTG A**Y**A TGC | 2984 | 2984 |
| **Y3** | 5'-GTG ATA **Y**GC | 2984 | 2984 |
| **Y4** | 3'-CAC **Y**AT ACG | 3055 | 3056 |
| **Y5** | 3'-CAC TA**Y** ACG | 3055 | 3056 |
| **Y6** | 3'-CAC **Y**A**Y** ACG | 3286 | 3287 |

[a] For structure of monomers **V** and **Y**, see Figure 1 in the main manuscript.

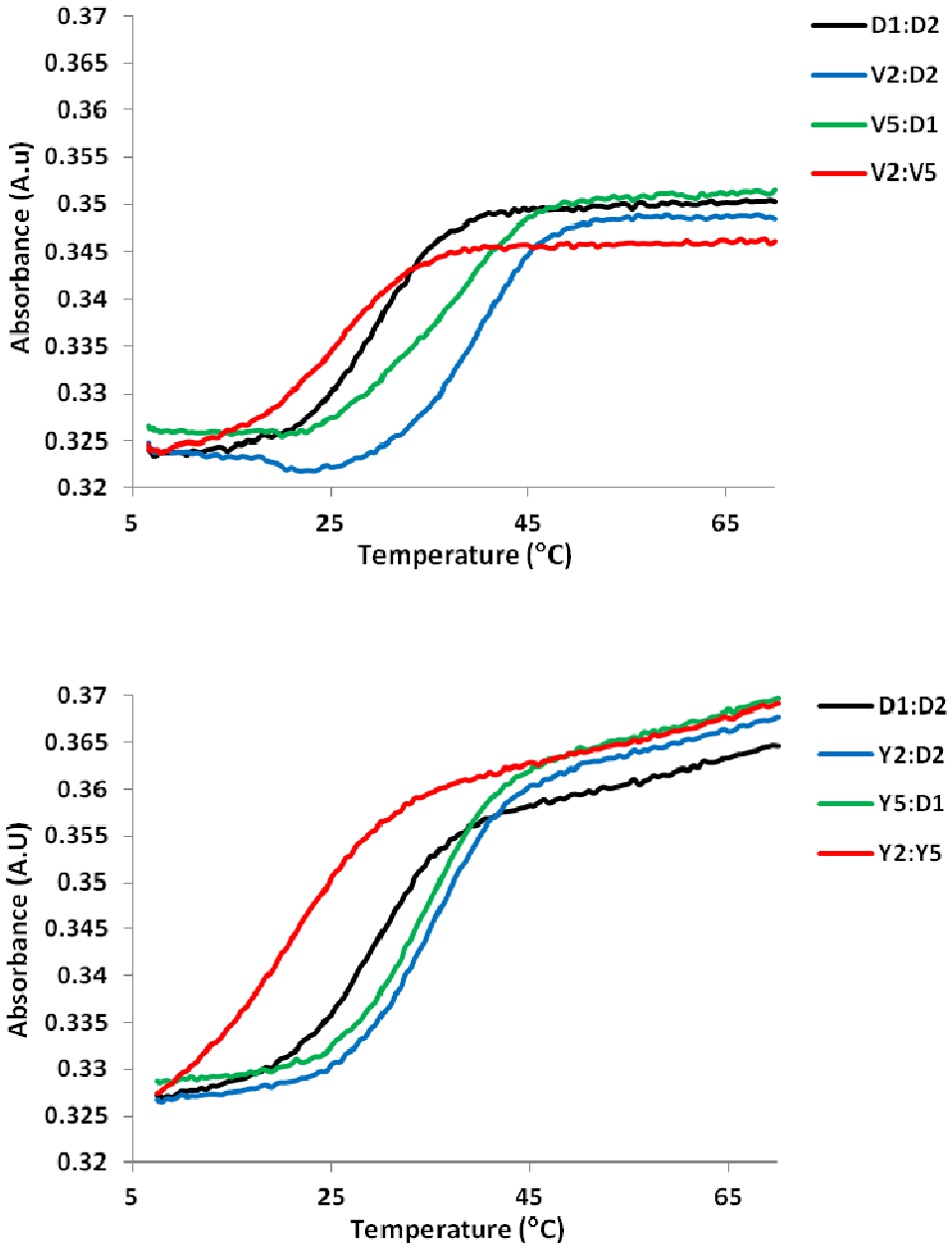


**Figure S1**. Thermal denaturation curves of **V**- or **Y**-modified duplexes and reference duplex **D1**:**D2**. For experimental conditions, see Table 1.

**Table S2**. DNA-selectivity of **B1-B6** ONs.[a]

| | | | ΔΔ$T_m$/mod (DNA-RNA) [°C] | | |
|---|---|---|---|---|---|
| **ON** | **Duplex** | **B =** | **U**[b] | **V** | **Y** |
| **B1**<br>**D2** | 5′-G**B**G ATA TGC<br>3′-CAC TAT ACG | | +7.0 | +14.5 | +9.0 |
| **B2**<br>**D2** | 5′-GTG A**B**A TGC<br>3′-CAC TAT ACG | | +9.0 | +12.5 | +11.5 |
| **B3**<br>**D2** | 5′-GTG ATA **B**GC<br>3′-CAC TAT ACG | | +8.0 | +5.5 | +11.5 |
| **D1**<br>**B4** | 5′-GTG ATA TGC<br>3′-CAC **B**AT ACG | | +8.0 | +6.0 | +4.0 |
| **D1**<br>**B5** | 5′-GTG ATA TGC<br>3′-CAC TA**B** ACG | | +10.5 | +9.0 | +7.0 |
| **D1**<br>**B6** | 5′-GTG ATA TGC<br>3′-CAC **B**A**B** ACG | | +7.3 | - | +6.5 |

[a] DNA selectivity defined as ΔΔ$T_m$/mod (DNA-RNA) = Δ$T_m$/mod (vs DNA) - Δ$T_m$/mod (vs RNA). [b] Data from reference S4 are included to facilitate comparison.

**Table S3**. Discrimination of singly mismatched RNA targets by **V2**, **Y2** and reference strands.[a] **V2** and **Y2** display less efficient discrimination than **D1** or **U2**, especially when a mismatched rC is opposite of the modified monomer.

| | | | RNA: 3′-CAC U**B**U ACG | | | |
|---|---|---|---|---|---|---|
| | | | $T_m$ [°C] | $\Delta T_m$[°C] | | |
| **ON** | **Sequence** | **B** = | A | C | G | U |
| **D1** | 5′-GTG ATA TGC | | **26.5** | <-16.5 | -4.5 | <-16.5 |
| **U2**[b] | 5′-GTG A**U**A TGC | | **31.0** | -17.5 | -3.5 | -9.5 |
| **V2** | 5′-GTG A**V**A TGC | | **24.5** | -11.0 | -2.5 | -8.5 |
| **Y2** | 5′-GTG A**Y**A TGC | | **21.5** | -9.0 | -4.0 | -9.0 |

[a] For conditions of thermal denaturation experiments, see Table 1. $T_m$'s of fully matched duplexes are shown in bold. $\Delta T_m$ = change in $T_m$ relative to fully matched DNA:RNA duplex. [b] Data from reference S4 are included to facilitate comparison.

**Table S4**. Discrimination of mismatched DNA targets by **Y6** and reference strands.[a] **Y6**, with two modifications positioned as next-nearest neighbors, discriminates DNA targets with a single central mismatched nucleotide opposite of the central adenosine residue with similar efficiency as reference strand **D2**, but lower efficiency than **U6**.

| | | | DNA : 5'-GTG A**B**A ACG | | | |
|---|---|---|---|---|---|---|
| | | | $T_m$ [°C] | $\Delta T_m$ [°C] | | |
| ON | Sequence | B = | T | A | C | G |
| **D2** | 3'-CAC TAT ACG | | **29.5** | -17.0 | -15.5 | -9.0 |
| **U6**[b] | 3'-CAC **U**A**U** ACG | | **43.5** | -24.0 | -17.0 | -14.0 |
| **Y6** | 3'-CAC **Y**A**Y** ACG | | **30.5** | -15.0 | -12.0 | -10.0 |

[a] For conditions of thermal denaturation experiments, see Table 1. $T_m$'s of fully matched duplexes are shown in bold. $\Delta T_m$ = change in $T_m$ relative to fully matched DNA:DNA duplex. [b] Data from reference S4 are included to facilitate comparison.

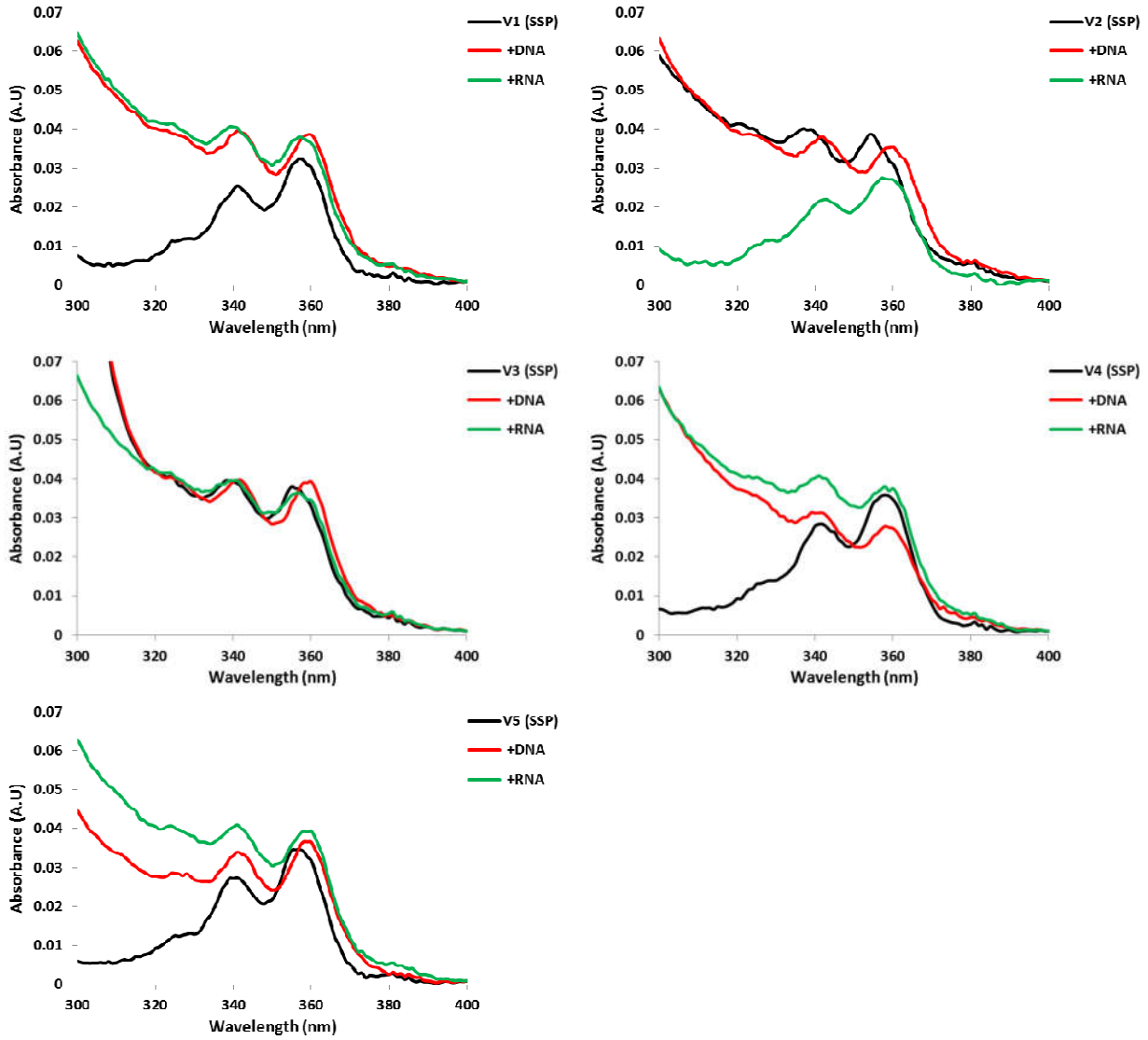


**Figure S2**. Absorption spectra of single-stranded probes (SSP) **V1-V5** and their corresponding duplexes with cDNA/cRNA. Spectra were recorded at $T = 5$ °C using each strand at 1.0 μM concentration in $T_m$ buffer.

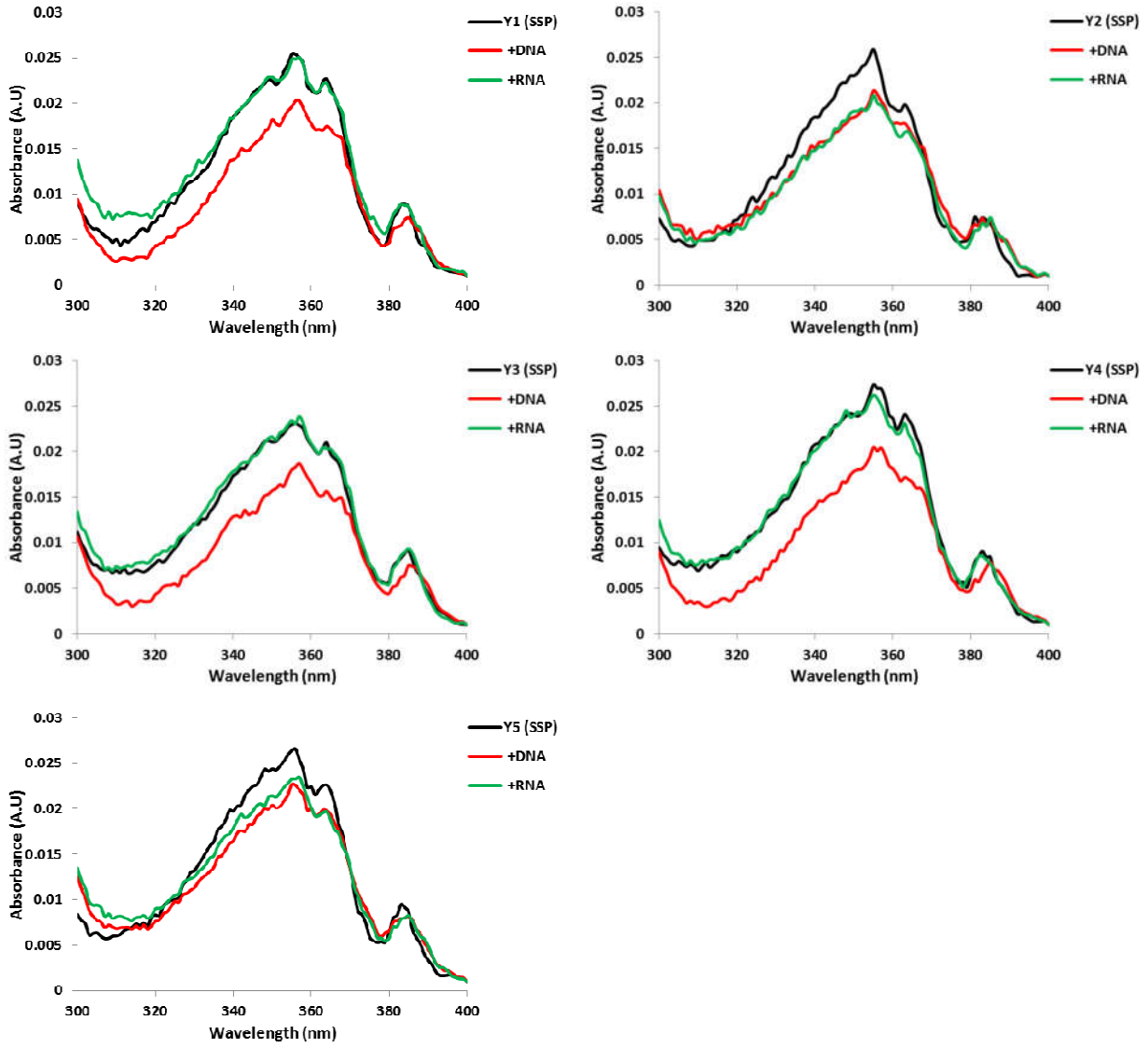


**Figure S3**. Absorption spectra of single-stranded **Y1-Y5** and their corresponding duplexes with cDNA/cRNA. Spectra were recorded at $T = 5$ °C using each strand at 1.0 μM concentration in $T_m$ buffer.

**Table S5**. Absorption maxima in the 340-365 nm region for single-stranded (SS) **U**/**V**/**Y**-modified ONs and the corresponding duplexes with cDNA or cRNA[a]

| | | | $\lambda_{max}[\Delta\lambda_{max}]$ (nm) | | | | | | | | |
|---|---|---|---|---|---|---|---|---|---|---|---|
| | | **B=** | **U**[b] | | | **V** | | | **Y** | | |
| ON | Sequence | | SS | +cDNA | +cRNA | SS | +cDNA | +cRNA | SS | +cDNA | +cRNA |
| **B1** | 5'-G**B**G ATA TGC | | 350 | 353 [+3] | 352 [+2] | 356 | 360 [+4] | 357 [+1] | 355 | 356 [+1] | 357 [+2] |
| **B2** | 5'-GTG A**B**A TGC | | 348 | 353 [+5] | 352 [+4] | 354 | 360 [+6] | 357 [+3] | 355 | 355 [±0] | 355 [±0] |
| **B3** | 5'-GTG ATA **B**GC | | 350 | 353 [+3] | 352 [+2] | 355 | 359 [+4] | 357 [+2] | 356 | 357 [+1] | 357 [+1] |
| **B4** | 3'-CAC **B**AT ACG | | 350 | 352 [+2] | 352 [+2] | 358 | 358 [±0] | 358 [±0] | 355 | 355 [±0] | 355 [±0] |
| **B5** | 3'-CAC TA**B** ACG | | 349 | 353 [+4] | 352 [+3] | 357 | 358 [+1] | 358 [+1] | 356 | 355 [-1] | 357 [+1] |

[a] Measurements were performed at 5 °C in $T_m$ buffer using a spectrophotometer and quartz optical cells with a 1.0 cm path length. [b] Data from reference S4 are included to facilitate comparison.

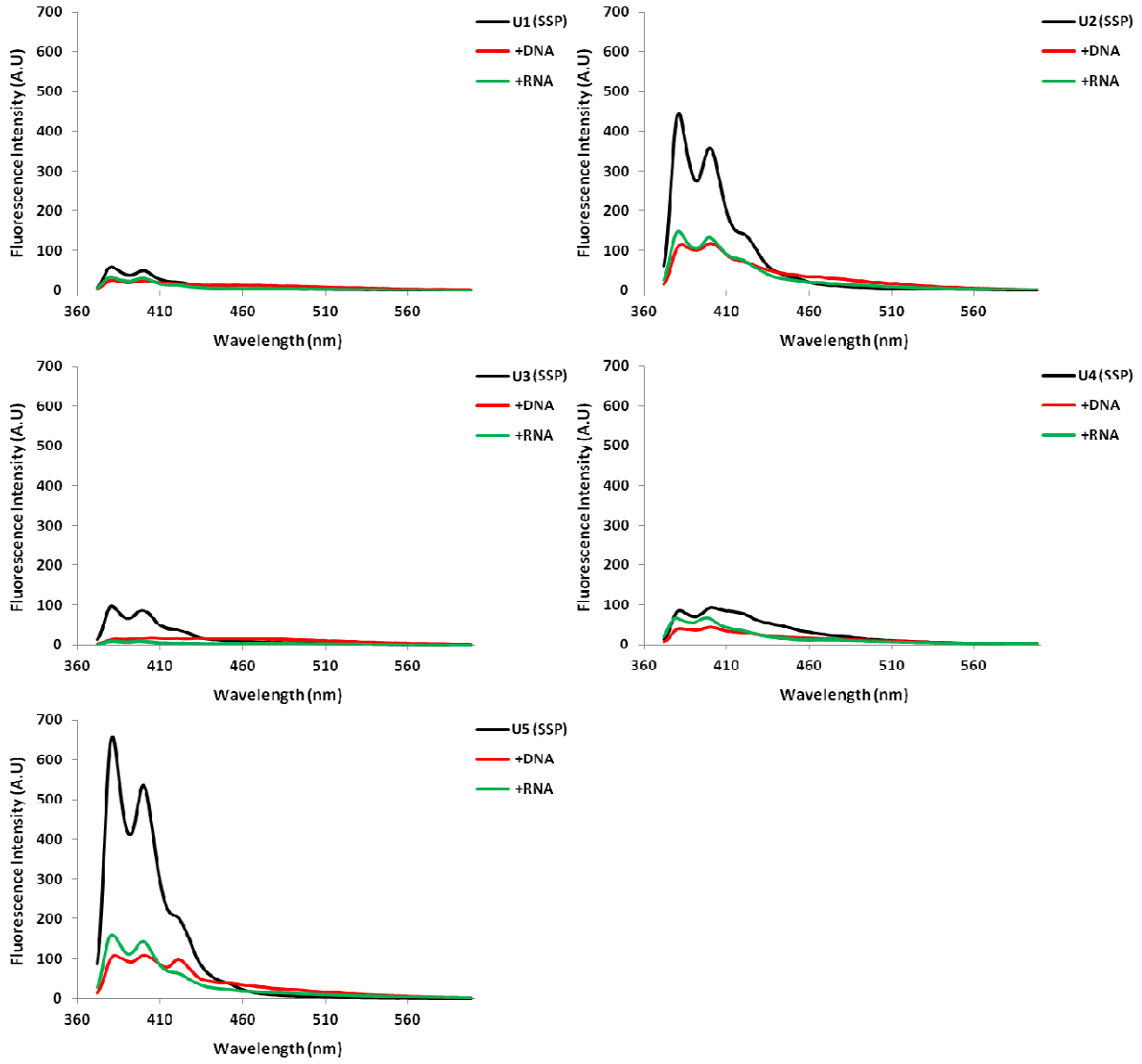


**Figure S4**. Steady-state fluorescence emission spectra of **U**-modified ONs and their corresponding duplexes with DNA/RNA targets. Spectra were recorded at $T$ = 5 °C using $\lambda_{ex}$ = 350 nm and each strand at 1.0 μM concentration in $T_m$ buffer. Spectra were previously reported in reference S5 (used with permission from the Royal Society of Chemistry) and are included to facilitate comparison.

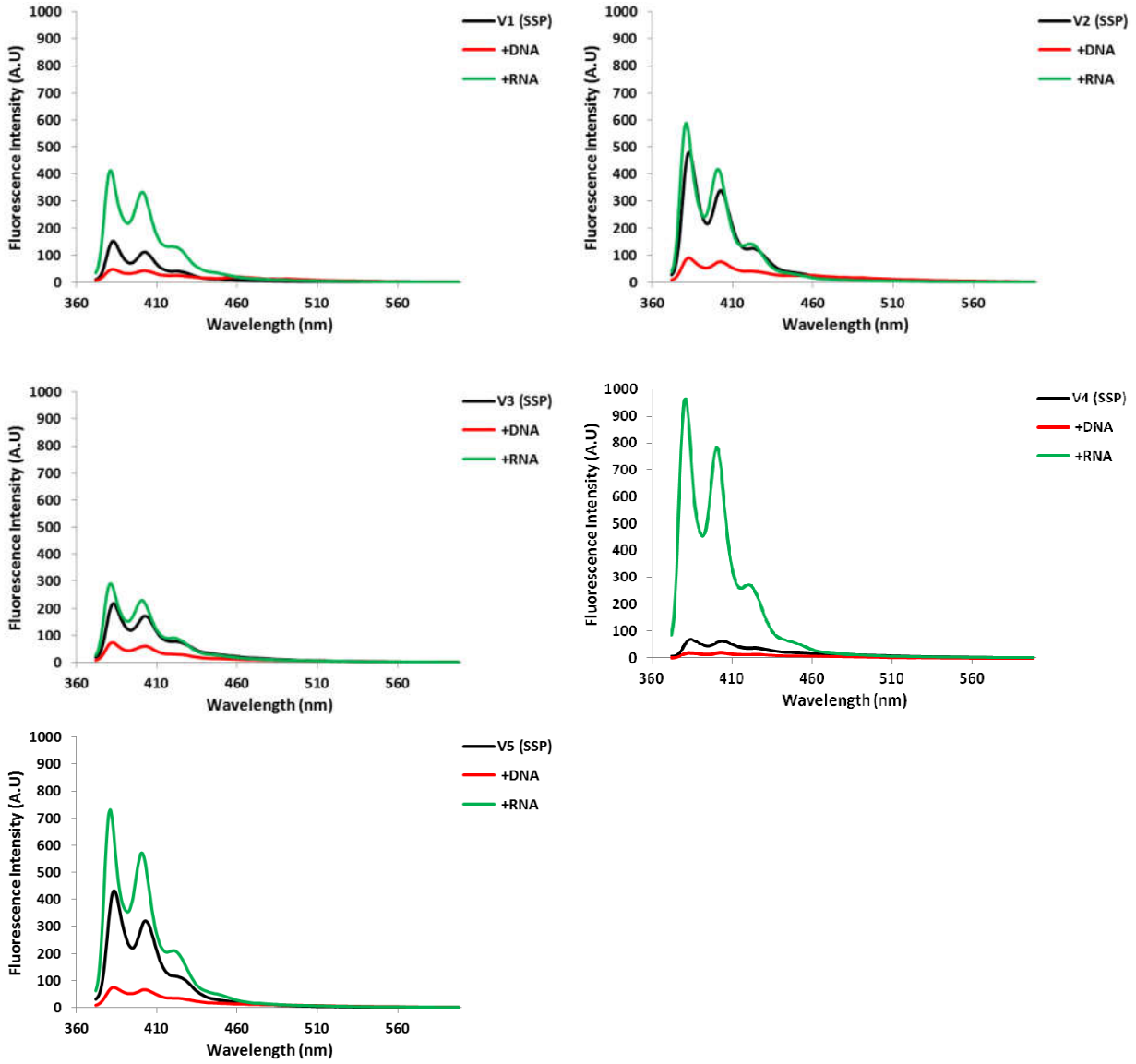


**Figure S5**. Steady-state fluorescence emission spectra of single-stranded probes (SSP) **V1-V5** and their corresponding duplexes with cDNA/cRNA. Spectra were recorded at $T = 5$ °C using $\lambda_{ex}$ = 350 nm and each strand at 1.0 μM concentration in $T_m$ buffer.

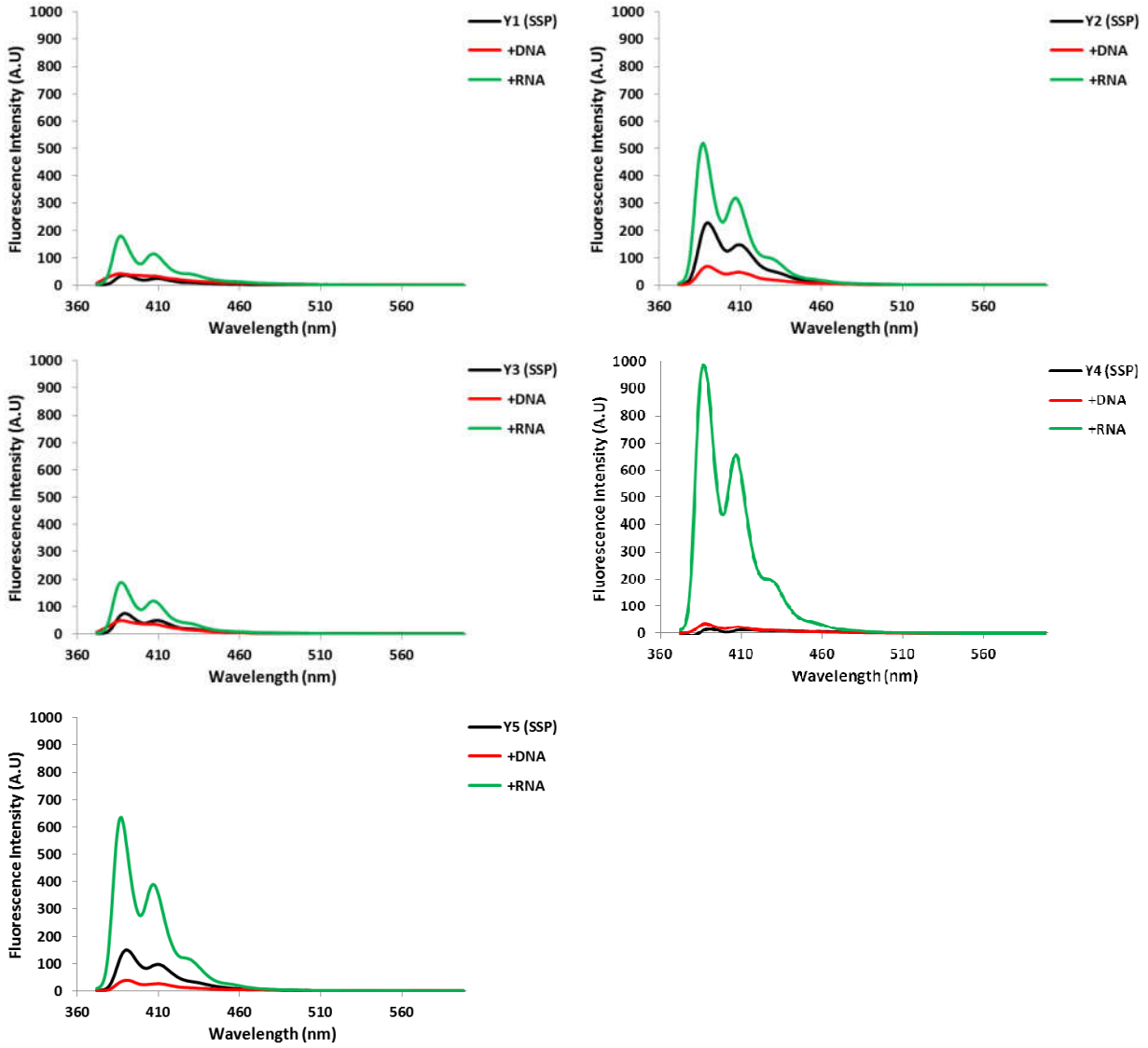


**Figure S6**. Steady-state fluorescence emission spectra of single-stranded probes (SSP) **Y1-Y5** and their corresponding duplexes with cDNA/cRNA. Spectra were recorded at $T$ = 5 °C using $\lambda_{ex}$ = 350 nm and each strand at 1.0 μM concentration in $T_m$ buffer.

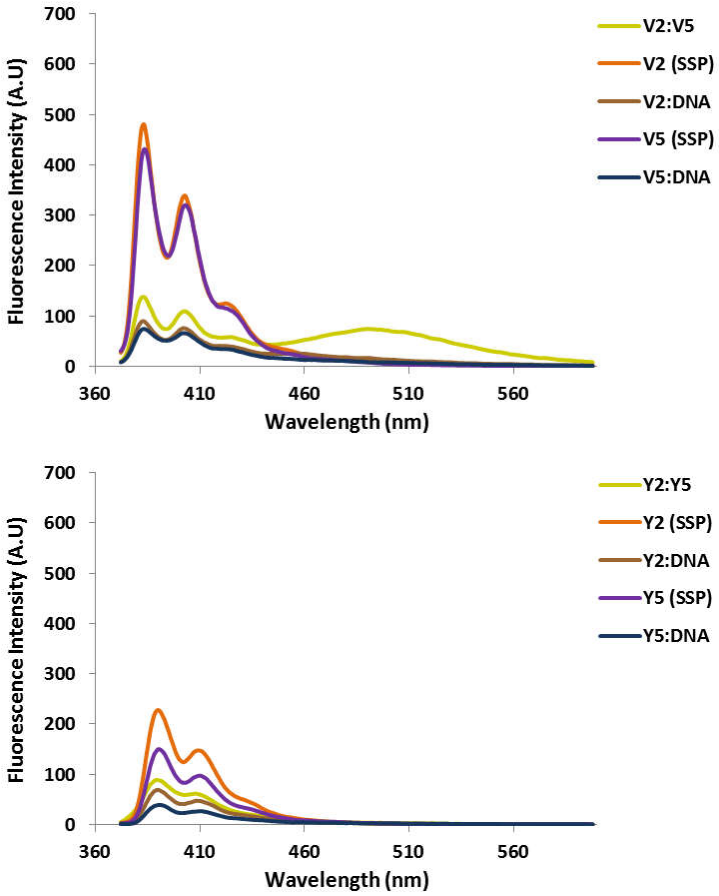


**Figure S7**. Steady-state fluorescence emission spectra of **B2** and **B5** ONs, the corresponding duplexes with cDNA, and double-stranded **B2**:**B5** probes with +1 interstrand zipper arrangements of the pyrene-functionalized monomers. Spectra were recorded at $T$ = 5 °C using $\lambda_{ex}$ = 350 nm and each strand at 1.0 μM concentration in $T_m$ buffer. SSP = single-stranded probe. Probe **V2**:**V5** displays a broad unstructured band at ~ 490 nm, indicative of a pyrene-pyrene excimer, which requires co-planar stacking of the pyrene moieties. No evidence of excimer formation is observed for **Y2**:**Y5**, presumably because the 1-methoxy and 7-*tert*-butyl substituents preclude pyrene-pyrene stacking. While it was not pursued in the present study, the excimer signal of **V2**:**V5** likely could have been used to monitor recognition of isosequential dsDNA targets in a similar fashion as described for other Invader probes.[S6]

**Table S6**. Change in enthalpy upon duplex formation ($\Delta H$) and change in enthalpy upon probe recognition of isosequential dsDNA target **D1**:**D4** ($\Delta H_{rec}$).[a]

| Probe | Zipper | Sequence | $\Delta H$ [$\Delta\Delta H$] (kJ/mol) | | | $\Delta H_{rec}$ (kJ/mol) |
|---|---|---|---|---|---|---|
| | | | upper strand vs cDNA | lower strand vs cDNA | probe duplex | |
| [b]**U1**<br>**U5** | **+4** | 5'-G**U**G ATA TGC<br>3'-CAC TA**U** ACG | -281±4 [+25] | -299±2 [+7] | -279±1 [+27] | +5 |
| [b]**U1**<br>**U4** | **+2** | 5'-G**U**G ATA TGC<br>3'-CAC **U**AT ACG | -281±4 [+25] | -300±7 [+6] | -248±8 [+58] | -27 |
| [b]**U2**<br>**U5** | +1 | 5'-GTG A**U**A TGC<br>3'-CAC TA**U** ACG | **-305±1 [+1]** | **-299±2 [+7]** | **-244±3 [+62]** | **-54** |
| [b]**U2**<br>**U4** | **-1** | 5'-GTG A**U**A TGC<br>3'-CAC **U**AT ACG | -305±1 [+1] | -300±7 [+6] | -296±6 [+10] | -3 |
| [b]**U3**<br>**U5** | **-1** | 5'-GTG ATA **U**GC<br>3'-CAC TA**U** ACG | -270±7 [+36] | -299±2 [+7] | -280±5 [+26] | +17 |
| [b]**U3**<br>**U4** | **-3** | 5'-GTG ATA **U**GC<br>3'-CAC **U**AT ACG | -270±7 [+36] | -300±7 [+6] | -309±4 [-3] | +45 |
| **V1**<br>**V5** | **+4** | 5'-G**V**G ATA TGC<br>3'-CAC TA**V** ACG | -278±6 [+28] | -273±3 [+33] | -225±5 [+81] | -20 |
| **V1**<br>**V4** | **+2** | 5'-G**V**G ATA TGC<br>3'-CAC **V**AT ACG | -278±6 [+28] | -288±28 [+18] | -251±2 [+55] | -9 |
| **V2**<br>**V5** | **+1** | 5'-GTG A**V**A TGC<br>3'-CAC TA**V** ACG | **-340±6 [-34]** | **-273±3 [+33]** | **-273±4 [+33]** | **-34** |
| **V2**<br>**V4** | **-1** | 5'-GTG A**V**A TGC<br>3'-CAC **V**AT ACG | -340±6 [-34] | -288±28 [+18] | -291±5 [+15] | -31 |
| **V3**<br>**V5** | **-1** | 5'-GTG ATA **V**GC<br>3'-CAC TA**V** ACG | -289±5 [+17] | -273±3 [+33] | -228±3 [+78] | -28 |
| **V3**<br>**V4** | **-3** | 5'-GTG ATA **V**GC<br>3'-CAC **V**AT ACG | -289±5 [+17] | -288±28 [+18] | -246±3 [+60] | -25 |
| **Y1**<br>**Y5** | +4 | 5'-G**Y**G ATA TGC<br>3'-CAC TA**Y** ACG | -302±2 [+4] | -319±5 [-13] | -273±3 [+33] | -42 |
| **Y1**<br>**Y4** | +2 | 5'-G**Y**G ATA TGC<br>3'-CAC **Y**AT ACG | -302±2 [+4] | -317±3 [-11] | -265±4 [+41] | -48 |
| **Y2**<br>**Y5** | +1 | 5'-GTG A**Y**A TGC<br>3'-CAC TA**Y** ACG | -326±1 [-20] | -319±5 [-13] | N/A | N/A |
| **Y2**<br>**Y4** | -1 | 5'-GTG A**Y**A TGC<br>3'-CAC **Y**AT ACG | -326±1 [-20] | -317±3 [-11] | -279±2 [+27] | -58 |
| **Y3**<br>**Y5** | -1 | 5'-GTG ATA **Y**GC<br>3'-CAC TA**Y** ACG | -275±1 [+31] | -319±5 [-13] | -272±2 [+34] | -16 |
| **Y3**<br>**Y4** | -3 | 5'-GTG ATA **Y**GC<br>3'-CAC **Y**AT ACG | -275±1 [+31] | -317±3 [-11] | -212±9 [+94] | -74 |

[a] $\Delta\Delta H$ is measured relative to $\Delta H$ for **D1**:**D4** = -306 kJ/mol. $\Delta H_{rec}$ = $\Delta H$ (upper strand vs cDNA) + $\Delta H$ (lower strand vs cDNA) - $\Delta H$ (probe duplex) - $\Delta H$ (dsDNA target). "±" denotes standard deviation. N/A = lack of a clear lower base line prevented determination of this value. [b]Data, previously reported in reference S5, are included to facilitate comparison.

**Table S7**. Change in entropy at 293 K upon duplex formation ($-T^{293}\Delta S$) and change in entropy upon probe recognition of isosequential dsDNA target **D1**:**D4** ($-T^{293}\Delta S_{rec}$).[a]

| Probe | Zipper | Sequence | $-T^{293}\Delta S$ [$\Delta(T^{293}\Delta S)$] (kJ/mol) | | | $-T^{293}\Delta S_{rec}$ (kJ/mol) |
|---|---|---|---|---|---|---|
| | | | upper strand vs cDNA | lower strand vs cDNA | probe duplex | |
| **U1**<br>**U5** | **+4** | 5'-G**U**G ATA TGC<br>3'-CAC TA**U** ACG | 235±3 [-30] | 247±6 [-18] | 224±1 [-41] | -7 |
| **U1**<br>**U4** | **+2** | 5'-G**U**G ATA TGC<br>3'-CAC **U**AT ACG | 235±3 [-30] | 254±6 [-11] | 203±8 [-62] | +21 |
| **U2**<br>**U5** | **+1** | 5'-GTG A**U**A TGC<br>3'-CAC TA**U** ACG | **251±1 [-14]** | **247±6 [-18]** | **204±3 [-61]** | **+29** |
| **U2**<br>**U4** | **-1** | 5'-GTG A**U**A TGC<br>3'-CAC **U**AT ACG | 251±1 [-14] | 254±6 [-11] | 245±5 [-20] | -5 |
| **U3**<br>**U5** | **-1** | 5'-GTG ATA **U**GC<br>3'-CAC TA**U** ACG | 220±7 [-45] | 247±6 [-18] | 225±5 [-40] | -23 |
| **U3**<br>**U4** | **-3** | 5'-GTG ATA **U**GC<br>3'-CAC **U**AT ACG | 220±7 [-45] | 254±6 [-11] | 256±3 [-9] | -47 |
| **V1**<br>**V5** | **+4** | 5'-G**V**G ATA TGC<br>3'-CAC TA**V** ACG | 233±6 [-32] | 224±3 [-41] | 178±5 [-87] | +14 |
| **V1**<br>**V4** | **+2** | 5'-G**V**G ATA TGC<br>3'-CAC **V**AT ACG | 233±6 [-32] | 247±28 [-18] | 205±2 [-60] | +10 |
| **V2**<br>**V5** | **+1** | 5'-GTG A**V**A TGC<br>3'-CAC TA**V** ACG | **285±6 [+20]** | **224±3 [-41]** | **233±4 [-32]** | **+11** |
| **V2**<br>**V4** | **-1** | 5'-GTG A**V**A TGC<br>3'-CAC **V**AT ACG | 285±6 [+20] | 247±28 [-18] | 241±4 [-24] | +26 |
| **V3**<br>**V5** | **-1** | 5'-GTG ATA **V**GC<br>3'-CAC TA**V** ACG | 243±4 [-22] | 224±3 [-41] | 181±3 [-84] | +21 |
| **V3**<br>**V4** | **-3** | 5'-GTG ATA **V**GC<br>3'-CAC **V**AT ACG | 243±4 [-22] | 247±28 [-18] | 203±3 [-62] | +22 |
| **Y1**<br>**Y5** | +4 | 5'-G**Y**G ATA TGC<br>3'-CAC TA**Y** ACG | 261±2 [-4] | 270±4 [+5] | 227±3 [-38] | +39 |
| **Y1**<br>**Y4** | +2 | 5'-G**Y**G ATA TGC<br>3'-CAC **Y**AT ACG | 261±2 [-4] | 279±3 [+14] | 224±4 [-41] | +51 |
| **Y2**<br>**Y5** | +1 | 5'-GTG A**Y**A TGC<br>3'-CAC TA**Y** ACG | 276±1 [+11] | 270±4 [+5] | N/A | N/A |
| **Y2**<br>**Y4** | -1 | 5'-GTG A**Y**A TGC<br>3'-CAC **Y**AT ACG | 276±1 [+11] | 279±3 [+14] | 237±2 [-28] | +53 |
| **Y3**<br>**Y5** | -1 | 5'-GTG ATA **Y**GC<br>3'-CAC TA**Y** ACG | 231±1 [-34] | 270±4 [+5] | 226±2 [-39] | +10 |
| **Y3**<br>**Y4** | -3 | 5'-GTG ATA **Y**GC<br>3'-CAC **Y**AT ACG | 231±1 [-34] | 279±3 [+14] | 174±9 [-91] | +71 |

[a] $\Delta(T^{293}\Delta S)$ is measured relative to $-T^{293}\Delta S$ for **D1**:**D2** = 265 kJ/mol. $-T^{293}\Delta S_{rec} = T^{293}\Delta S$ (upper strand vs cDNA) + $T^{293}\Delta S$ (lower strand vs cDNA) - $T^{293}\Delta S$ (probe duplex) - $T^{293}\Delta S$ (dsDNA target). "±" denotes standard deviation. N/A = the lack of a clear lower base line prevented determination of this value. [b]Data, previously reported in reference S5, are included to facilitate comparison.

*Additional background discussion regarding the* $\Delta G_{rec}^{293}$ *term.* The $\Delta G_{rec}^{293}$ term, which we define as $\Delta G_{rec}^{293}$ = $\Delta G^{293}$ (**ONX**:cDNA) + $\Delta G^{293}$ (cDNA:**ONY**) - $\Delta G^{293}$ (**ONX**:**ONY**) - $\Delta G^{293}$ (dsDNA), describes the thermodynamic driving force for Invader-mediated recognition of a *linear* dsDNA target with the same core sequence as the Invader probe (e.g., 5'-GTGATATGC : 3'-CACTATACG for the probes shown in Table 4). While $\Delta G_{rec}^{293}$ is not a direct measure of the thermodynamic driving force for recognition of model target **DH1** (Figure 4) or more complex targets, it is a useful term to assess different Invader designs relative to each other. The $\Delta G^{293}$ (dsDNA) component – i.e., the change in free energy associated with formation of the dsDNA target region – will likely be considerably more negative (i.e., more stable) for model target **DH1**, whereas the $\Delta G^{293}$ (**ONX**:cDNA) and $\Delta G^{293}$ (cDNA:**ONY**) terms are not expected to deviate substantially in the formed recognition complexes save for potential stacking interactions with nucleotides in the $T_{10}$-loop. We did not experimentally determine the $\Delta G^{293}$ (**ONX**:cDNA) and $\Delta G^{293}$ (cDNA:**ONY**) terms as they need to be determined simultaneously, which is experimentally challenging. Consequently, we expect $\Delta G_{rec}^{293}$ for Invader-mediated recognition of **DH1** to be less favorable than for recognition of the corresponding isosequential dsDNA targets, which is supported by our experimental observations (e.g., no recognition of **DH1** is observed with **V2**:**V5** despite a $\Delta G_{rec}^{293}$ value of -23 kJ/mol, Figure 4 and Table 4). However, we have found that $\Delta G_{rec}$ values for Invader-mediated recognition of linear isosequential dsDNA targets scale to more complex targets such as DNA hairpins (i.e., dsDNA recognition more likely to ensue with probes with highly negative $\Delta G_{rec}^{293}$ values), aiding probe optimization – e.g., see references S5, S7 and S8.

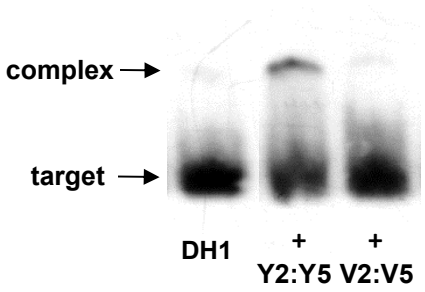


**Figure S8**. Electrophoretogram from experiments in which **Y2**:**Y5** or **V2**:**V5** probes were pre-annealed with **DH1** (heating to 90 °C for 2 min, followed by slow cooling to room temperature) followed by incubation in the HEPES buffer (50 mM HEPES, 100 mM NaCl, 5 mM $MgCl_2$, pH 7.2, 10% sucrose, 1.44 mM spermine tetrahyrdochloride) for 15 h at room temperature.

**References**.

S1) R. G. Harvey, M. Konieczny and J. Pataki, *J. Org. Chem*., 1983, **48**, 2930-2932.

S2) T. Yamato, M. Fujimoto, Y. Nagano, A. Miyazawa and M. Tashiro, *Org. Prep. Proc. Int*., 1997, **29**, 321–329.

S3) V. V. Filichev, I. V. Astakhova, A. D. Malakhov, V. A. Korshun and E. B. Pedersen, *Chem. Eur. J*. 2008, **14**, 9968–9980.

S4) S. Karmakar, B. A. Anderson, R. L. Rathje, S. Andersen, T. B. Jensen, P. E. Nielsen and P. J. Hrdlicka, *J. Org. Chem*., 2011, **76**, 7119–7131.

S5) S. Karmakar, A. S. Madsen, D. C. Guenther, B. C. Gibbons and P. J. Hrdlicka, *Org. Biomol. Chem*., 2014, **12**, 7758–7773.

S6) S. P. Sau, T. S. Kumar and P. J. Hrdlicka, *Org. Biomol. Chem*., 2010, **8**, 2028–2036.

S7) S. Karmakar, D. C. Guenther and P. J. Hrdlicka, *J. Org. Chem*., 2013, **78**, 12040–12048.

S8) D. C. Guenther, G. H. Anderson, B. A. Anderson, S. Karmakar and P. J. Hrdlicka, *Chem. Sci*., 2015, **6**, 5006–5015.

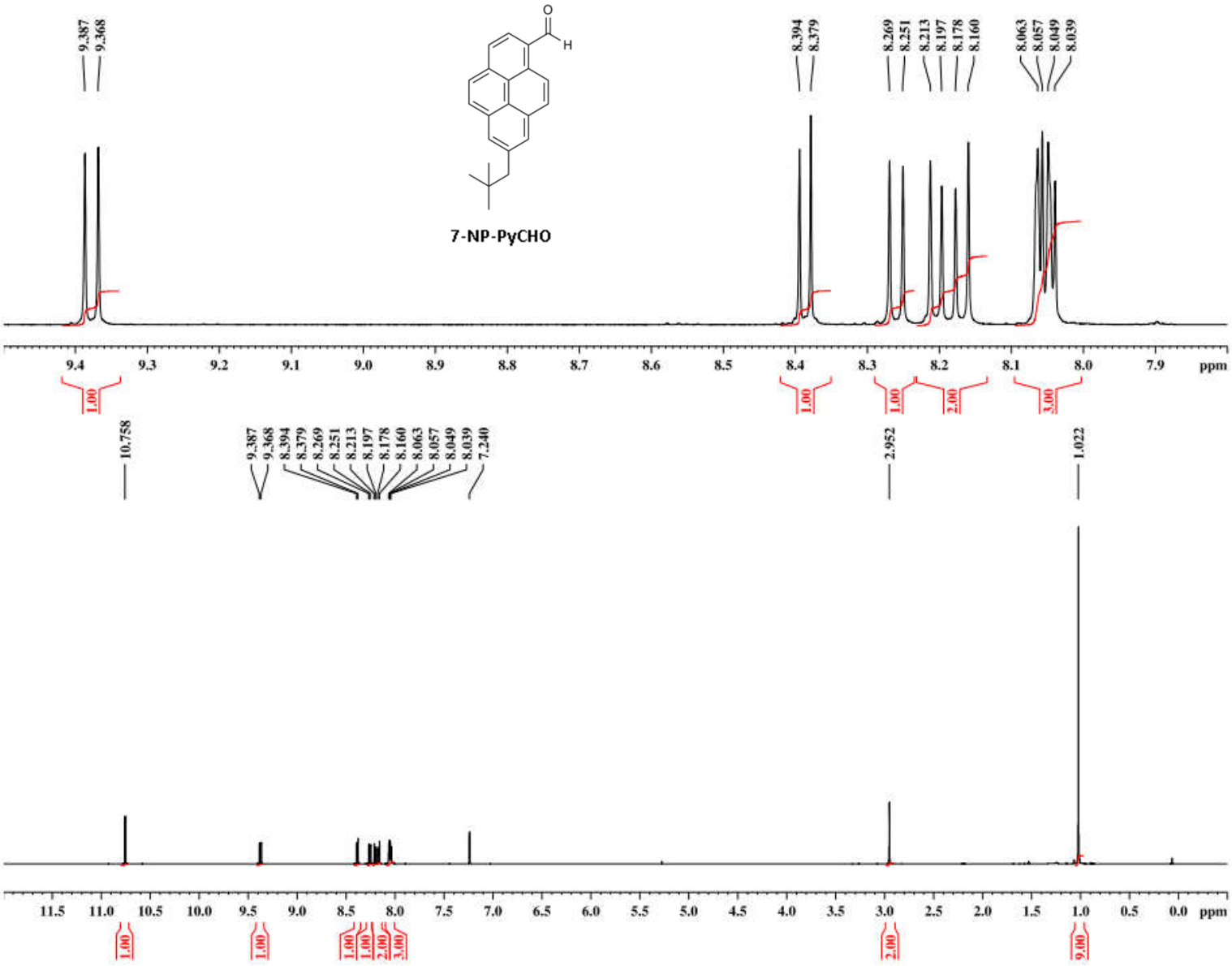
9.387
9.368
8.394
8.379
8.269
8.251
8.213
8.197
8.178
8.160
8.063
8.057
8.049
8.039
7-NP-PyCHO
ppm
10.758
7.240
2.952
1.022

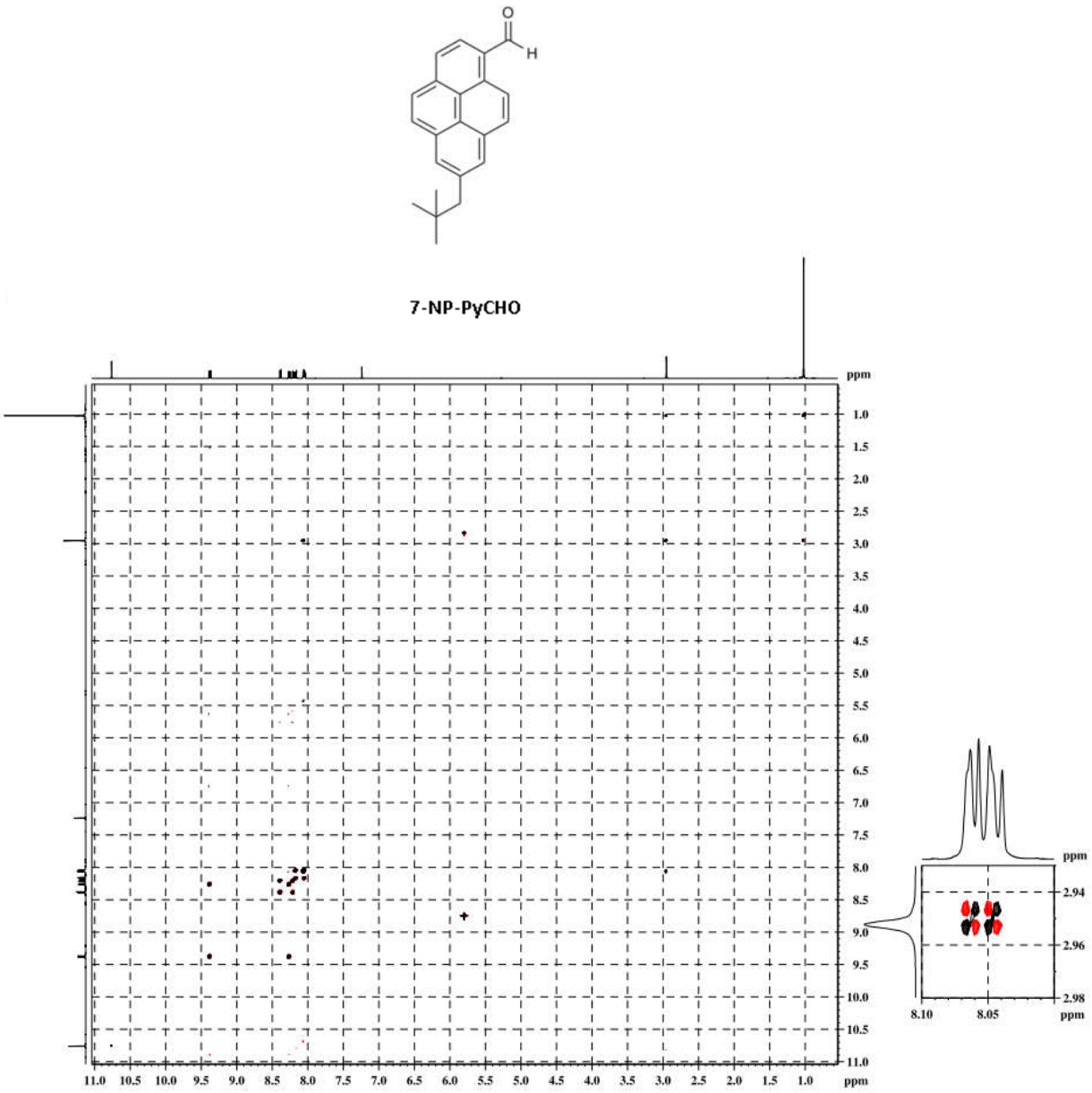
O
H
7-NP-PyCHO
ppm
1.0
1.5
2.0
2.5
3.0
3.5
4.0
4.5
5.0
5.5
6.0
6.5
7.0
7.5
8.0
8.5
9.0
9.5
10.0
10.5
11.0
11.0 10.5 10.0 9.5 9.0 8.5 8.0 7.5 7.0 6.5 6.0 5.5 5.0 4.5 4.0 3.5 3.0 2.5 2.0 1.5 1.0 ppm
ppm
2.94
2.96
2.98
8.10
8.05
ppm

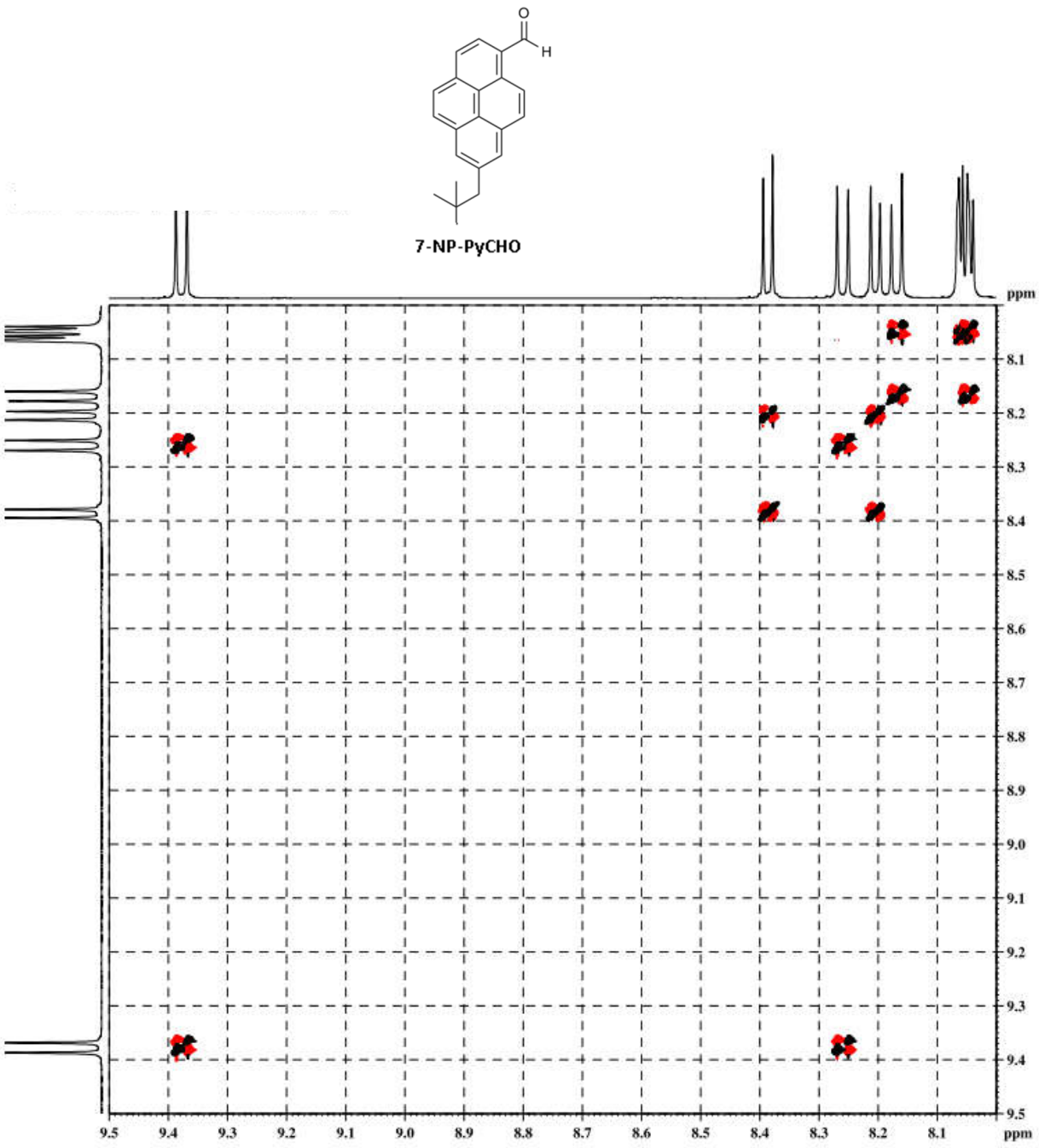
O
H
7-NP-PyCHO
ppm
8.1
8.2
8.3
8.4
8.5
8.6
8.7
8.8
8.9
9.0
9.1
9.2
9.3
9.4
9.5
9.5
9.4
9.3
9.2
9.1
9.0
8.9
8.8
8.7
8.6
8.5
8.4
8.3
8.2
8.1
ppm

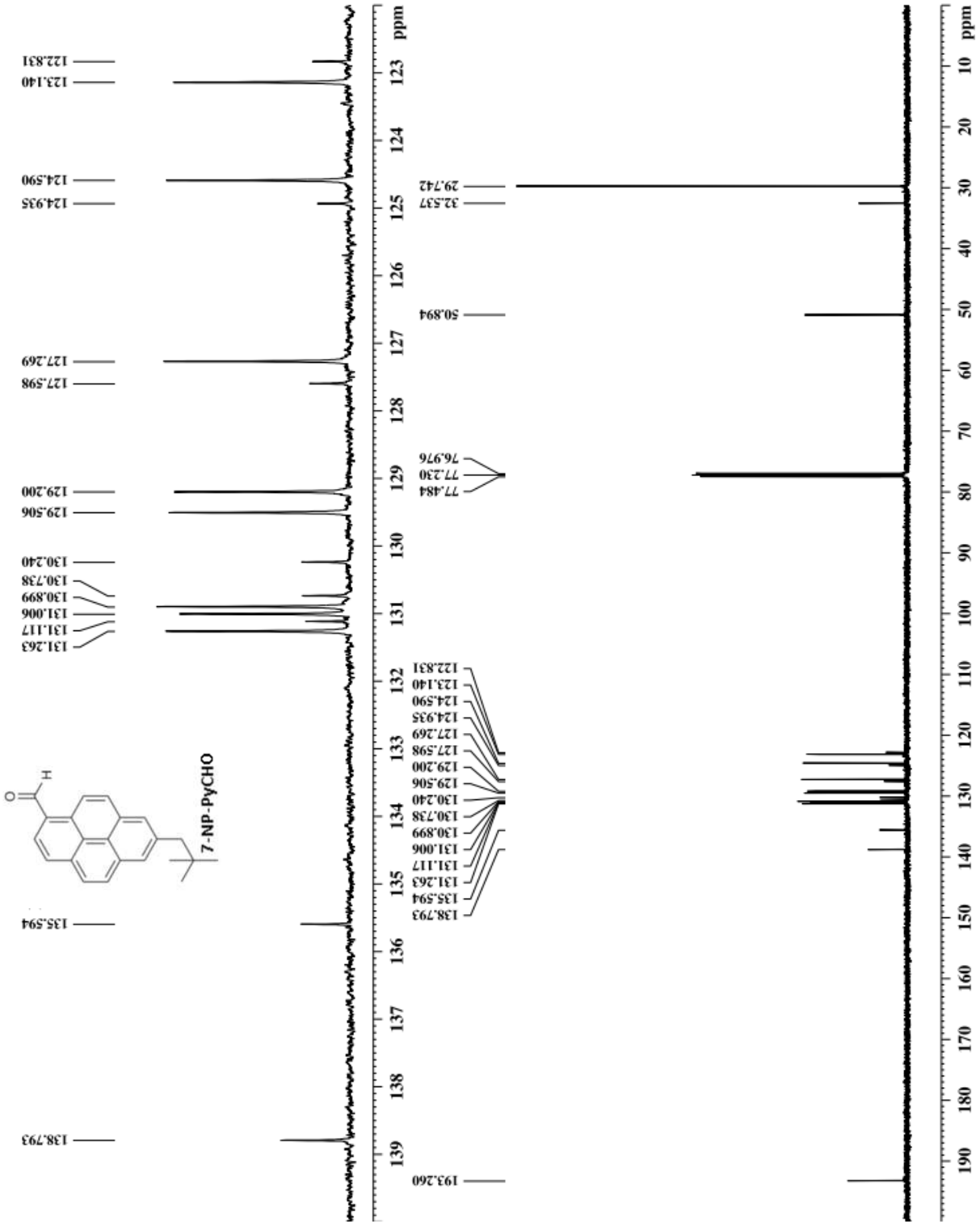
7-NP-PyCHO
O
H
193.260
138.793
135.594
131.263
131.117
131.006
130.899
130.738
130.240
129.506
129.200
127.598
127.269
124.935
124.590
123.140
122.831
77.484
77.230
76.976
50.894
32.537
29.742
ppm

29.743
50.893
7-NP-PyCHO
131.272
131.011
130.904
129.511
129.202
127.271
124.592
123.139
ppm

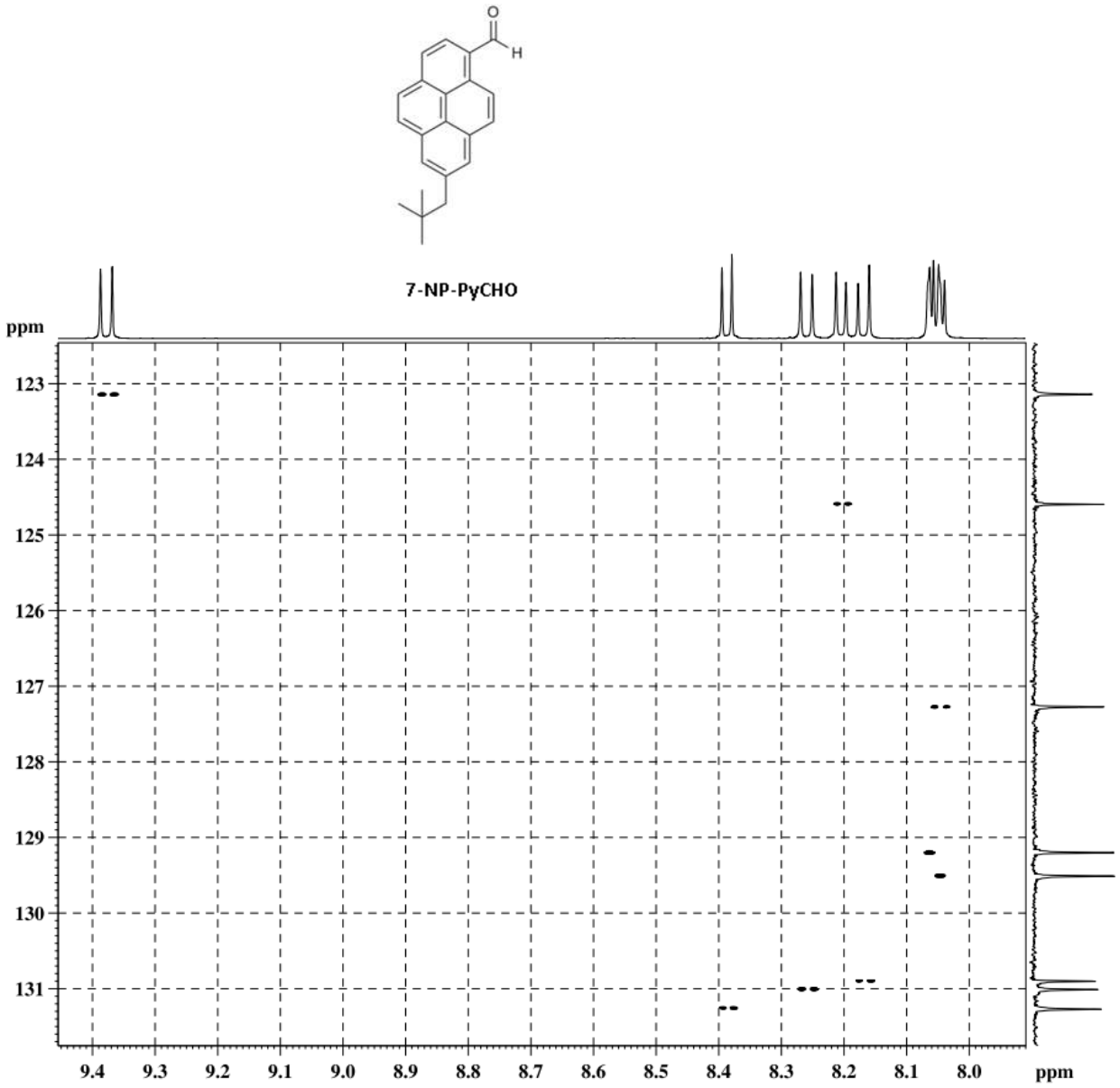
O
H
7-NP-PyCHO
ppm
123
124
125
126
127
128
129
130
131
9.4
9.3
9.2
9.1
9.0
8.9
8.8
8.7
8.6
8.5
8.4
8.3
8.2
8.1
8.0
ppm

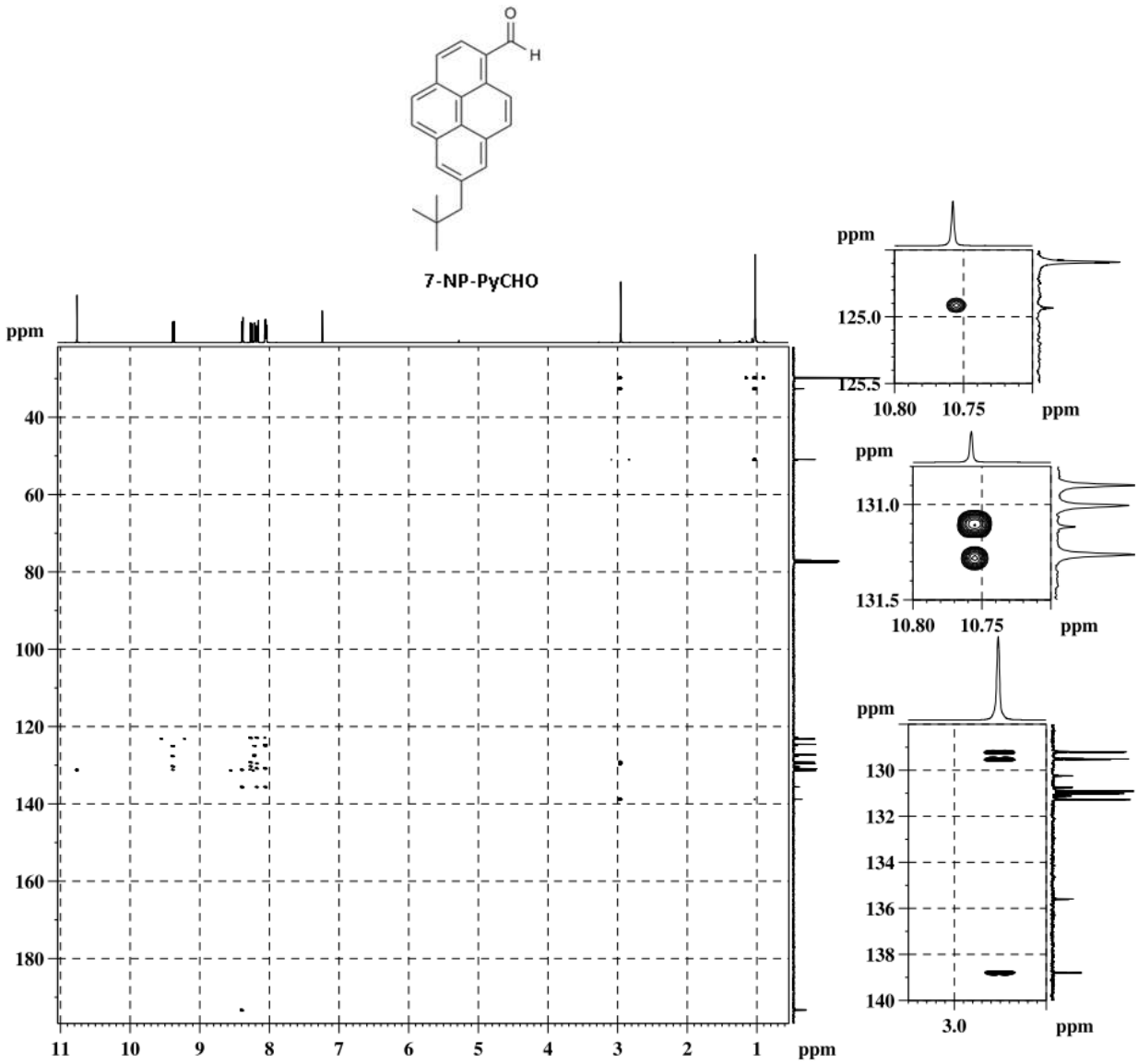
7-NP-PyCHO
ppm
40
60
80
100
120
140
160
180
11
10
9
8
7
6
5
4
3
2
1
ppm
ppm
125.0
125.5
10.80
10.75
ppm
ppm
131.0
131.5
10.80
10.75
ppm
ppm
130
132
134
136
138
140
3.0
ppm

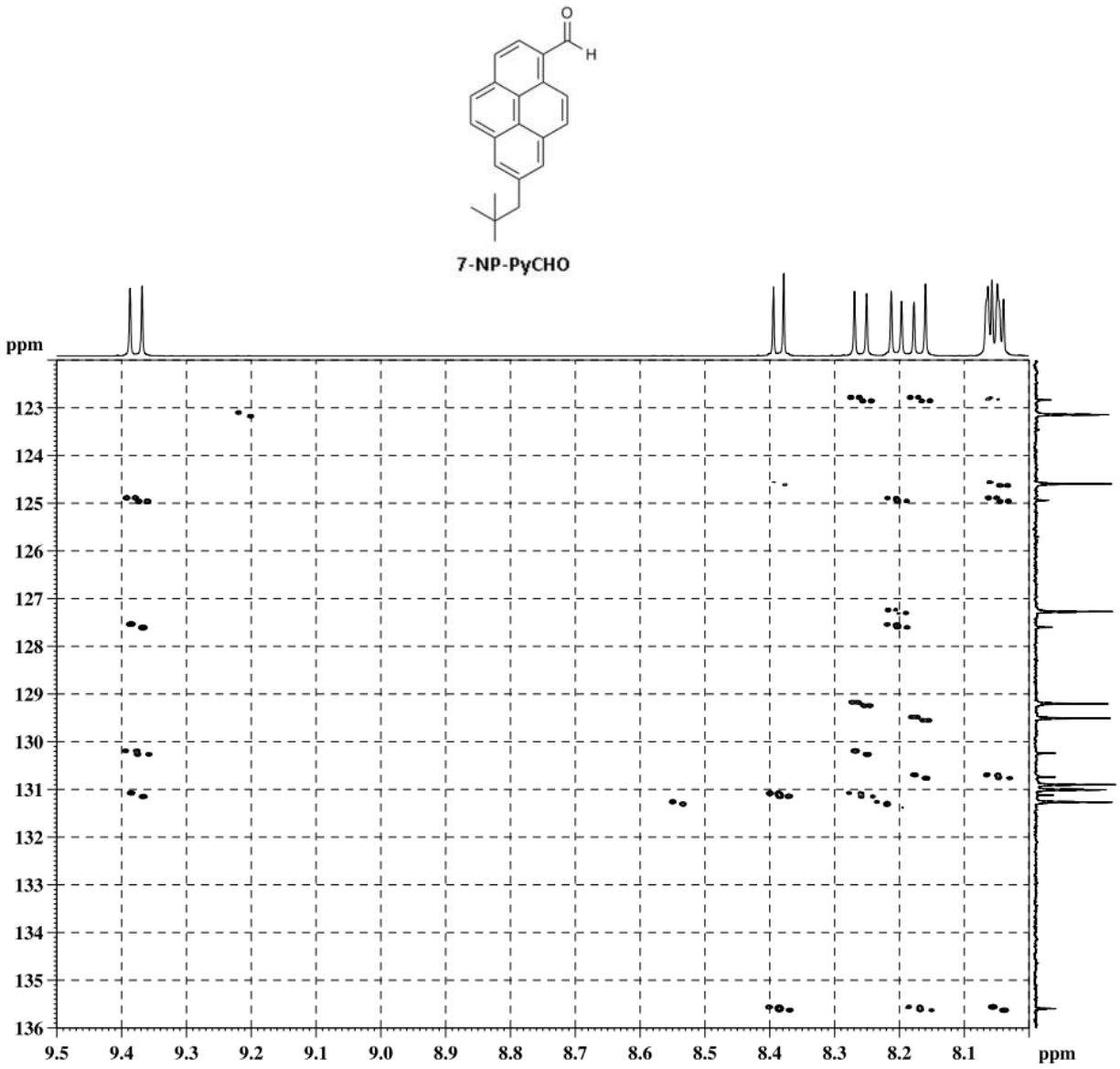
O
H
7-NP-PyCHO
ppm
123
124
125
126
127
128
129
130
131
132
133
134
135
136
9.5
9.4
9.3
9.2
9.1
9.0
8.9
8.8
8.7
8.6
8.5
8.4
8.3
8.2
8.1
ppm

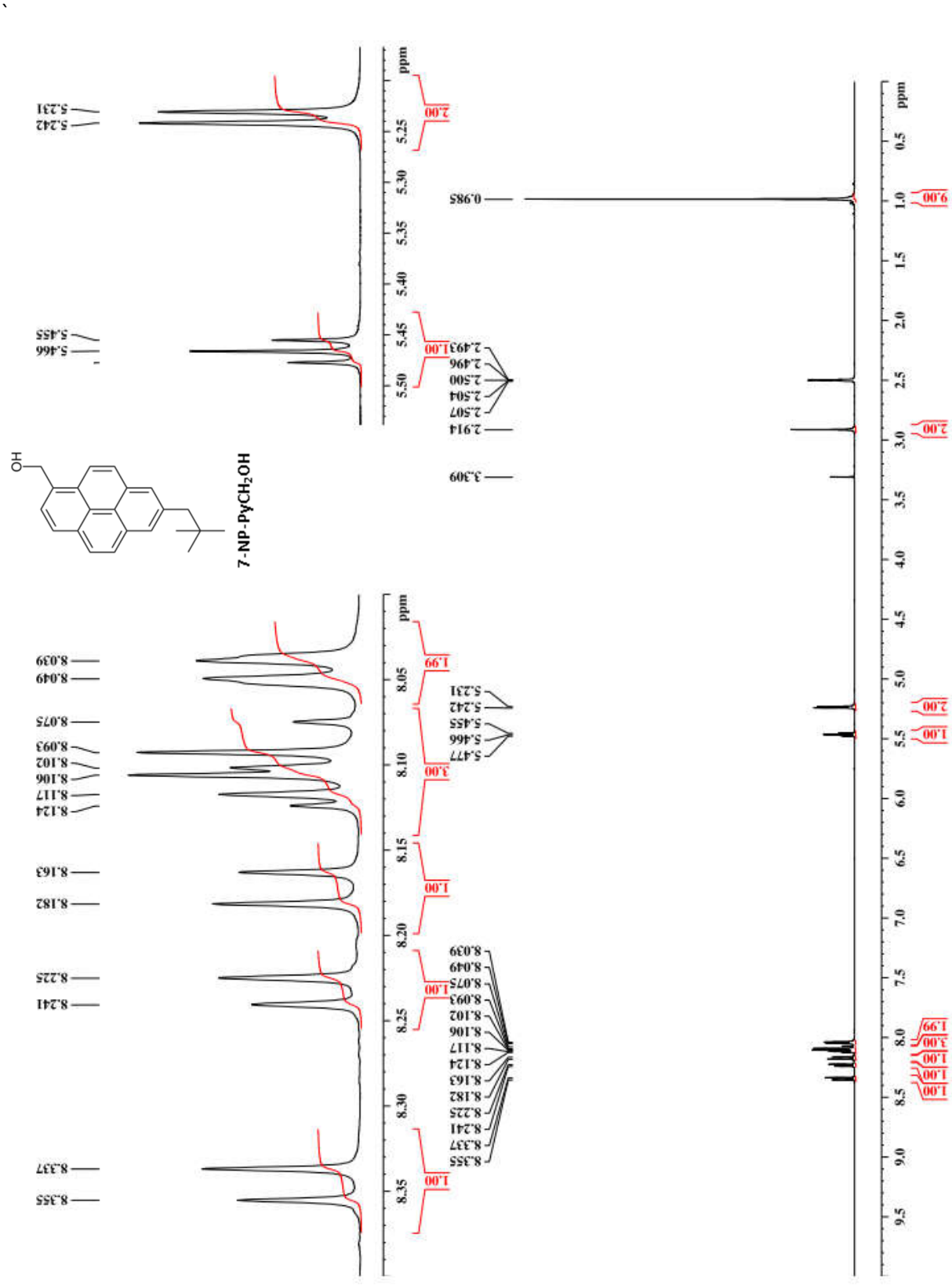
7-NP-PyCH2OH
OH
0.985
2.914
2.493
2.496
2.500
2.504
2.507
3.309
5.231
5.242
5.455
5.466
5.477
8.039
8.049
8.075
8.093
8.102
8.106
8.117
8.124
8.163
8.182
8.225
8.241
8.337
8.355
ppm

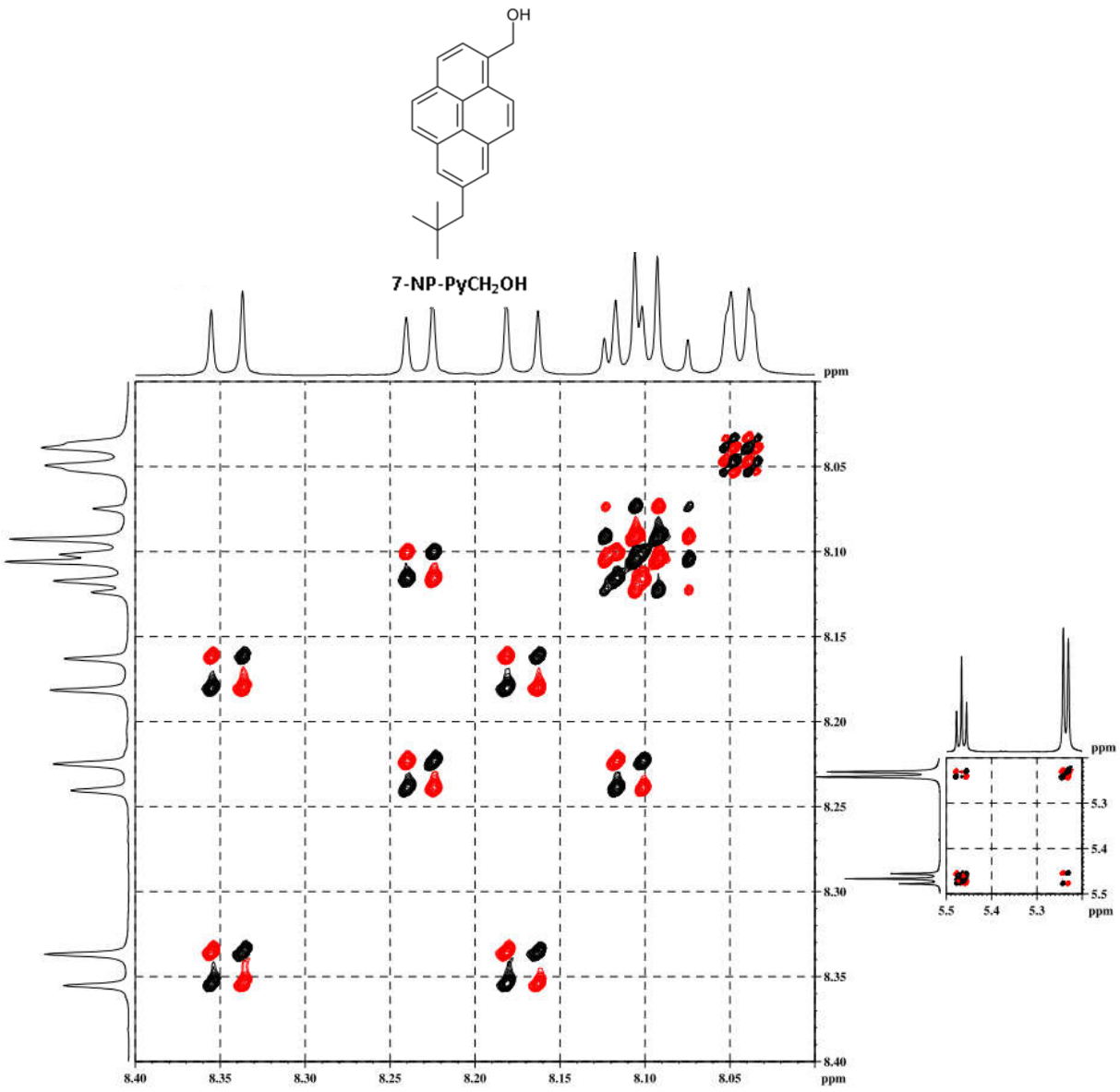
OH
7-NP-PyCH2OH
ppm
8.05
8.10
8.15
8.20
8.25
8.30
8.35
8.40
ppm
5.3
5.4
5.5
ppm

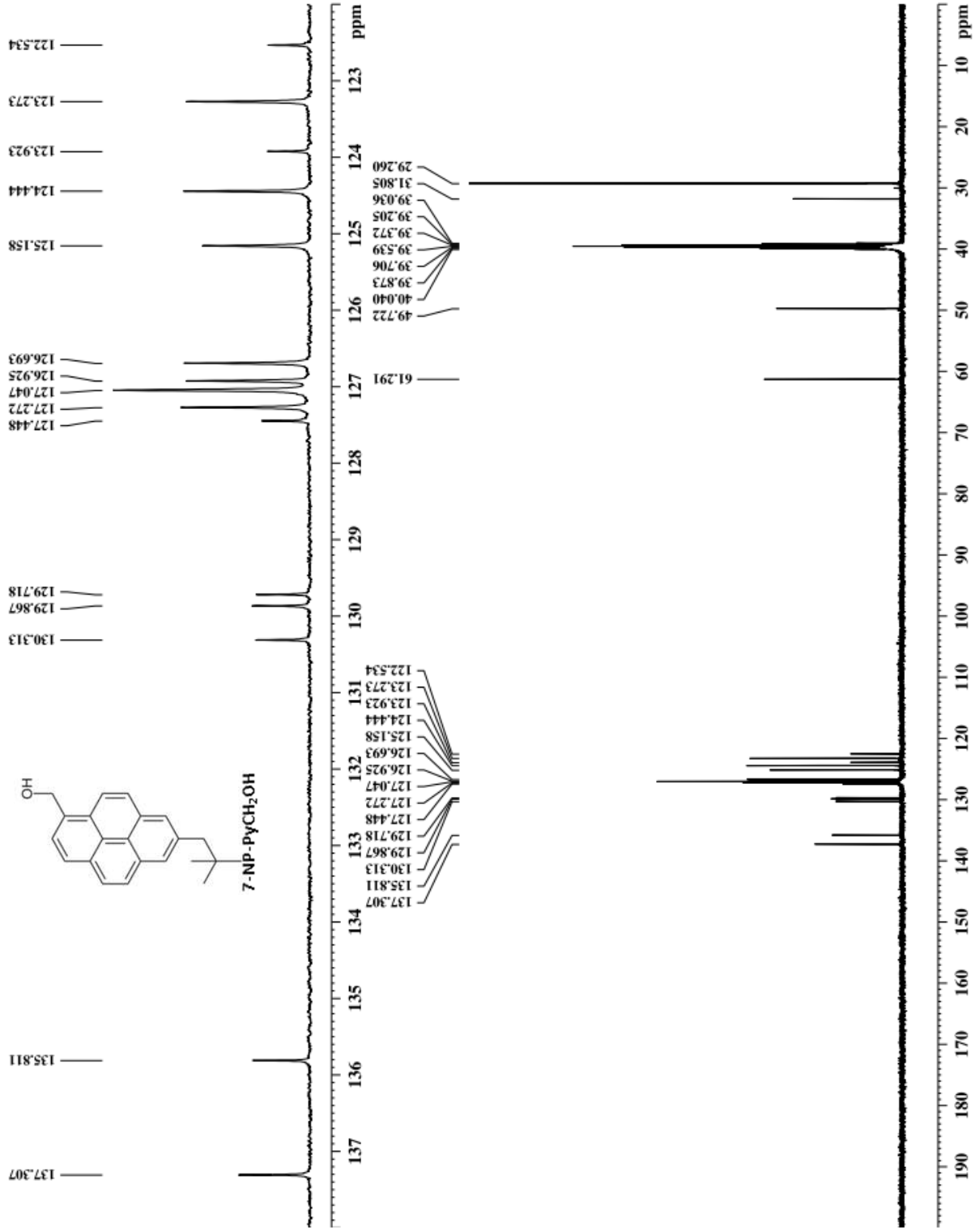
7-NP-PyCH2OH
OH
137.307
135.811
130.313
129.867
129.718
127.448
127.272
127.047
126.925
126.693
125.158
124.444
123.923
123.273
122.534
61.291
49.722
40.040
39.873
39.706
39.539
39.372
39.205
39.036
31.805
29.260
ppm

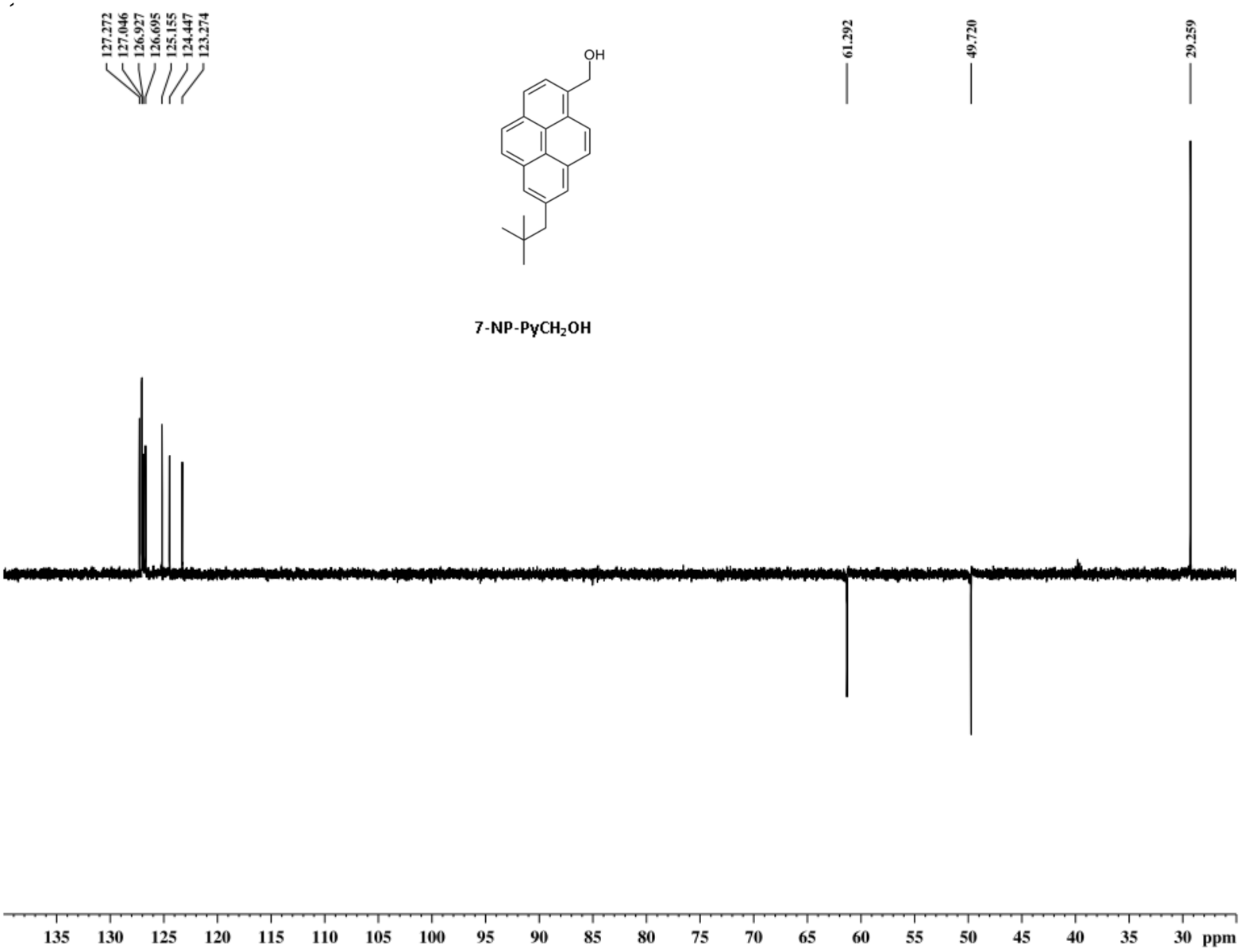
127.272
127.046
126.927
126.695
125.155
124.447
123.274
OH
61.292
49.720
29.259
7-NP-PyCH2OH
135 130 125 120 115 110 105 100 95 90 85 80 75 70 65 60 55 50 45 40 35 30 ppm

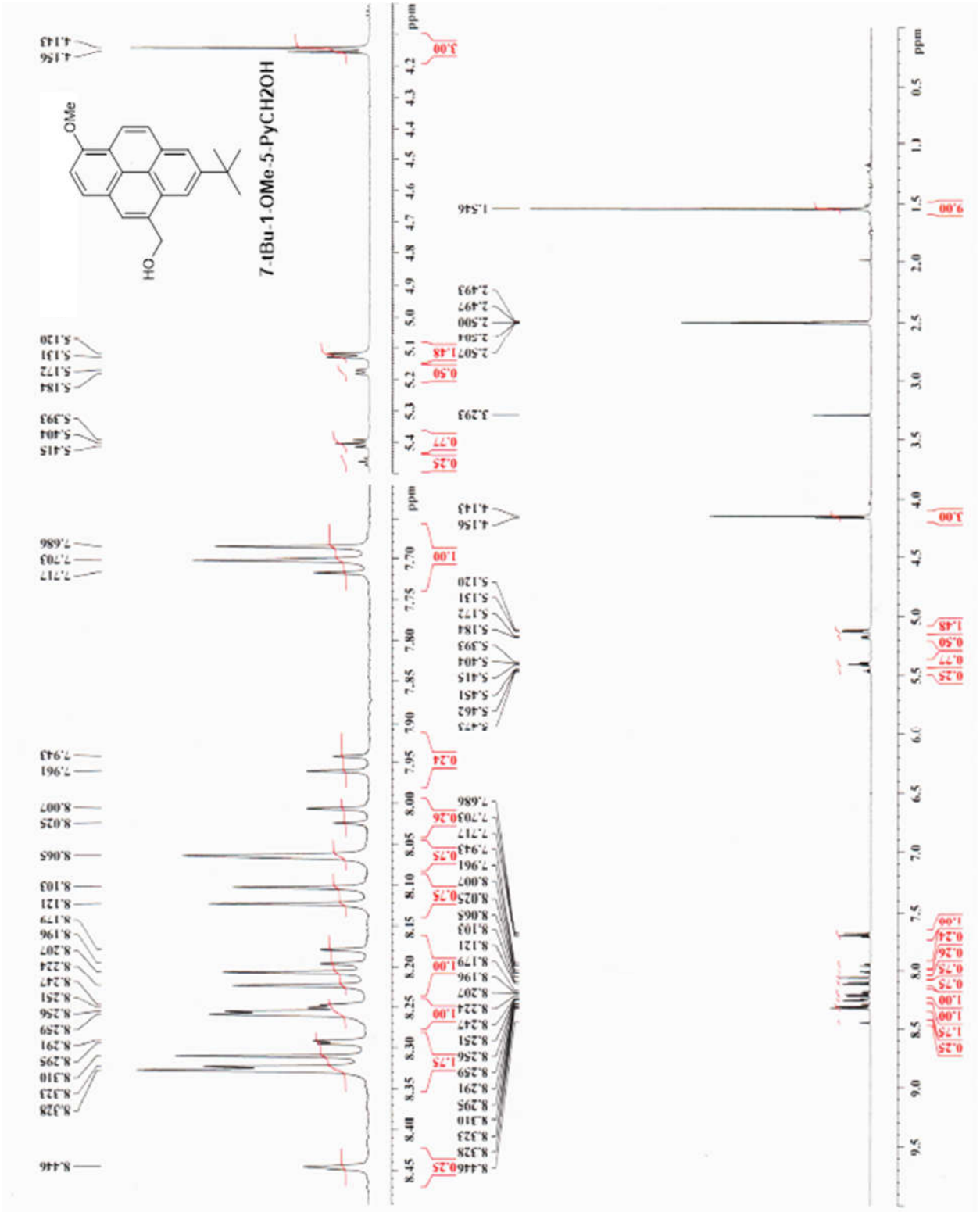
7-tBu-1-OMe-5-PyCH2OH
OMe
HO

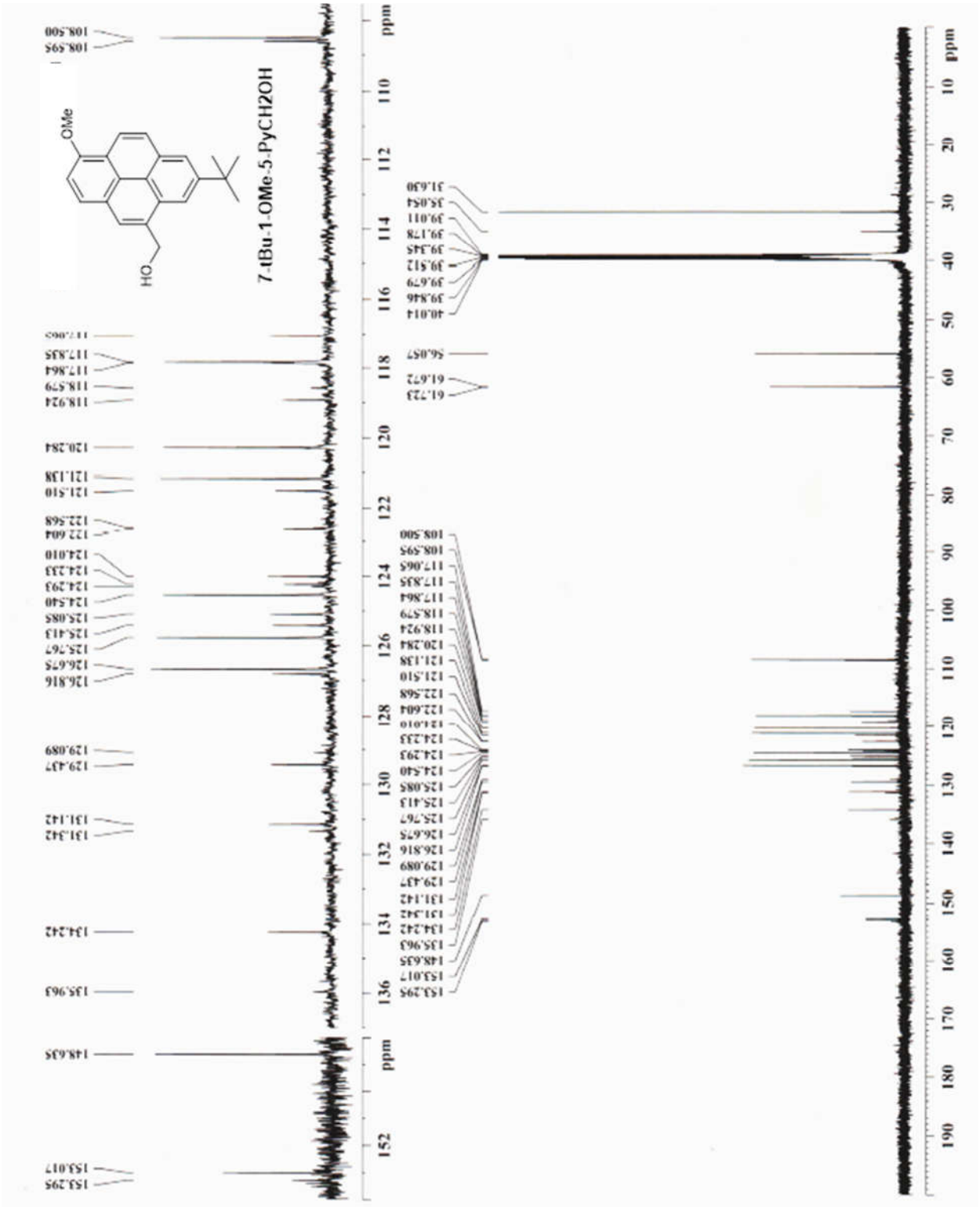
7-tBu-1-OMe-5-PyCH2OH
OMe
HO
ppm

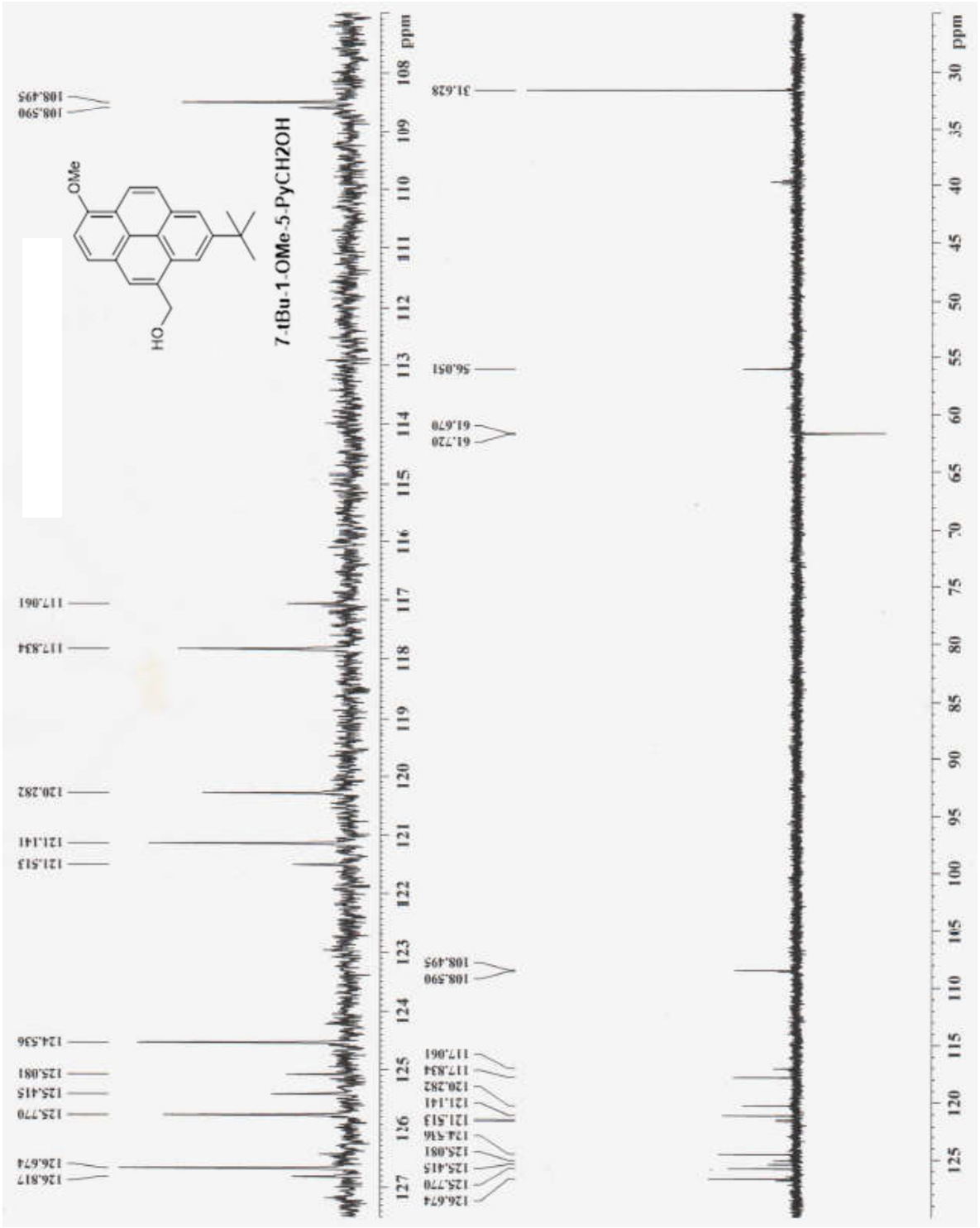
7-tBu-1-OMe-5-PyCH2OH
OMe
HO
108.590
108.495
117.061
117.834
120.282
121.141
121.513
124.536
125.081
125.415
125.770
126.817
126.674
31.628
56.051
61.720
61.670
ppm

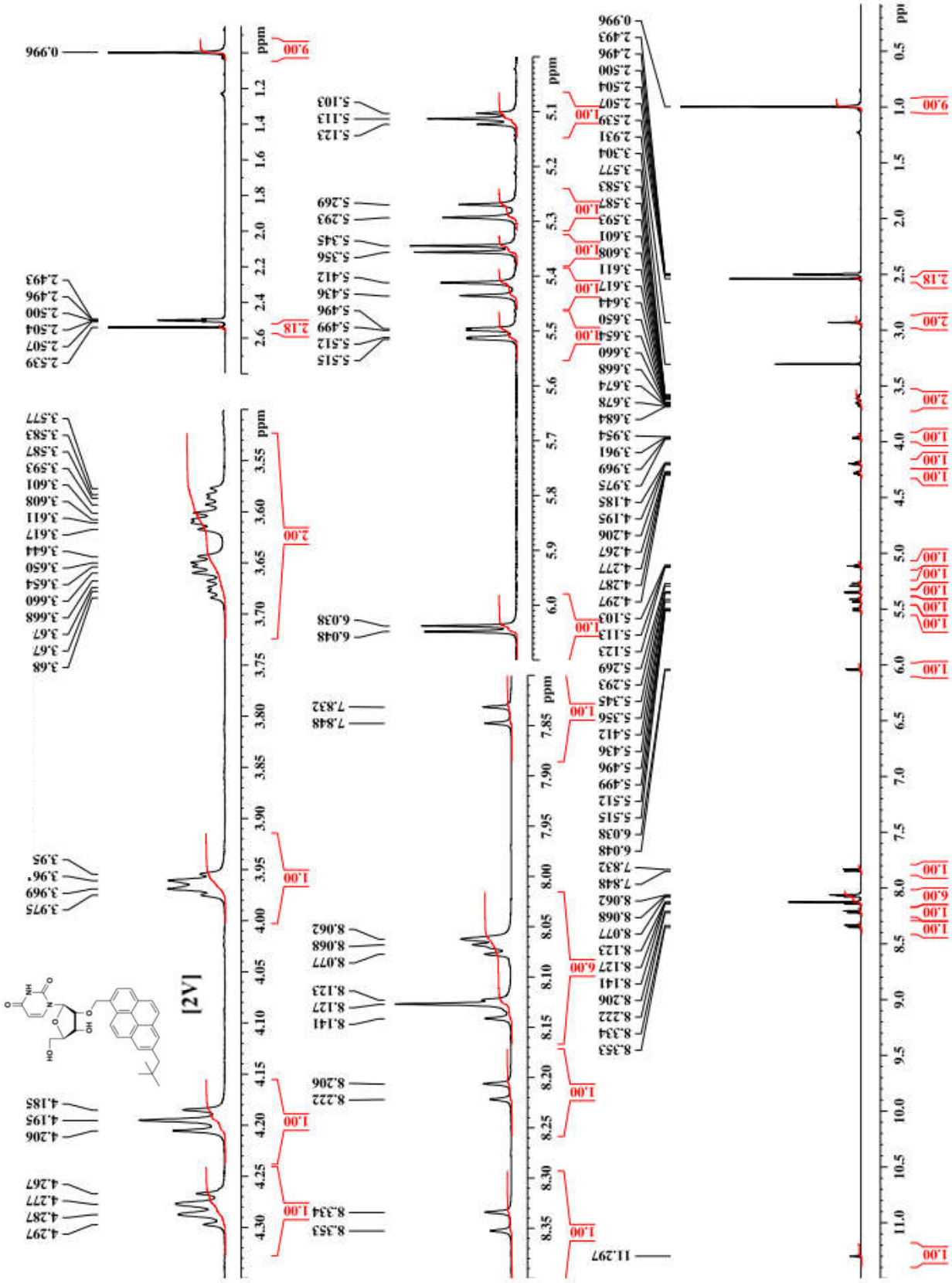
[2V]

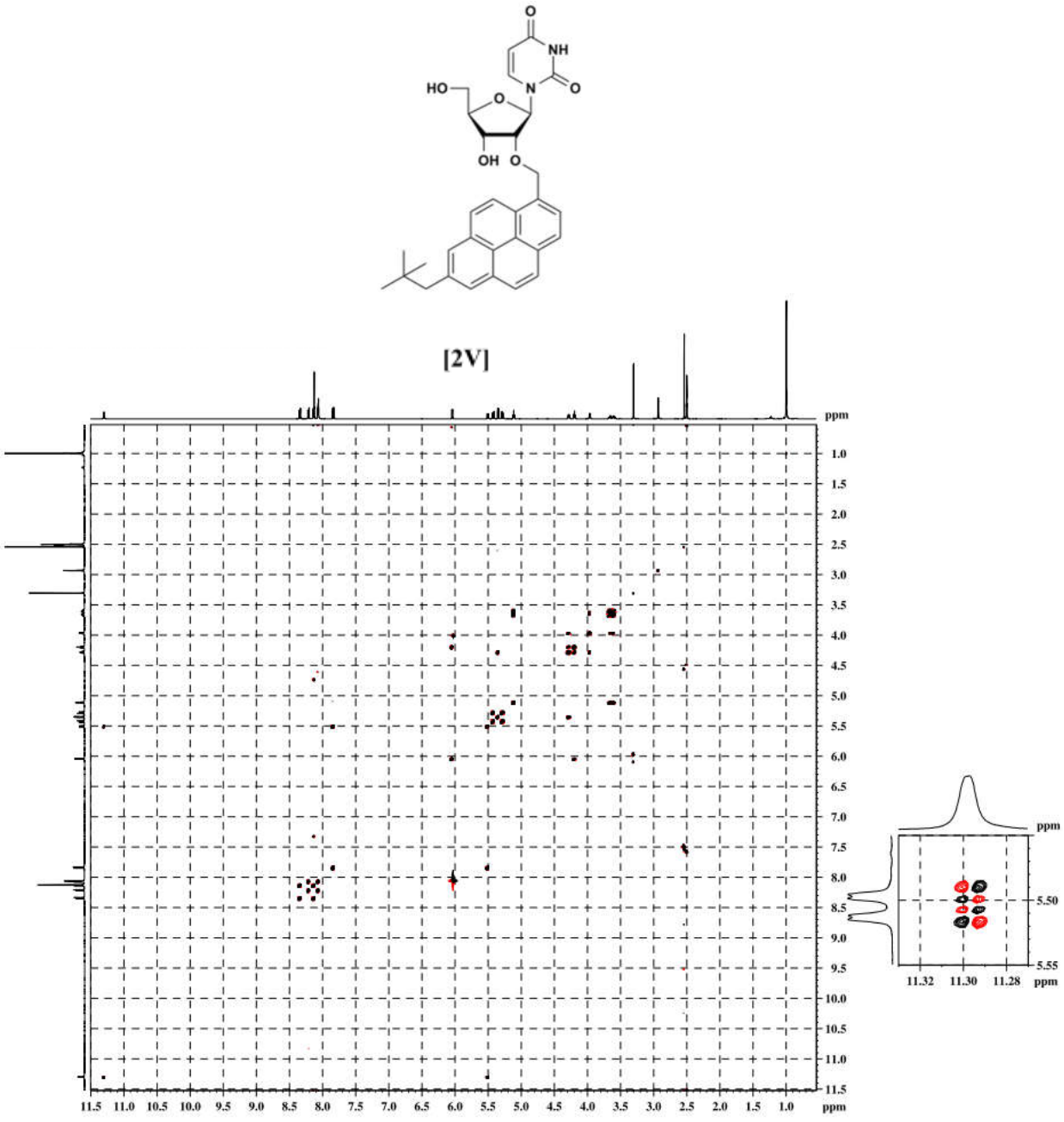
[2V]
ppm
11.5 11.0 10.5 10.0 9.5 9.0 8.5 8.0 7.5 7.0 6.5 6.0 5.5 5.0 4.5 4.0 3.5 3.0 2.5 2.0 1.5 1.0
11.32 11.30 11.28 ppm
5.50
5.55

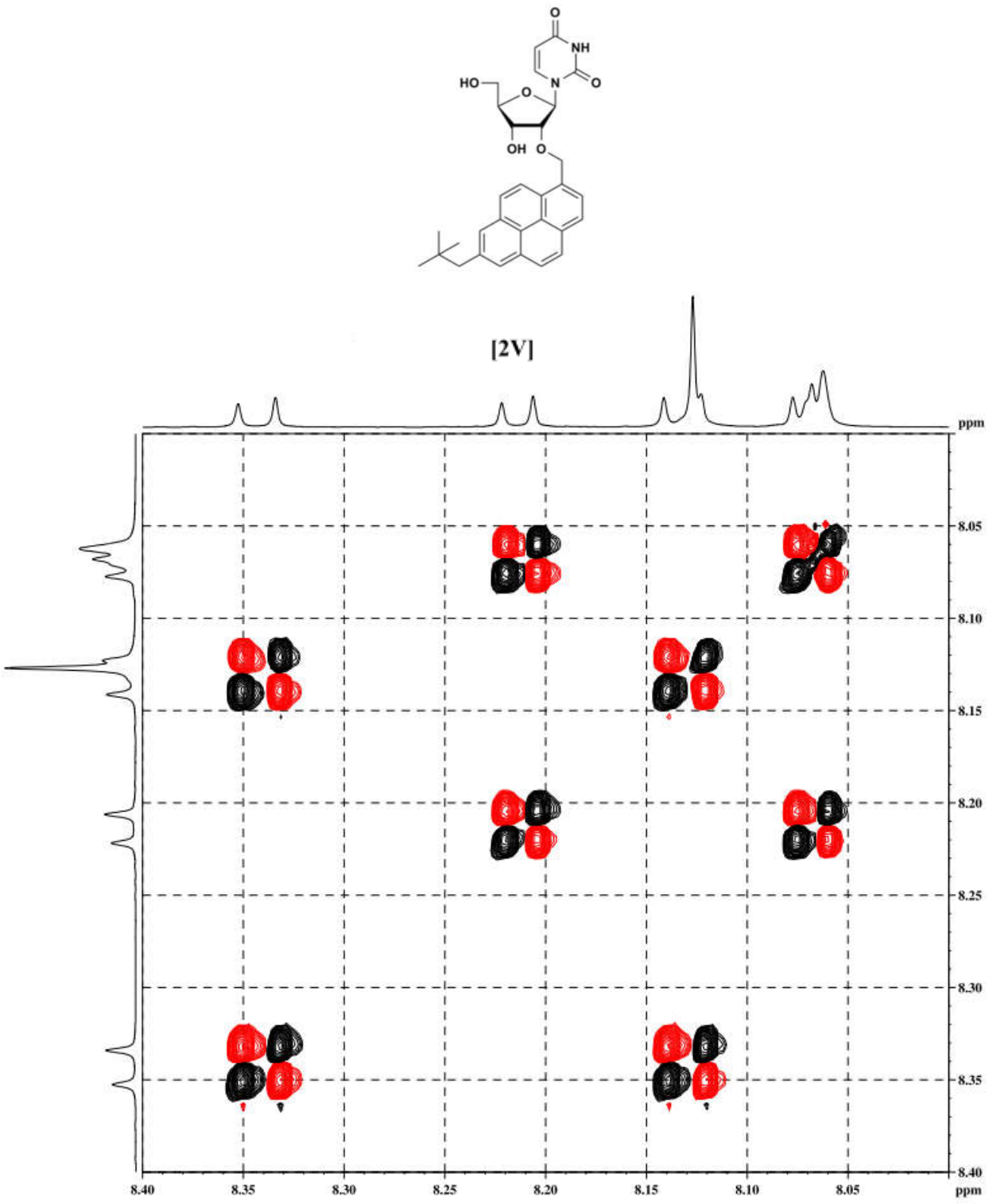
[2V]
ppm
8.05
8.10
8.15
8.20
8.25
8.30
8.35
8.40
8.40
8.35
8.30
8.25
8.20
8.15
8.10
8.05
ppm

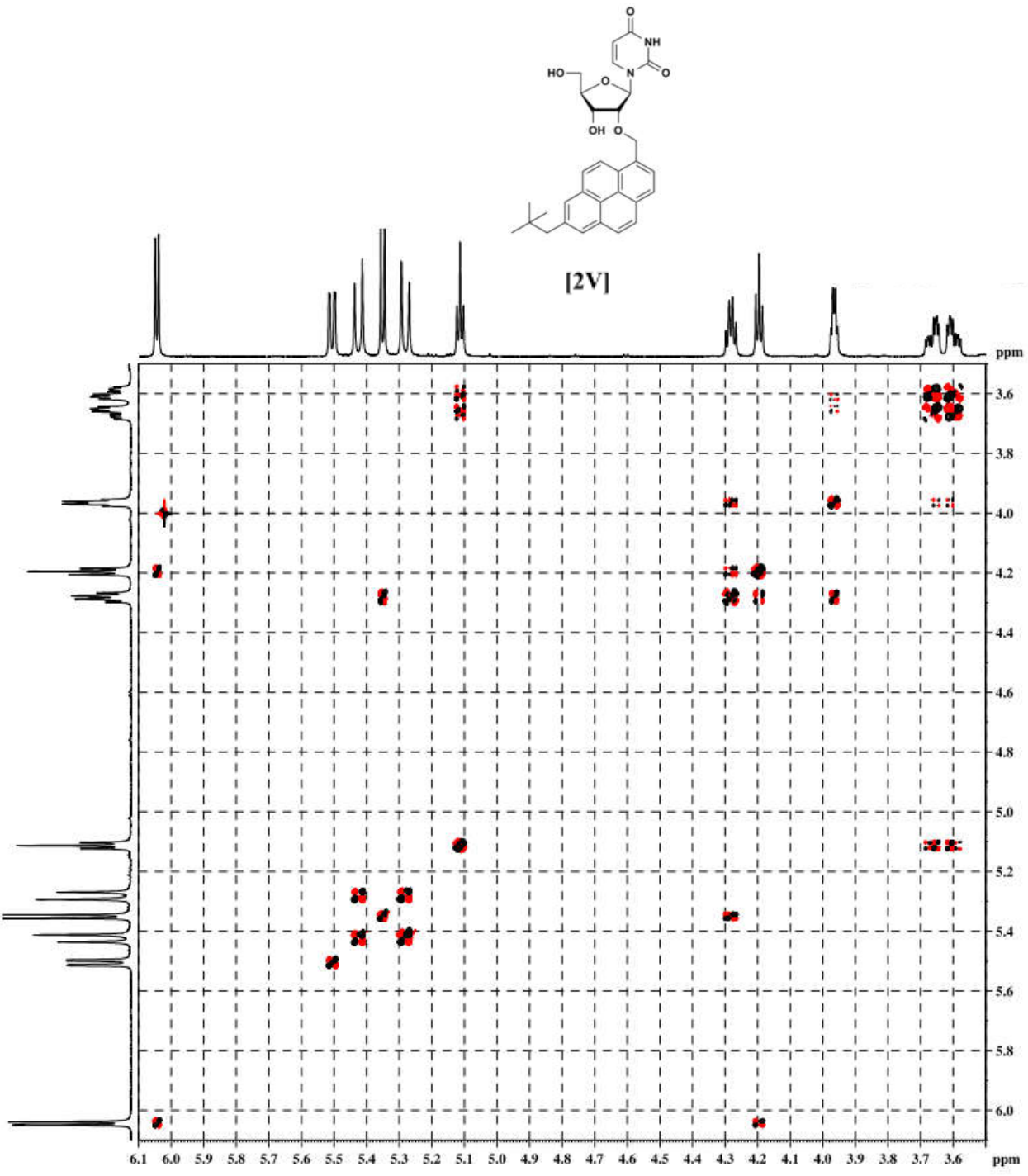
[2V]
ppm
6.1 6.0 5.9 5.8 5.7 5.6 5.5 5.4 5.3 5.2 5.1 5.0 4.9 4.8 4.7 4.6 4.5 4.4 4.3 4.2 4.1 4.0 3.9 3.8 3.7 3.6 ppm
3.6 3.8 4.0 4.2 4.4 4.6 4.8 5.0 5.2 5.4 5.6 5.8 6.0

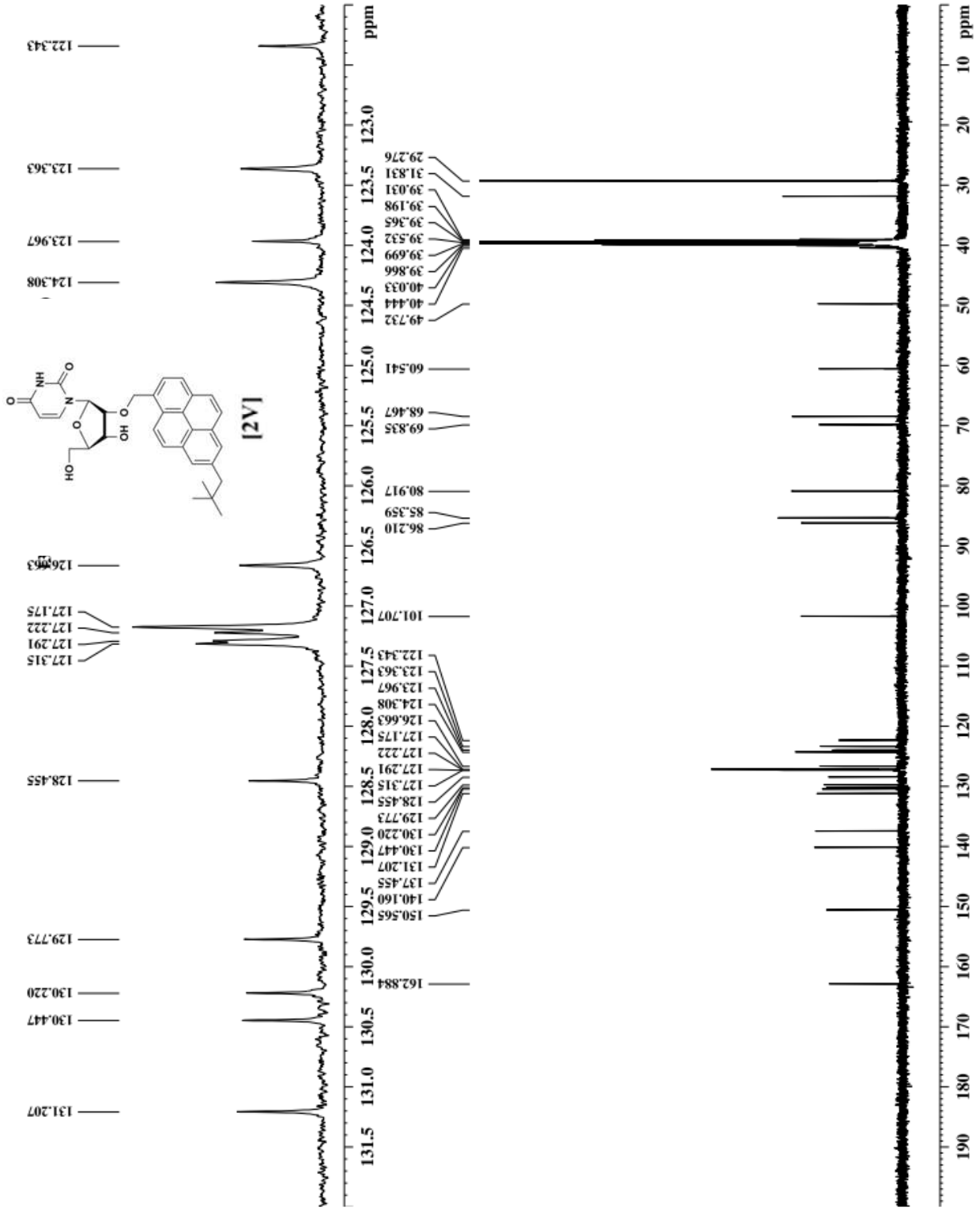
[2V]

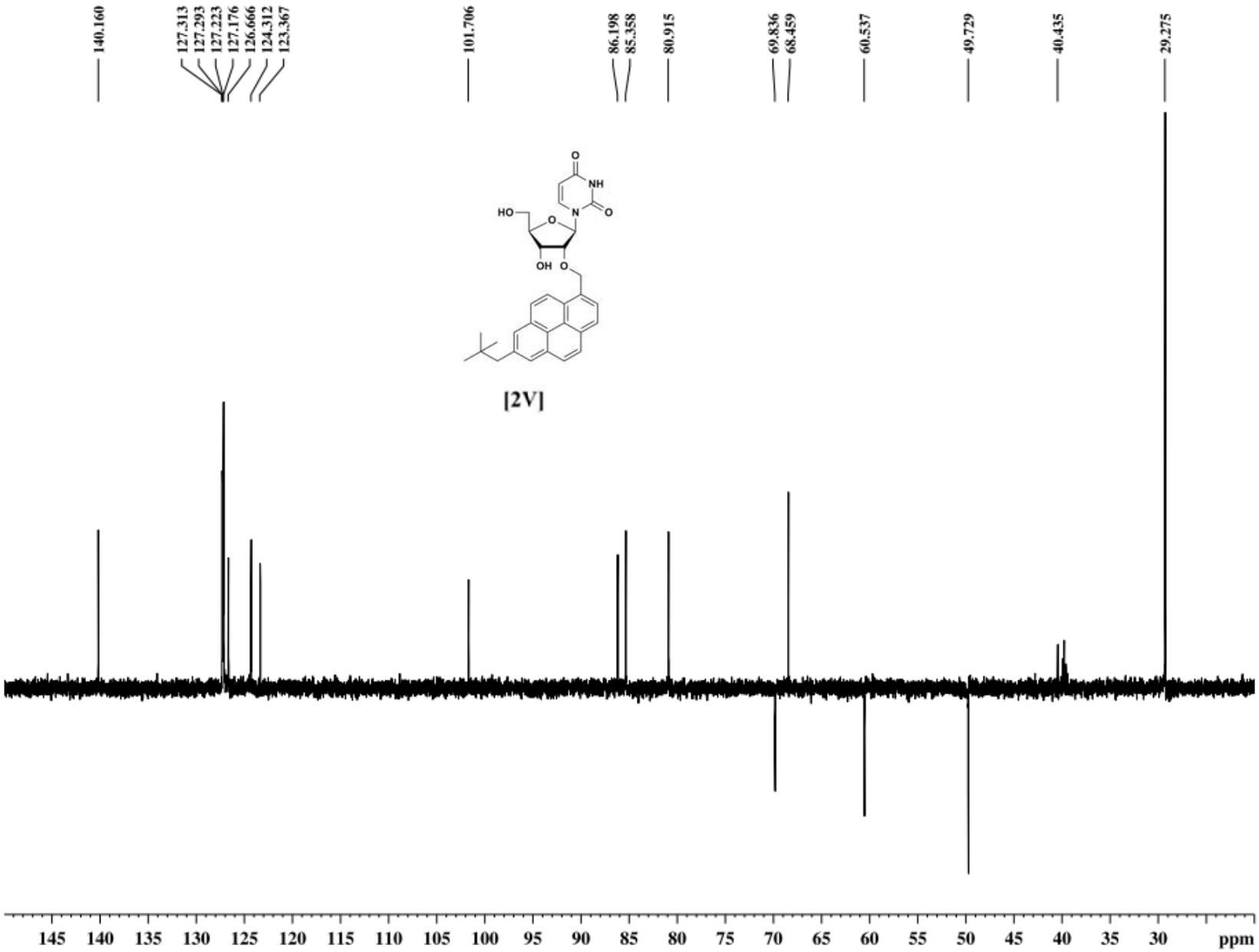
140.160
127.313
127.293
127.223
127.176
126.666
124.312
123.367
101.706
86.198
85.358
80.915
69.836
68.459
60.537
49.729
40.435
29.275
HO
O
NH
N
O
OH
O
[2V]
145 140 135 130 125 120 115 110 105 100 95 90 85 80 75 70 65 60 55 50 45 40 35 30 ppm

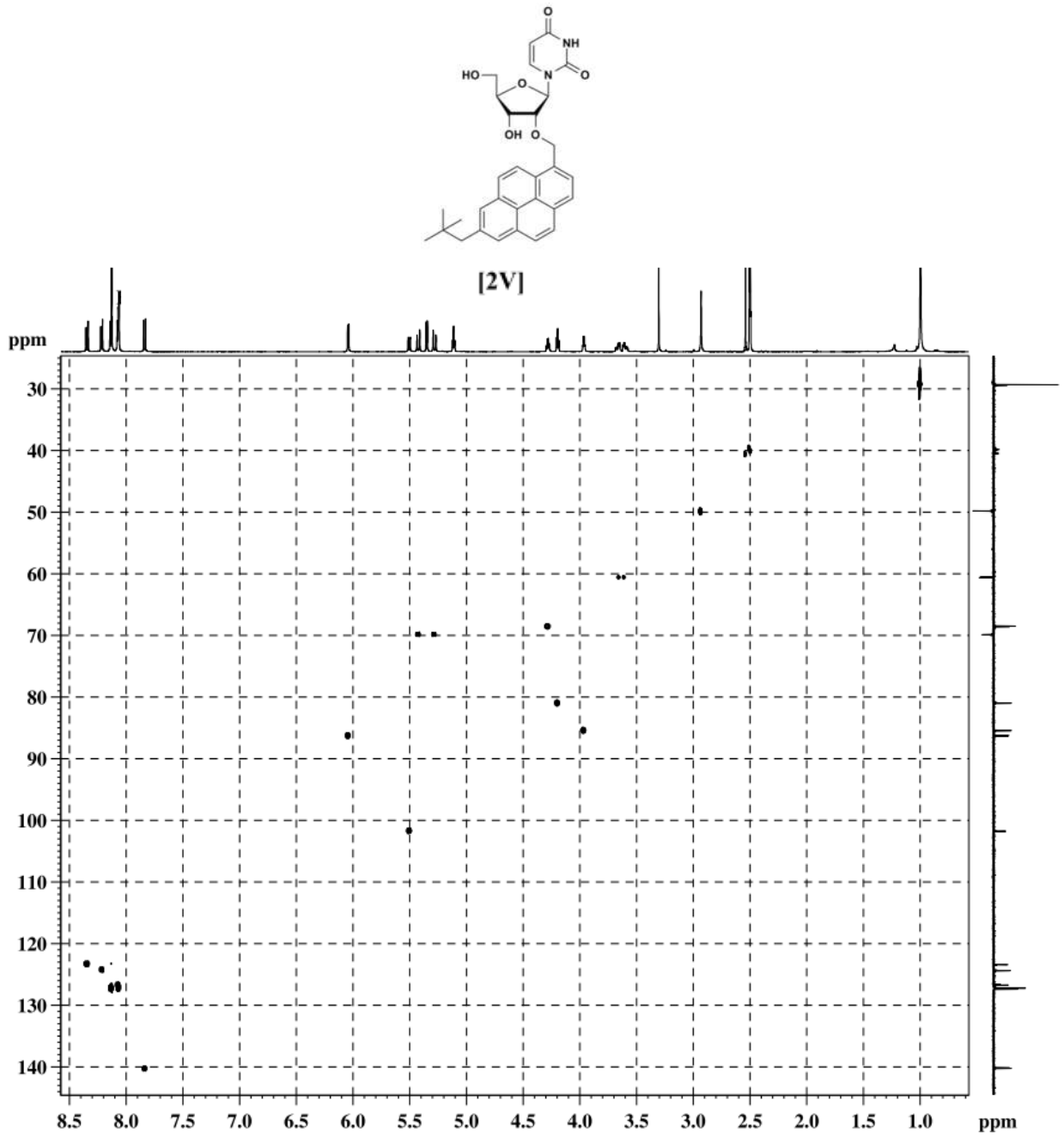
[2V]
ppm
30
40
50
60
70
80
90
100
110
120
130
140
8.5
8.0
7.5
7.0
6.5
6.0
5.5
5.0
4.5
4.0
3.5
3.0
2.5
2.0
1.5
1.0
ppm

`

`

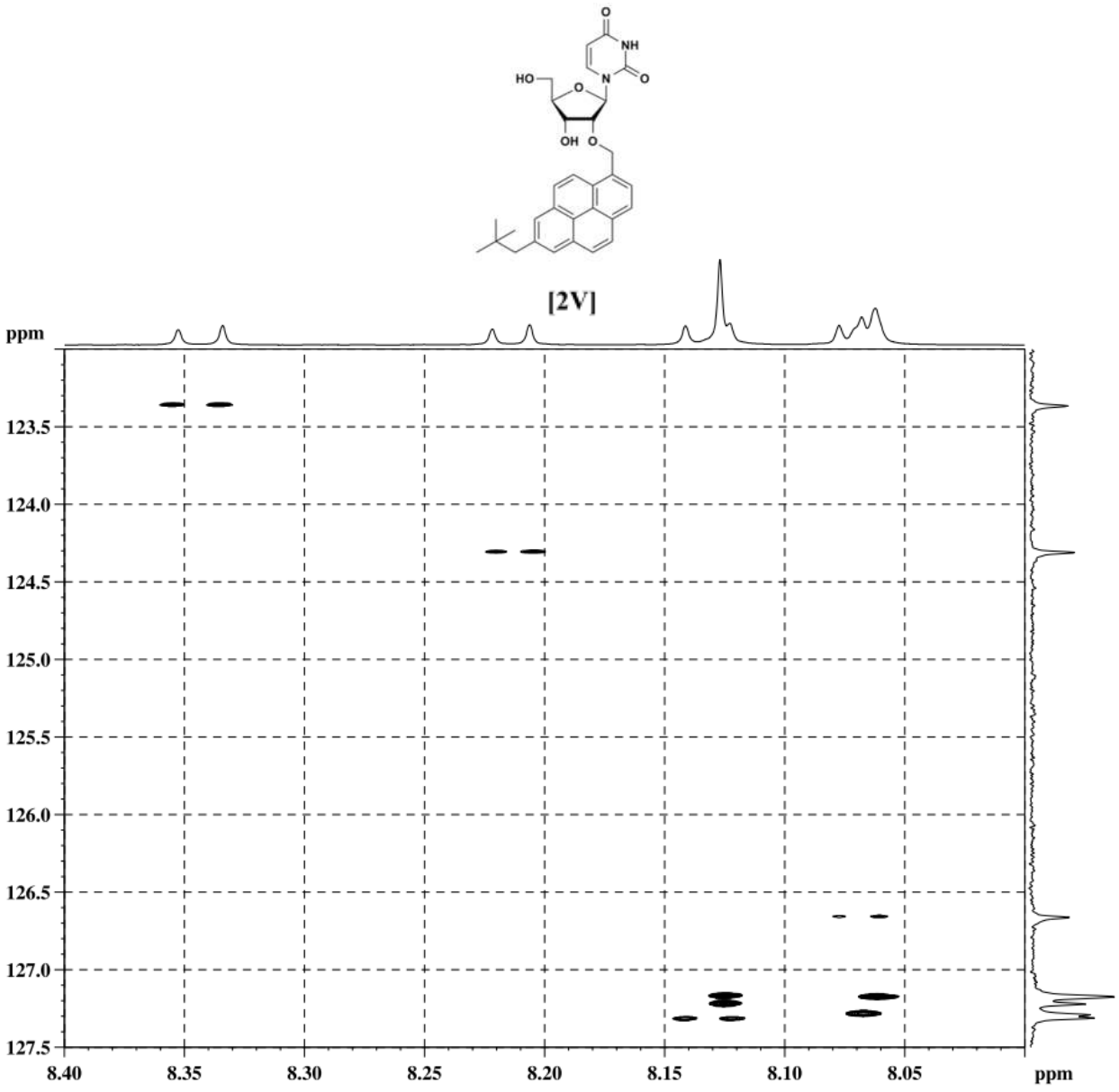
[2V]
ppm
123.5
124.0
124.5
125.0
125.5
126.0
126.5
127.0
127.5
8.40
8.35
8.30
8.25
8.20
8.15
8.10
8.05
ppm

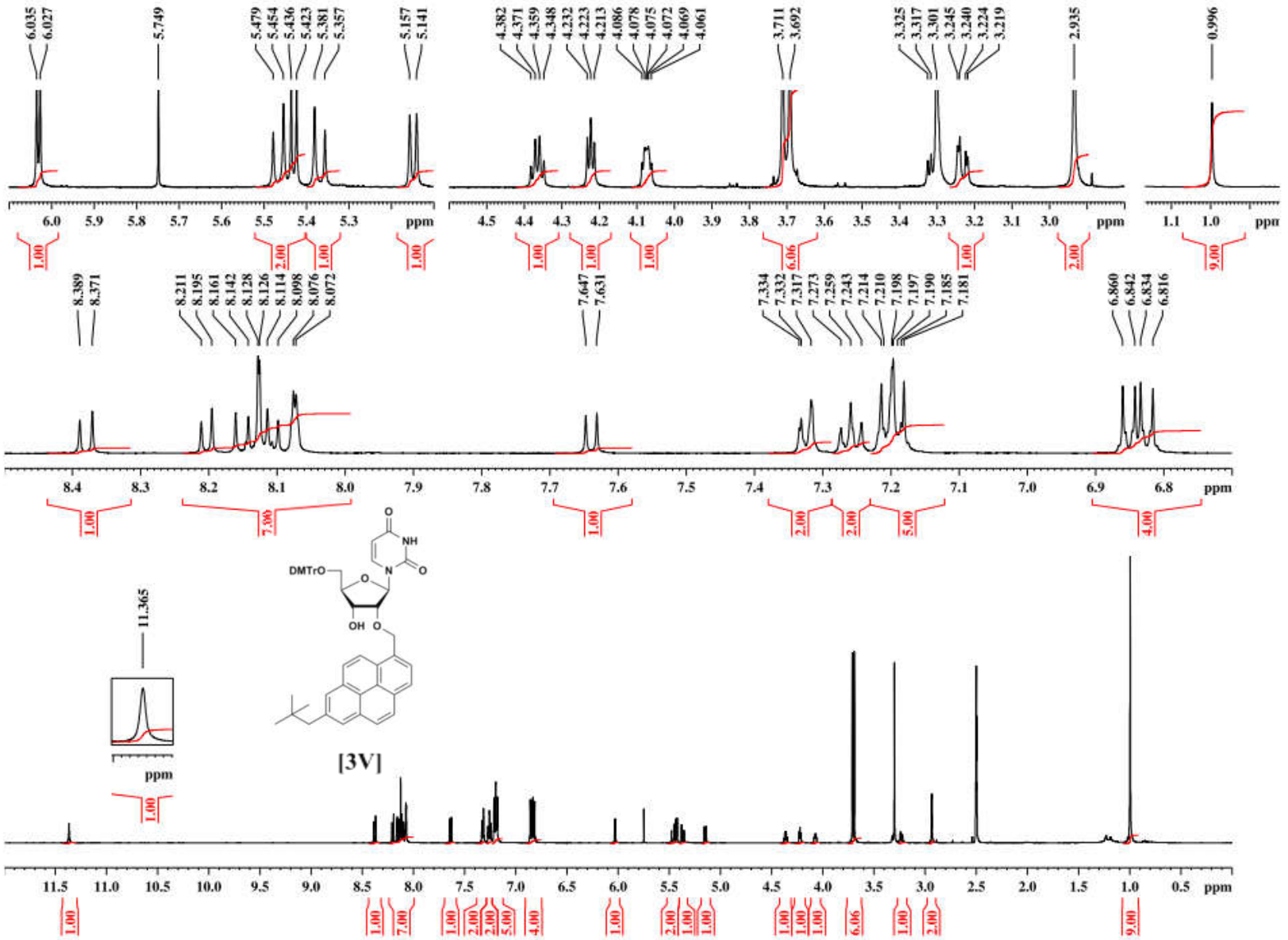
6.035
6.027
5.749
5.479
5.454
5.436
5.423
5.381
5.357
5.157
5.141
4.382
4.371
4.359
4.348
4.232
4.223
4.213
4.086
4.078
4.075
4.072
4.069
4.061
3.711
3.692
3.325
3.317
3.301
3.245
3.240
3.224
3.219
2.935
0.996
8.389
8.371
8.211
8.195
8.161
8.142
8.128
8.126
8.114
8.098
8.076
8.072
7.647
7.631
7.334
7.332
7.317
7.273
7.259
7.243
7.214
7.210
7.198
7.197
7.190
7.185
7.181
6.860
6.842
6.834
6.816
11.365
ppm
DMTrO
NH
N
O
OH
[3V]

`

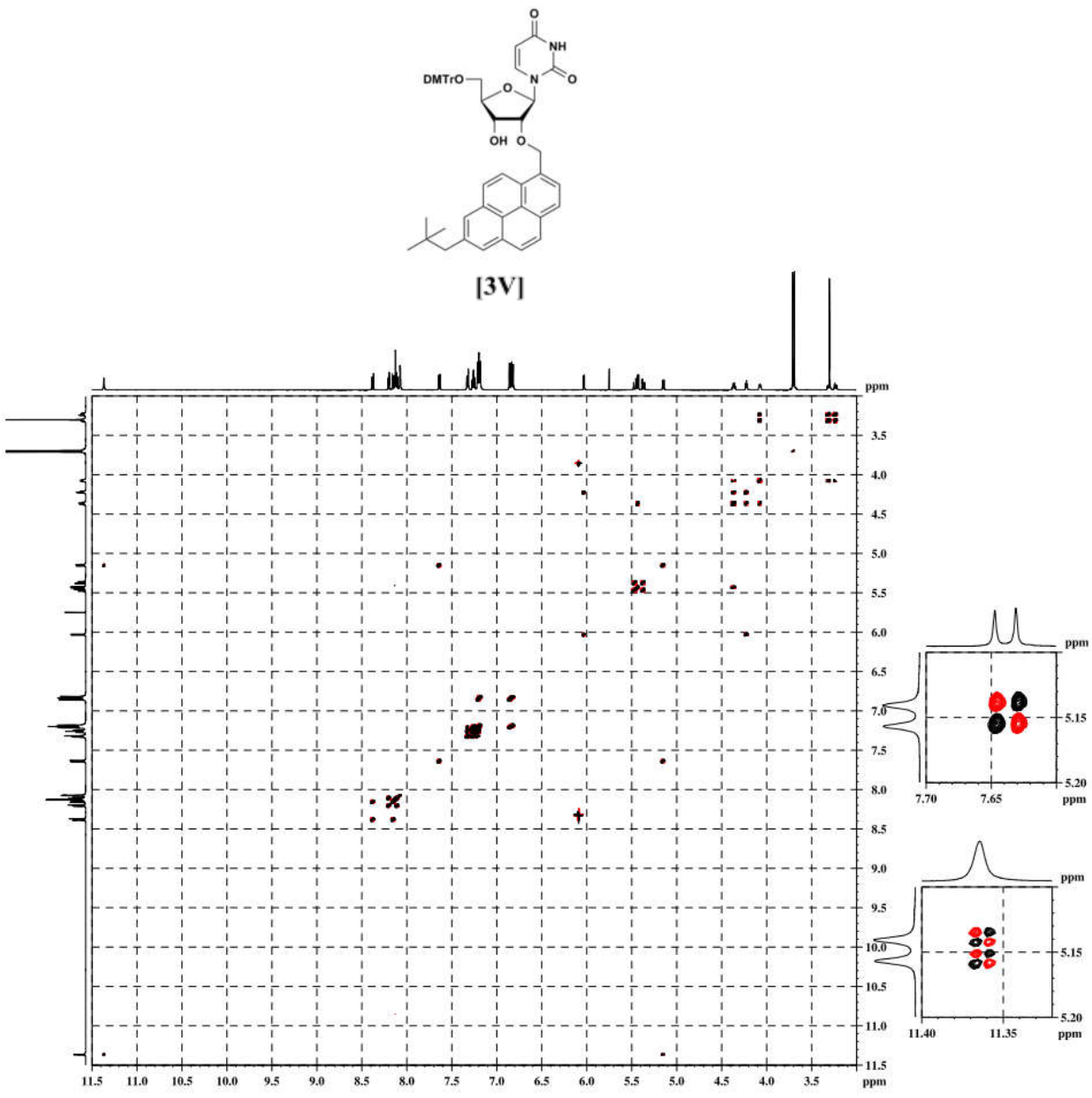
DMTrO
O
NH
N
O
OH
O
[3V]
ppm
11.5 11.0 10.5 10.0 9.5 9.0 8.5 8.0 7.5 7.0 6.5 6.0 5.5 5.0 4.5 4.0 3.5
7.70 7.65
5.15 5.20
11.40 11.35

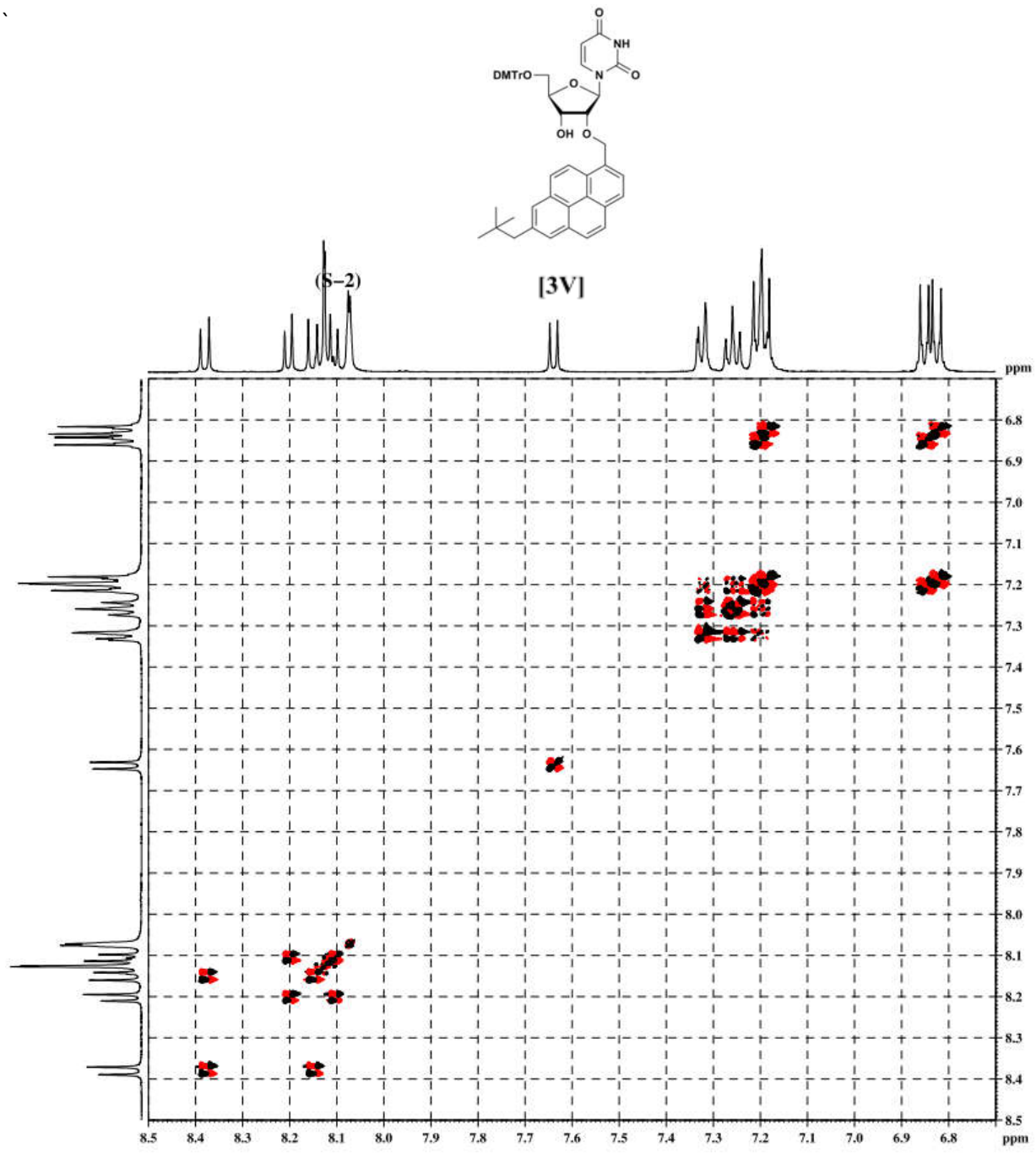
DMTrO
O
NH
N
O
OH
O
(S-2)
[3V]
ppm
6.8
6.9
7.0
7.1
7.2
7.3
7.4
7.5
7.6
7.7
7.8
7.9
8.0
8.1
8.2
8.3
8.4
8.5
8.5
8.4
8.3
8.2
8.1
8.0
7.9
7.8
7.7
7.6
7.5
7.4
7.3
7.2
7.1
7.0
6.9
6.8
ppm

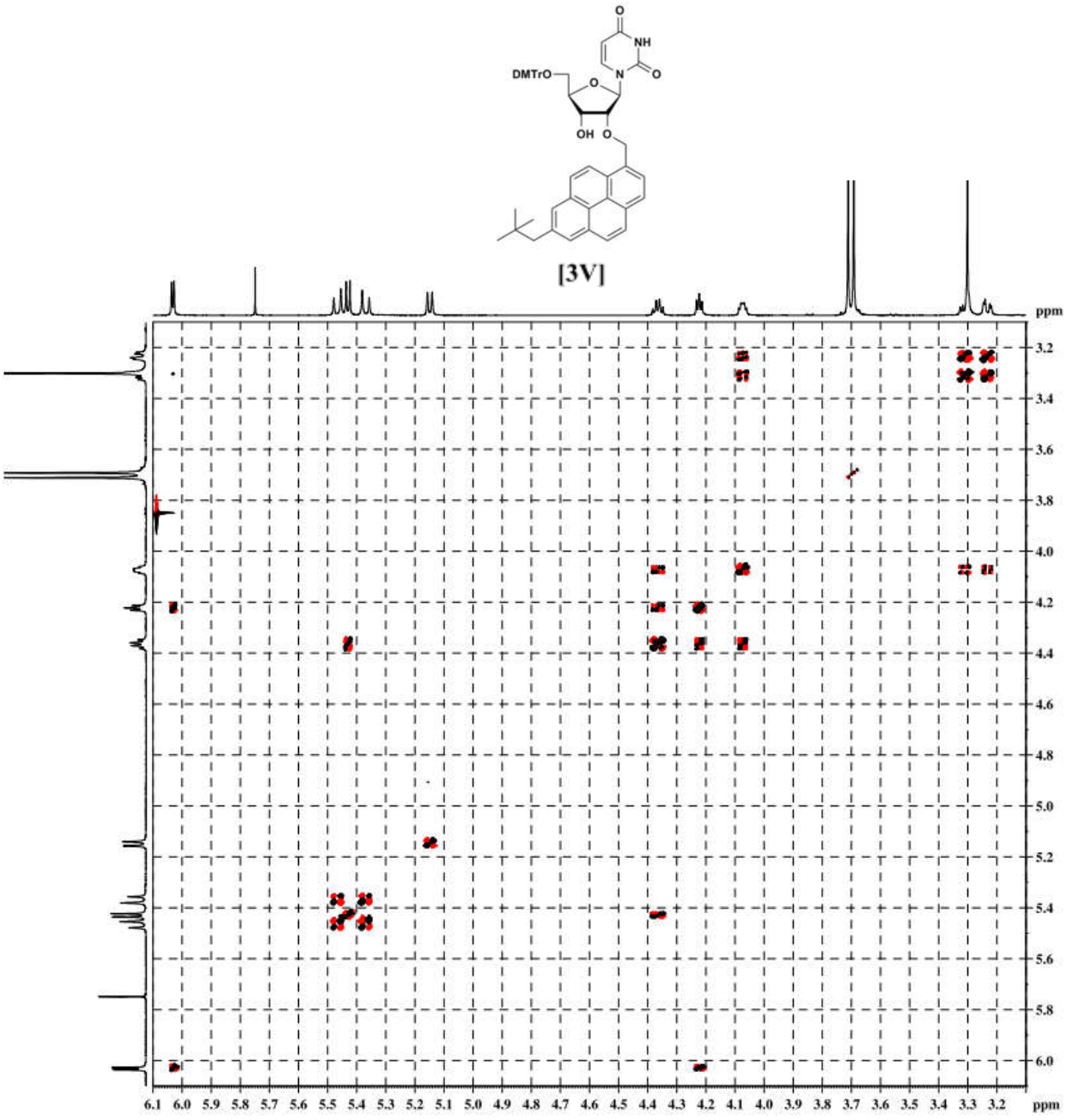
DMTrO
NH
O
N
OH
[3V]
ppm
3.2
3.4
3.6
3.8
4.0
4.2
4.4
4.6
4.8
5.0
5.2
5.4
5.6
5.8
6.0
6.1 6.0 5.9 5.8 5.7 5.6 5.5 5.4 5.3 5.2 5.1 5.0 4.9 4.8 4.7 4.6 4.5 4.4 4.3 4.2 4.1 4.0 3.9 3.8 3.7 3.6 3.5 3.4 3.3 3.2
ppm

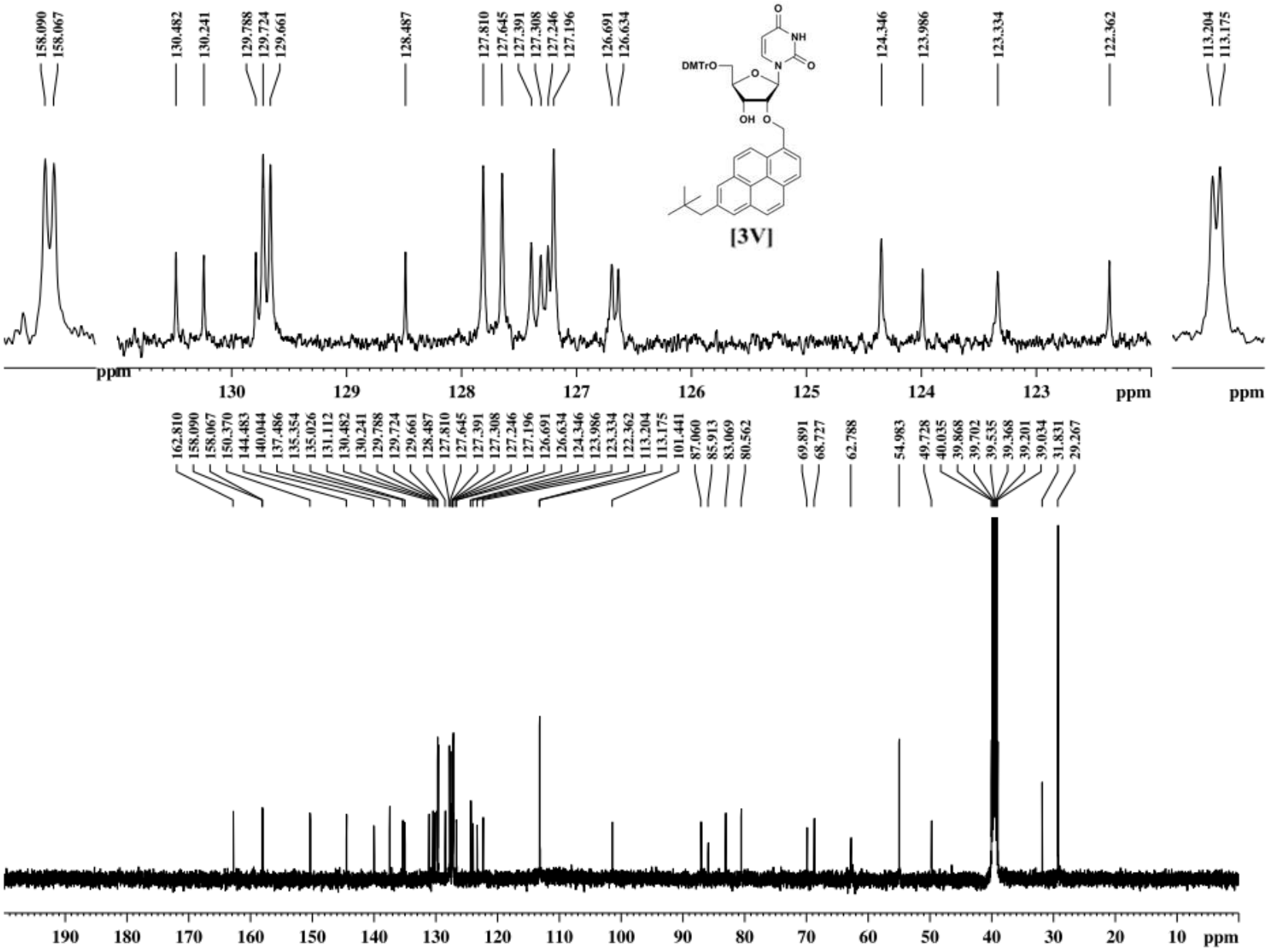
158.090
158.067
130.482
130.241
129.788
129.724
129.661
128.487
127.810
127.645
127.391
127.308
127.246
127.196
126.691
126.634
124.346
123.986
123.334
122.362
113.204
113.175
DMTrO
NH
OH
[3V]
ppm
130
129
128
127
126
125
124
123
ppm
ppm
162.810
158.090
158.067
150.370
144.483
140.044
137.486
135.354
135.026
131.112
130.482
130.241
129.788
129.724
129.661
128.487
127.810
127.645
127.391
127.308
127.246
127.196
126.691
126.634
124.346
123.986
123.334
122.362
113.204
113.175
101.441
87.060
85.913
83.069
80.562
69.891
68.727
62.788
54.983
49.728
40.035
39.868
39.702
39.535
39.368
39.201
39.034
31.831
29.267
190
180
170
160
150
140
130
120
110
100
90
80
70
60
50
40
30
20
10
ppm

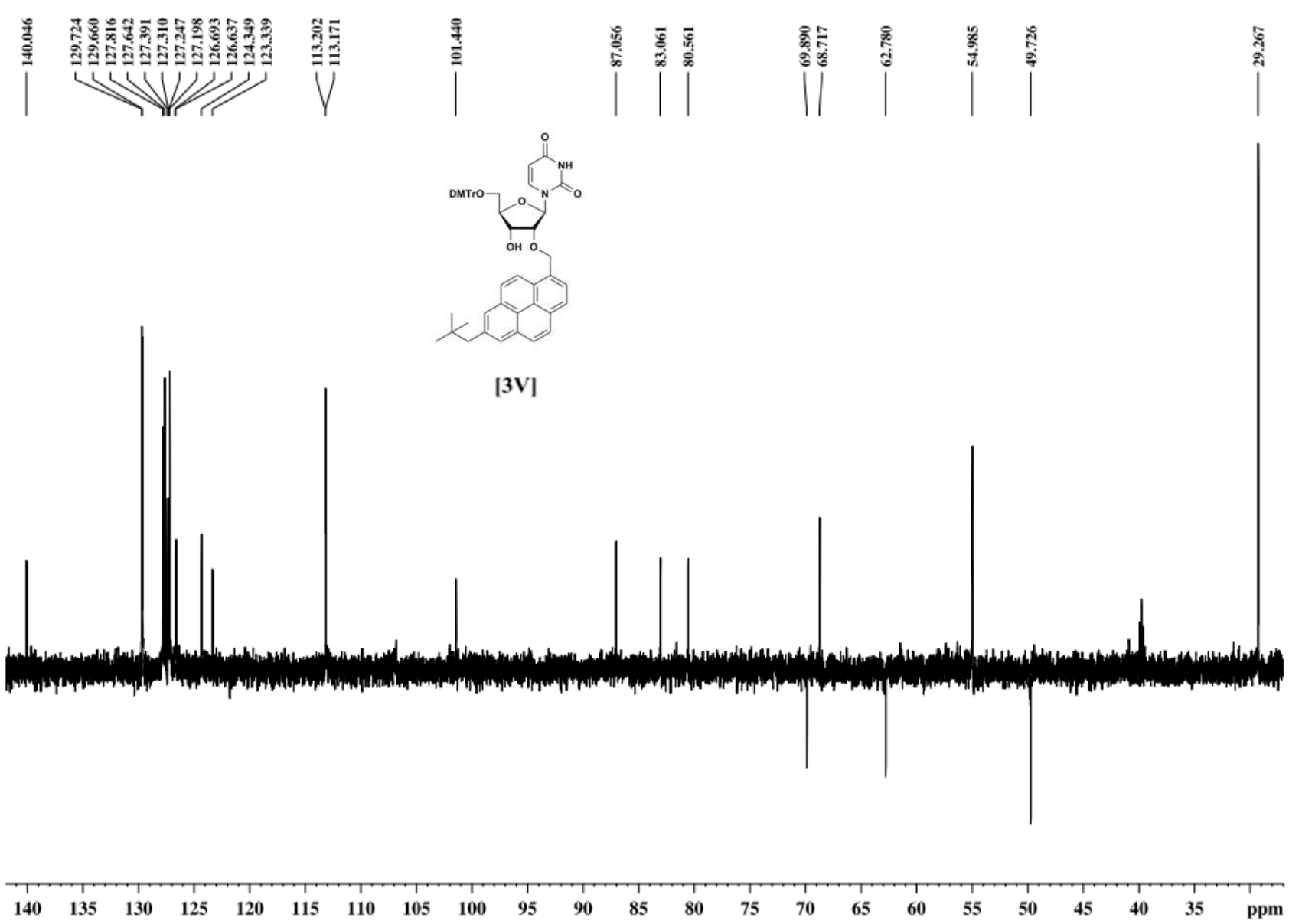
140.046
129.724
129.660
127.816
127.642
127.391
127.310
127.247
127.198
126.693
126.637
124.349
123.339
113.202
113.171
101.440
87.056
83.061
80.561
69.890
68.717
62.780
54.985
49.726
29.267
DMTrO
O
NH
N
O
OH
O
[3V]
140
135
130
125
120
115
110
105
100
95
90
85
80
75
70
65
60
55
50
45
40
35
ppm

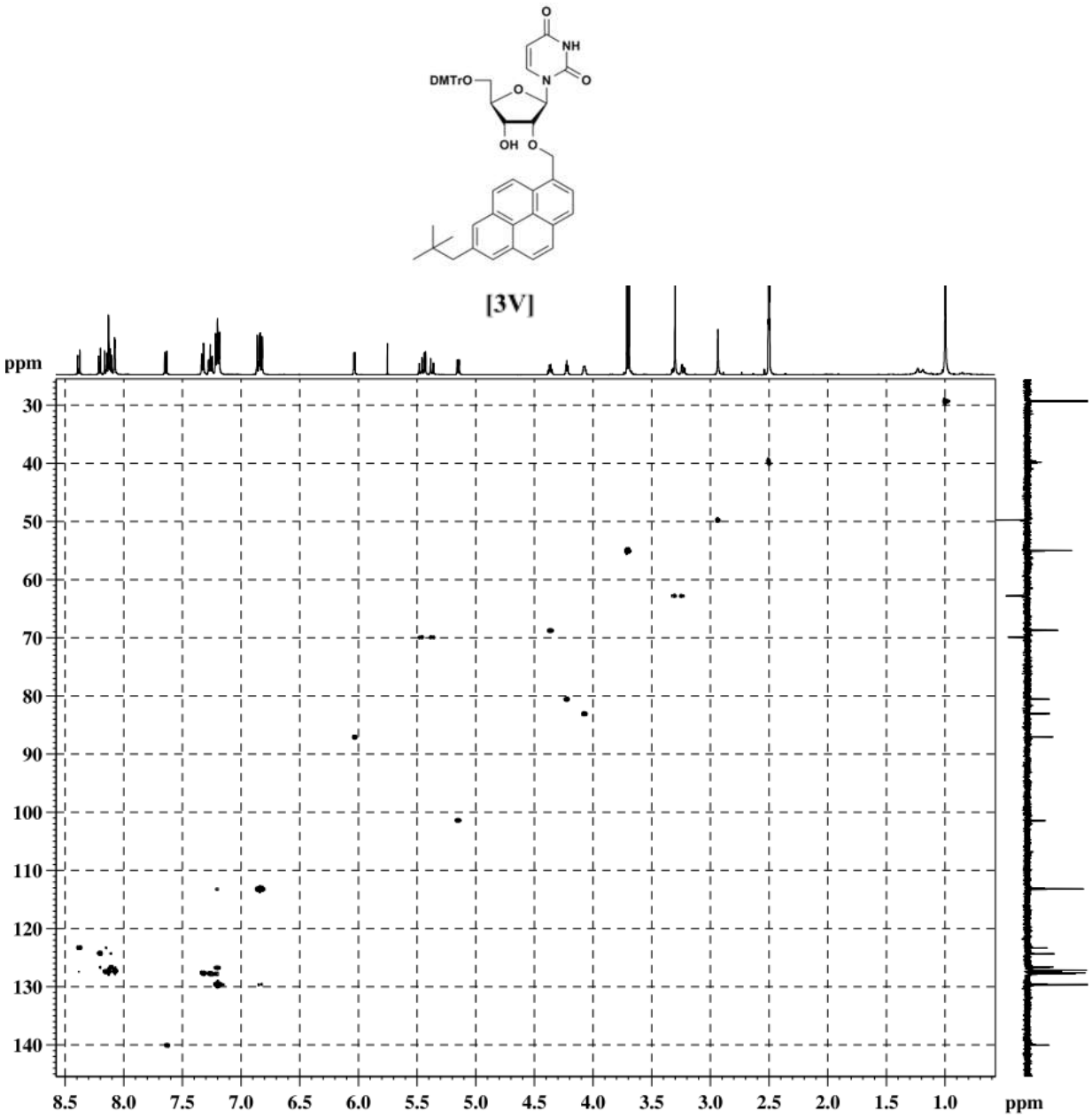
DMTrO
O
NH
N
O
OH
O
[3V]
ppm
30
40
50
60
70
80
90
100
110
120
130
140
8.5
8.0
7.5
7.0
6.5
6.0
5.5
5.0
4.5
4.0
3.5
3.0
2.5
2.0
1.5
1.0
ppm

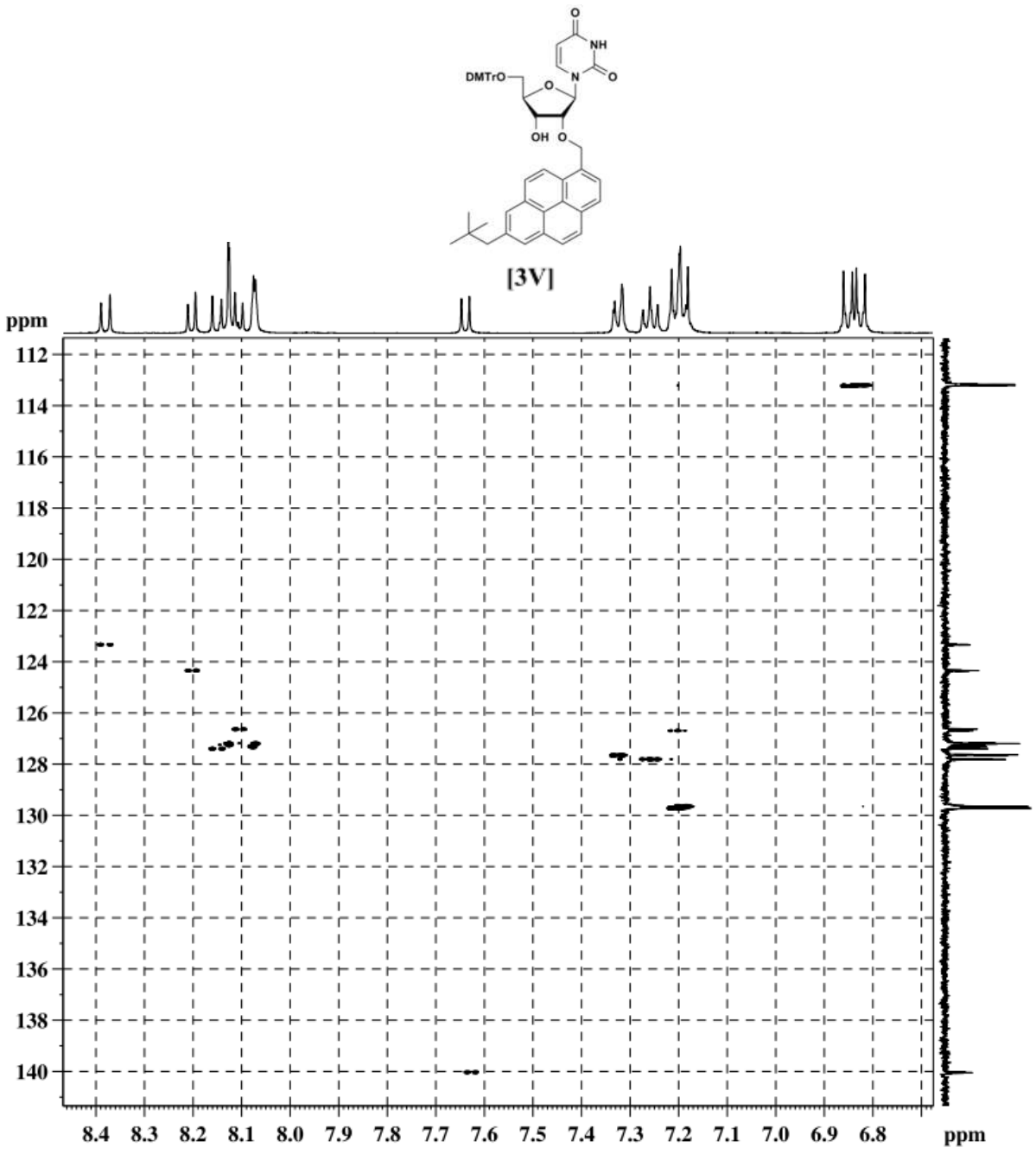
DMTrO
O
NH
N
O
OH
O
[3V]
ppm
112
114
116
118
120
122
124
126
128
130
132
134
136
138
140
8.4
8.3
8.2
8.1
8.0
7.9
7.8
7.7
7.6
7.5
7.4
7.3
7.2
7.1
7.0
6.9
6.8
ppm

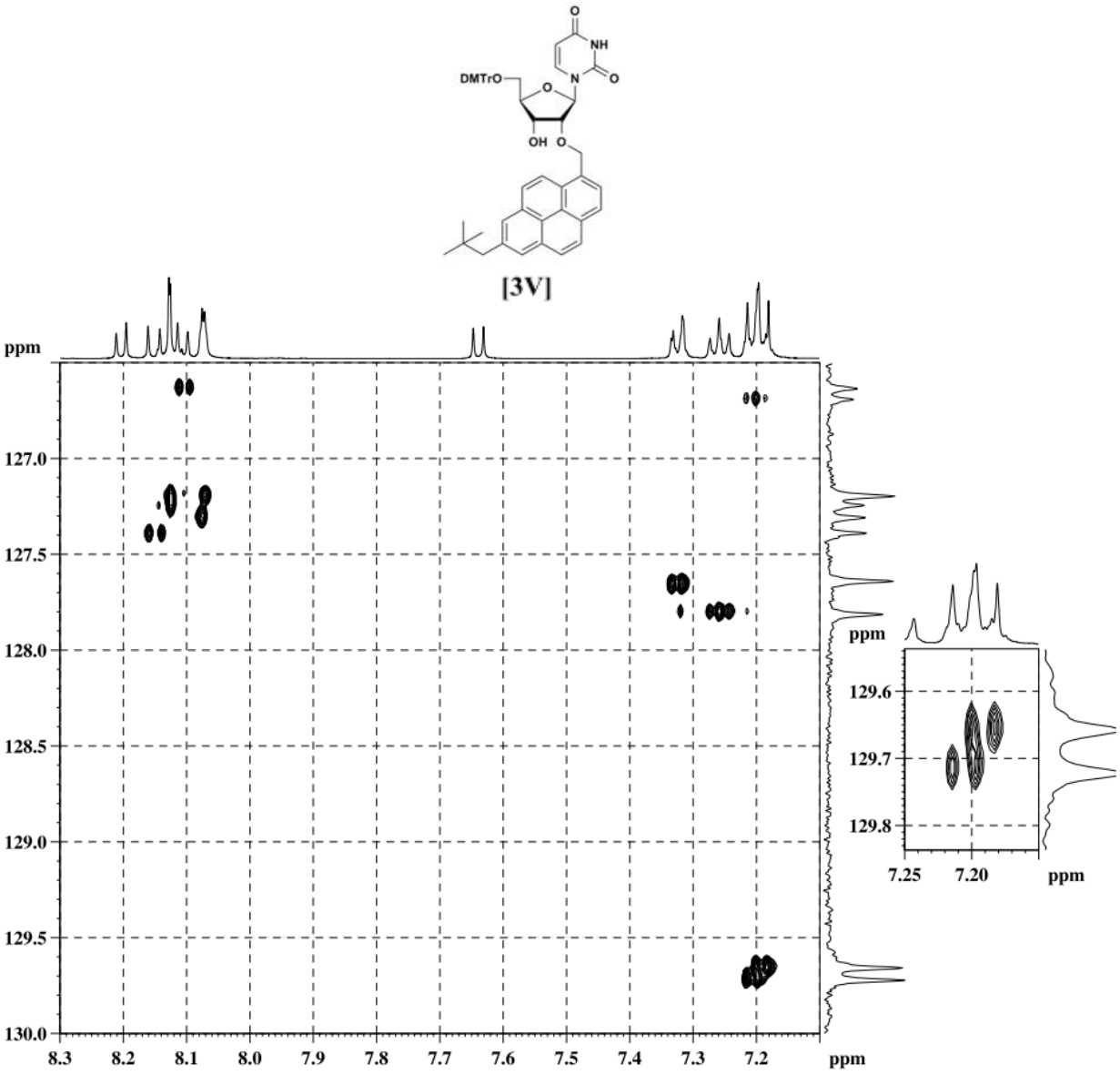
DMTrO
O
NH
N
O
OH
O
[3V]
ppm
127.0
127.5
128.0
128.5
129.0
129.5
130.0
8.3
8.2
8.1
8.0
7.9
7.8
7.7
7.6
7.5
7.4
7.3
7.2
ppm
ppm
129.6
129.7
129.8
7.25
7.20
ppm

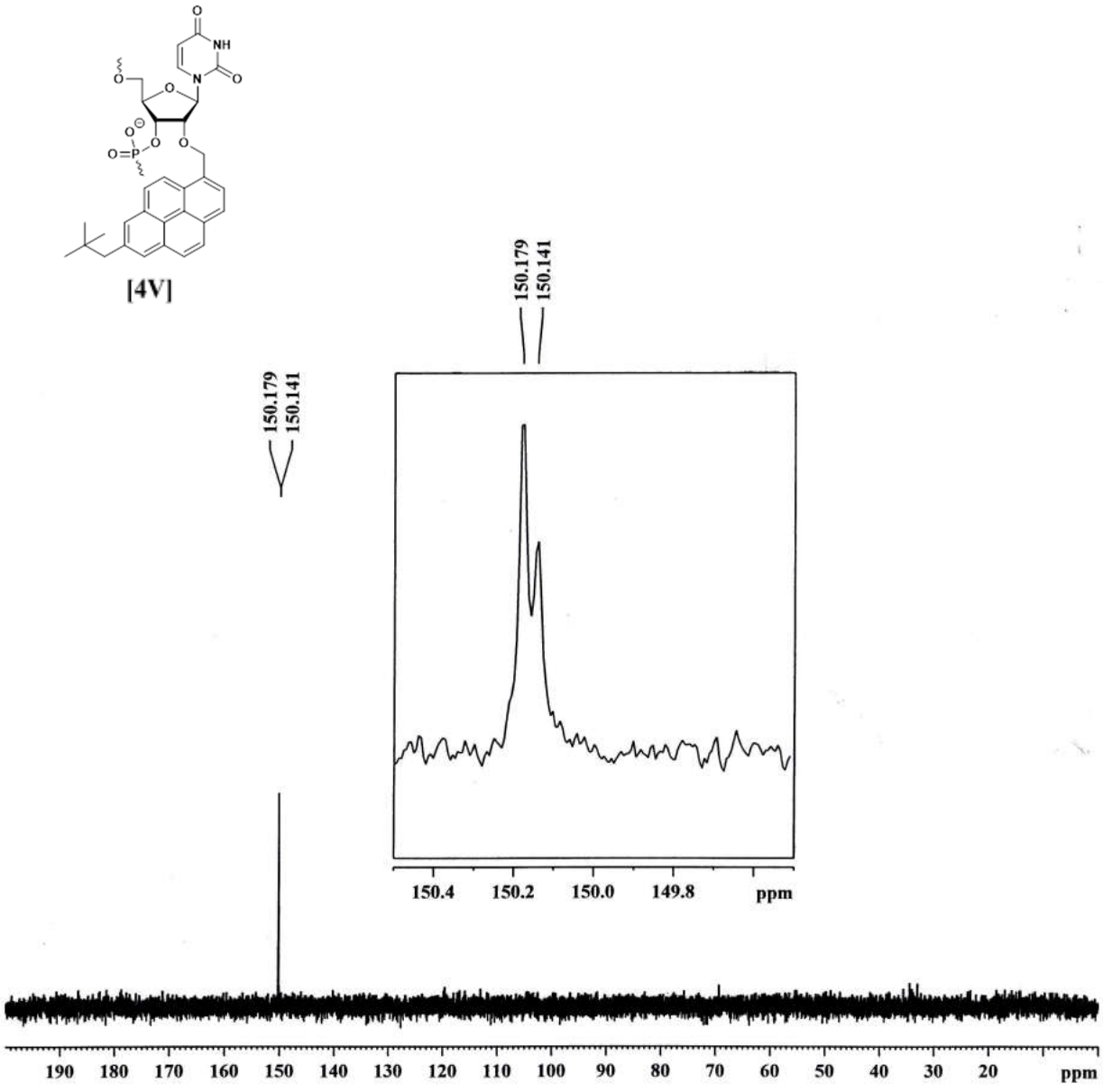
[4V]
150.179
150.141
150.179
150.141
150.4
150.2
150.0
149.8
ppm
190
180
170
160
150
140
130
120
110
100
90
80
70
60
50
40
30
20
ppm

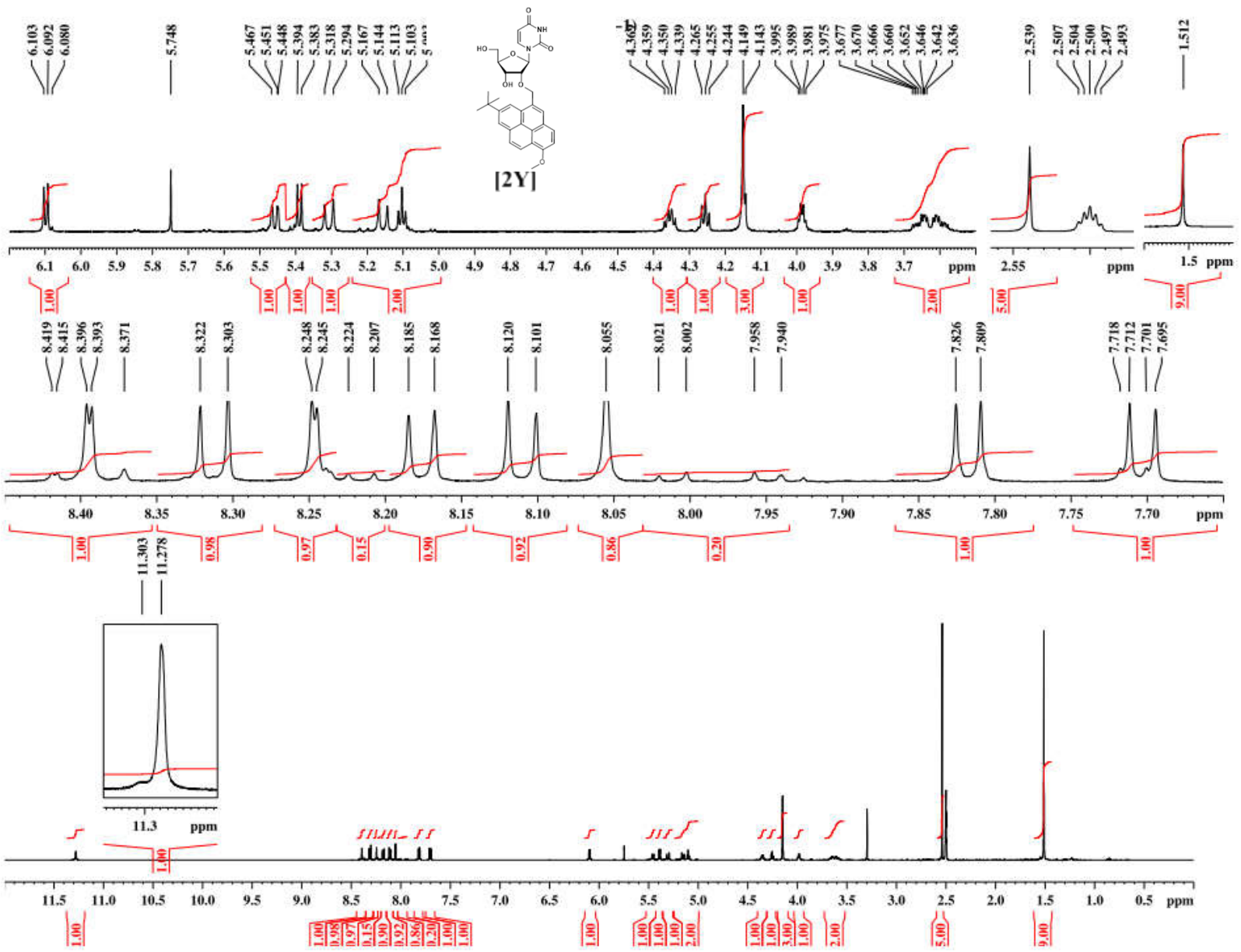
[2Y]

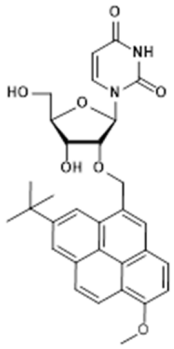
O
NH
HO
O
N
O
OH
O
O

**[2Y]**

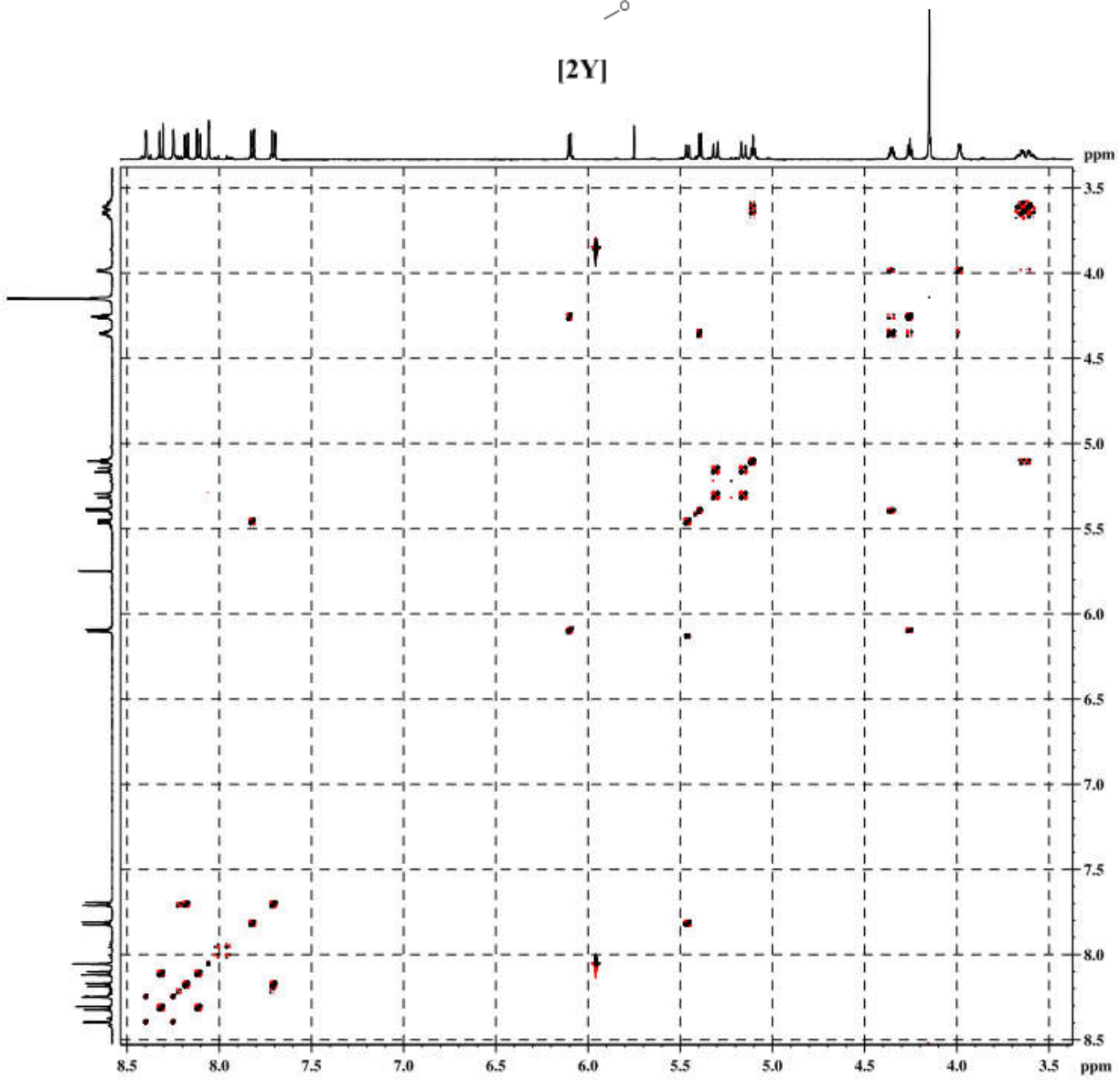
ppm
3.5
4.0
4.5
5.0
5.5
6.0
6.5
7.0
7.5
8.0
8.5
8.5
8.0
7.5
7.0
6.5
6.0
5.5
5.0
4.5
4.0
3.5
ppm

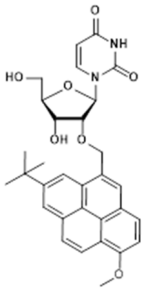
O
NH
HO
N
O
O
OH
O
O

**[2Y]**

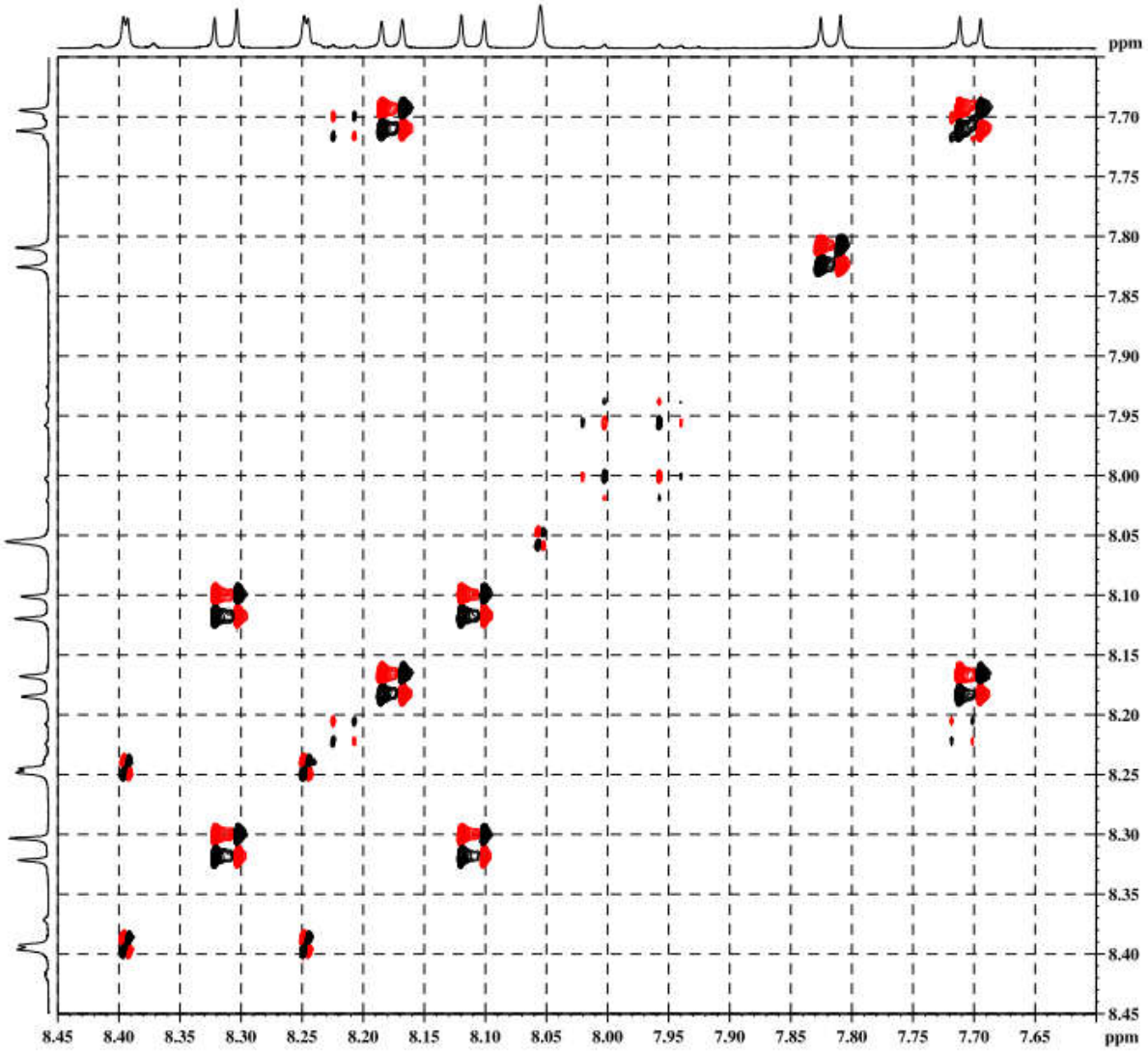
ppm
7.70
7.75
7.80
7.85
7.90
7.95
8.00
8.05
8.10
8.15
8.20
8.25
8.30
8.35
8.40
8.45
8.45 8.40 8.35 8.30 8.25 8.20 8.15 8.10 8.05 8.00 7.95 7.90 7.85 7.80 7.75 7.70 7.65
ppm

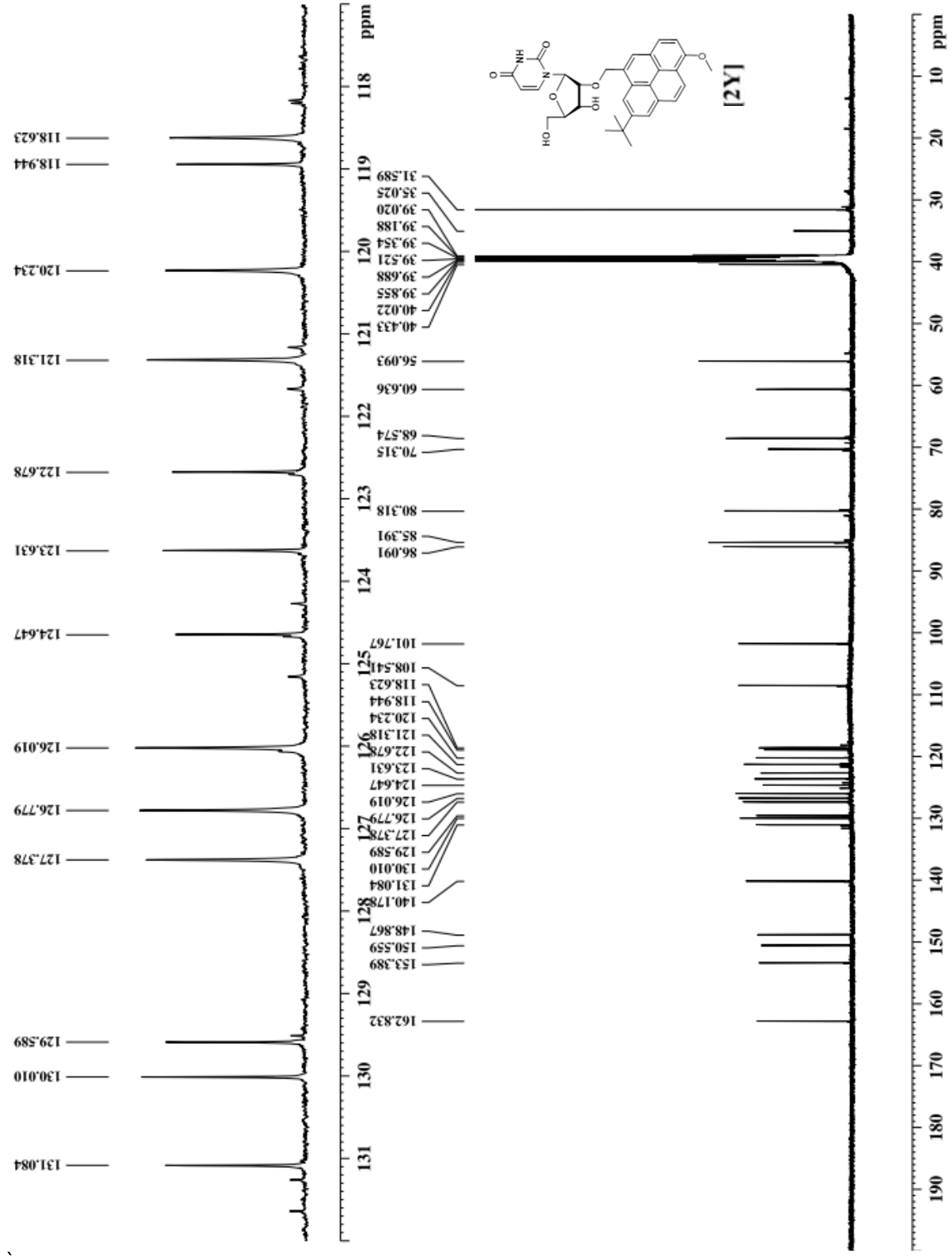
[2Y]
ppm

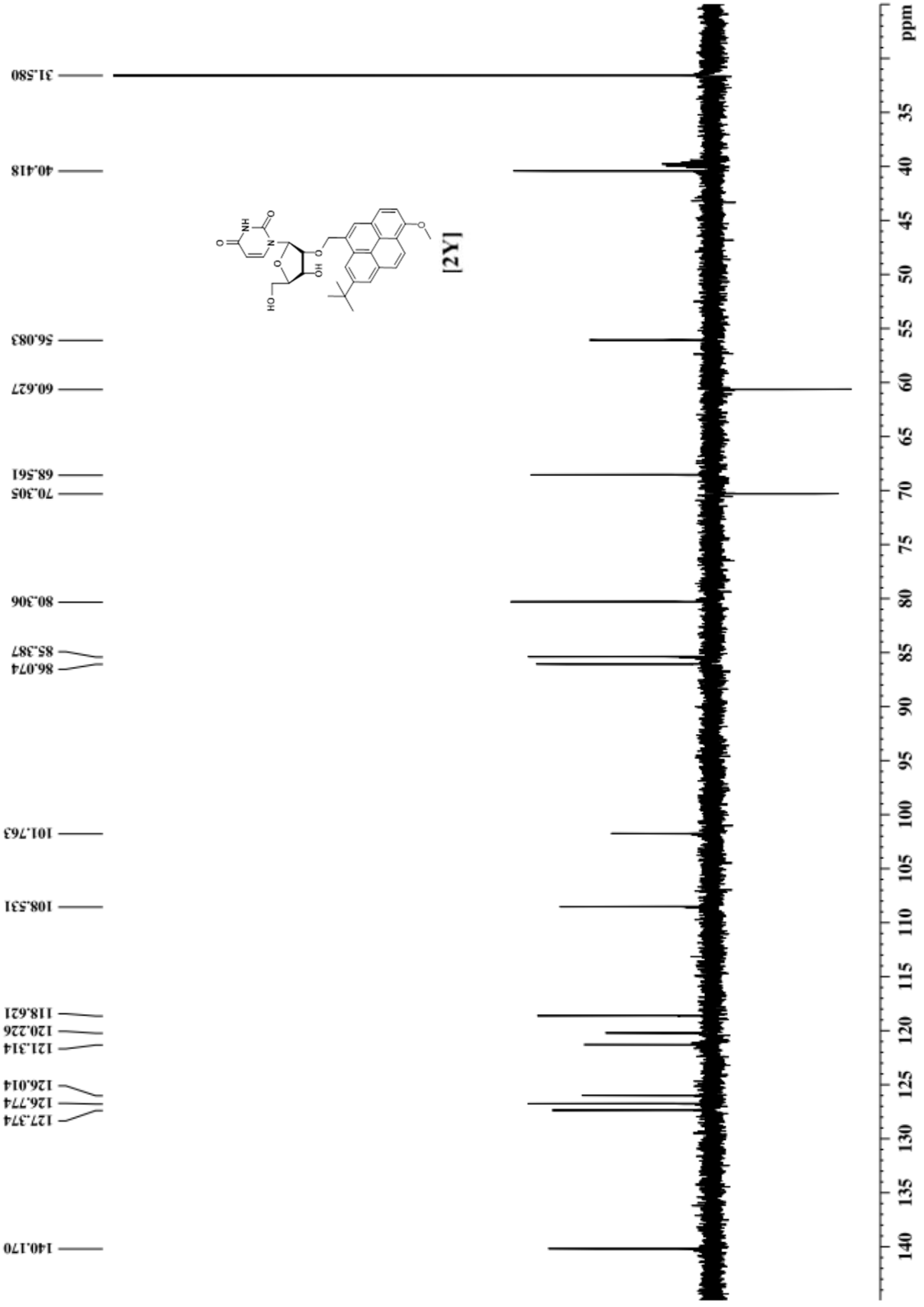
31.580
40.418
56.083
60.627
68.561
70.305
80.306
85.387
86.074
101.763
108.531
118.621
120.226
121.314
126.014
126.774
127.374
140.170
ppm
[2Y]

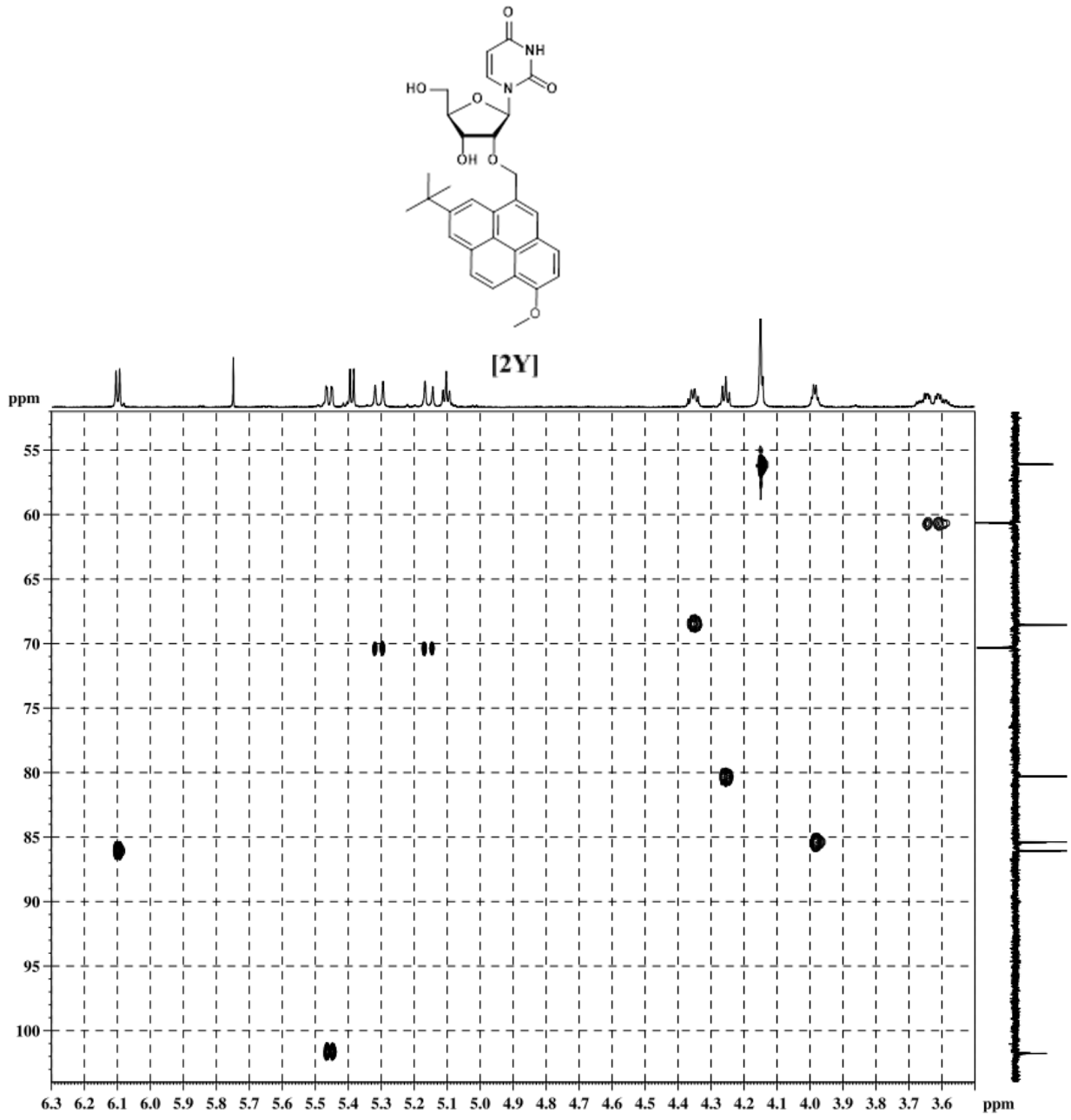
O
NH
HO
O
N
O
OH
O
O
[2Y]
ppm
55
60
65
70
75
80
85
90
95
100
6.3 6.2 6.1 6.0 5.9 5.8 5.7 5.6 5.5 5.4 5.3 5.2 5.1 5.0 4.9 4.8 4.7 4.6 4.5 4.4 4.3 4.2 4.1 4.0 3.9 3.8 3.7 3.6
ppm

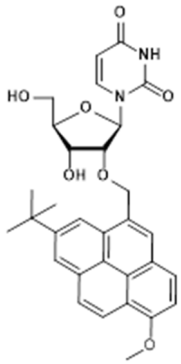
O
NH
HO
N
O
O
OH
O
O

**[2Y]**

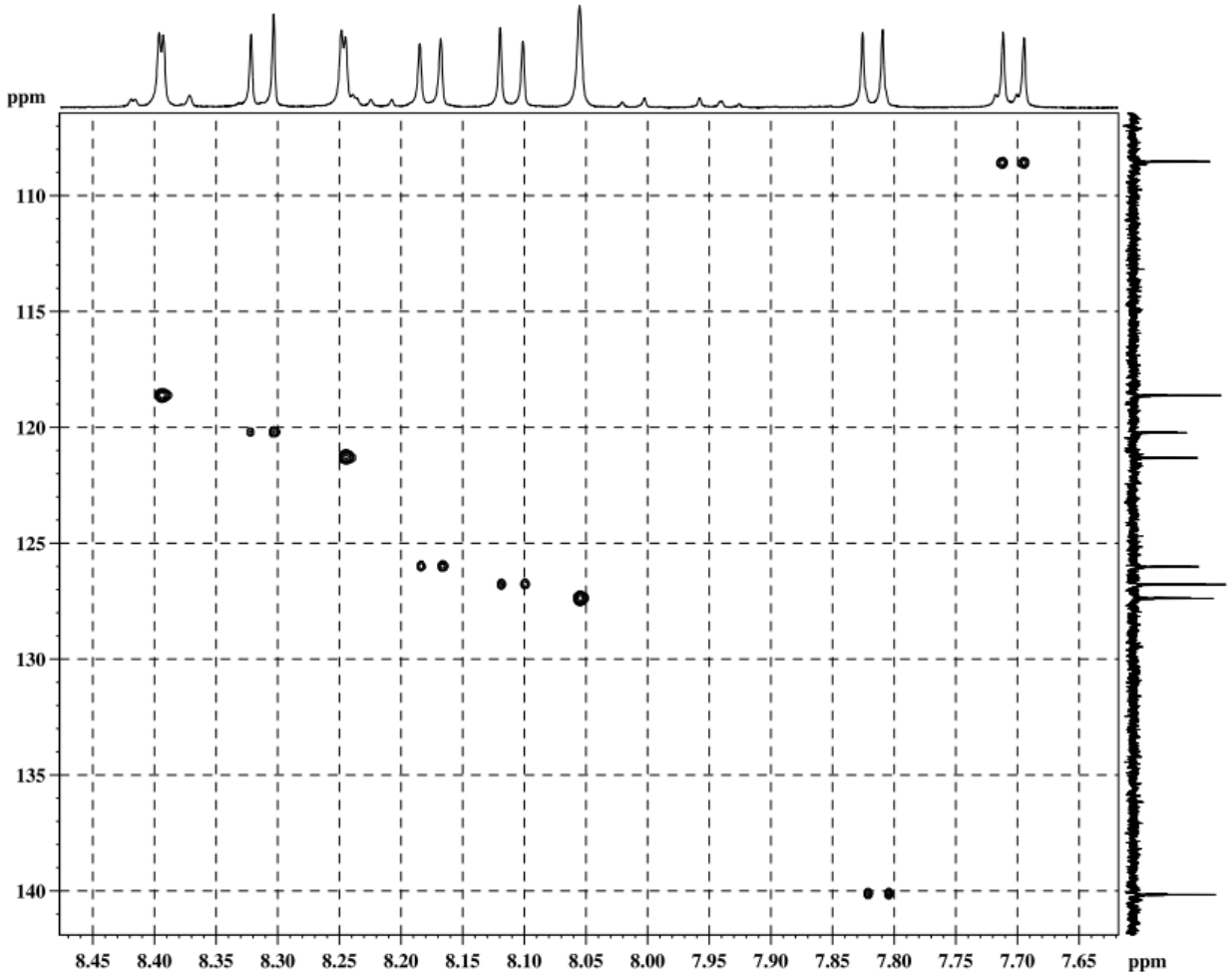
ppm
110
115
120
125
130
135
140
8.45
8.40
8.35
8.30
8.25
8.20
8.15
8.10
8.05
8.00
7.95
7.90
7.85
7.80
7.75
7.70
7.65
ppm

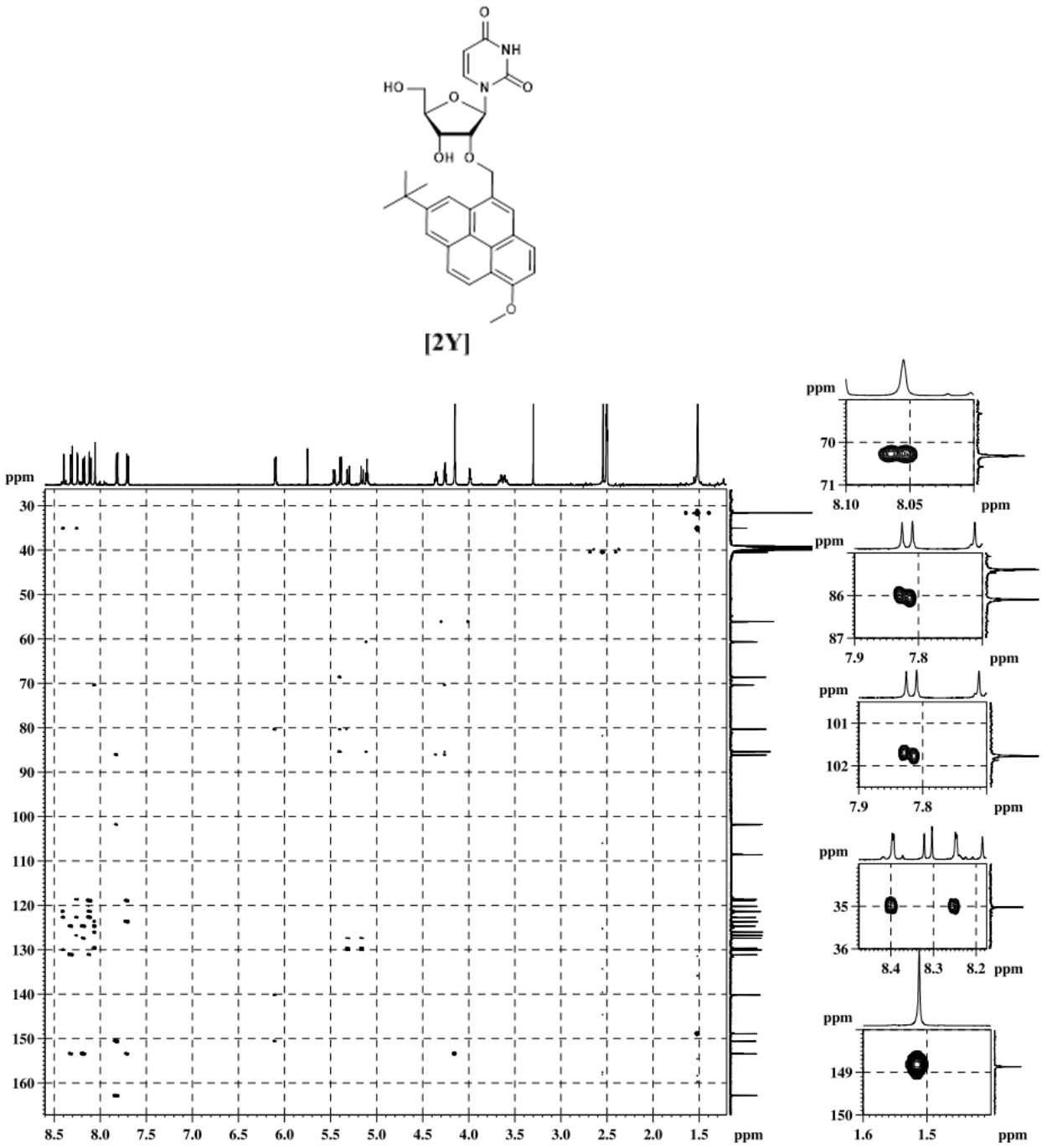
O
NH
HO
N
O
O
OH
O
O
[2Y]
ppm
30
40
50
60
70
80
90
100
110
120
130
140
150
160
8.5
8.0
7.5
7.0
6.5
6.0
5.5
5.0
4.5
4.0
3.5
3.0
2.5
2.0
1.5
ppm
ppm
70
71
8.10
8.05
ppm
ppm
86
87
7.9
7.8
ppm
ppm
101
102
7.9
7.8
ppm
ppm
35
36
8.4
8.3
8.2
ppm
ppm
149
150
1.6
1.5
ppm

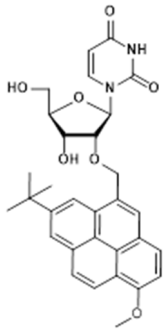

**[2Y]**

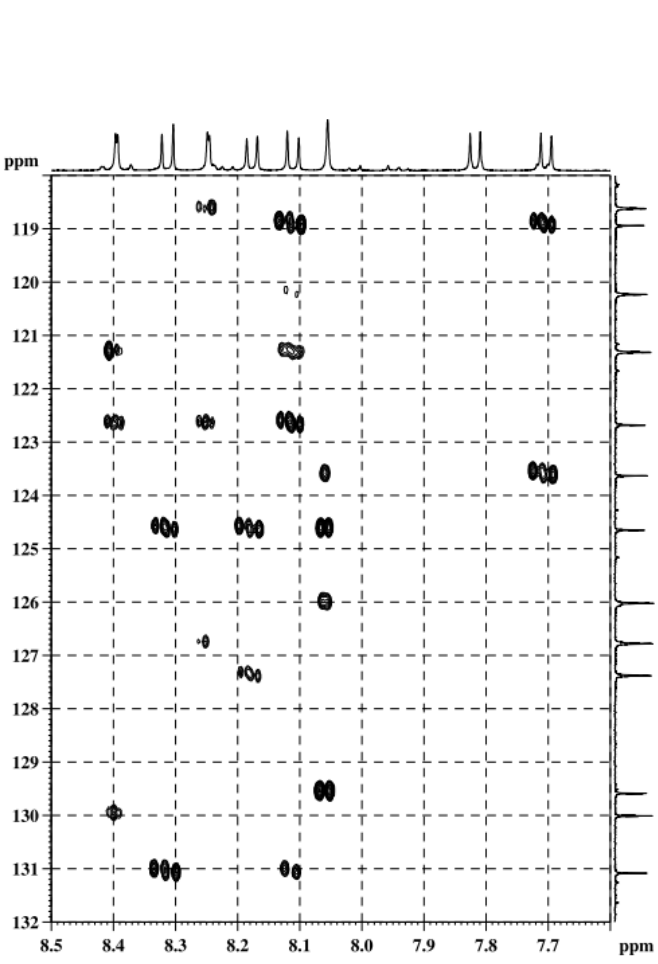
ppm
119
120
121
122
123
124
125
126
127
128
129
130
131
132
8.5 8.4 8.3 8.2 8.1 8.0 7.9 7.8 7.7
ppm

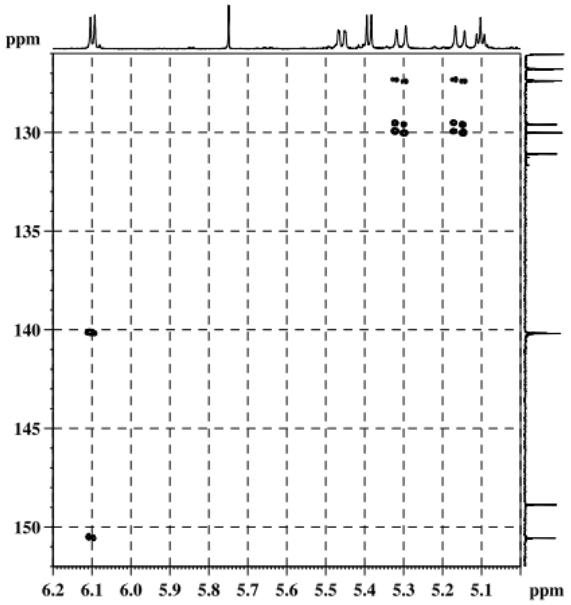
ppm
130
135
140
145
150
6.2 6.1 6.0 5.9 5.8 5.7 5.6 5.5 5.4 5.3 5.2 5.1
ppm

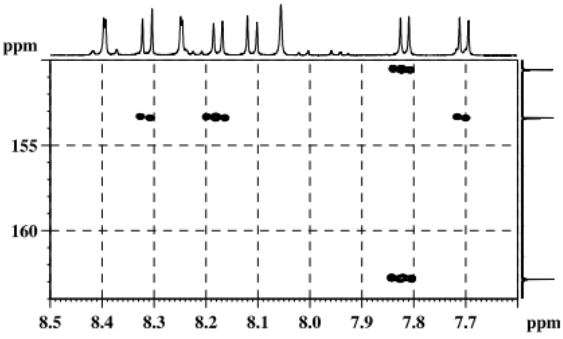
ppm
155
160
8.5 8.4 8.3 8.2 8.1 8.0 7.9 7.8 7.7
ppm

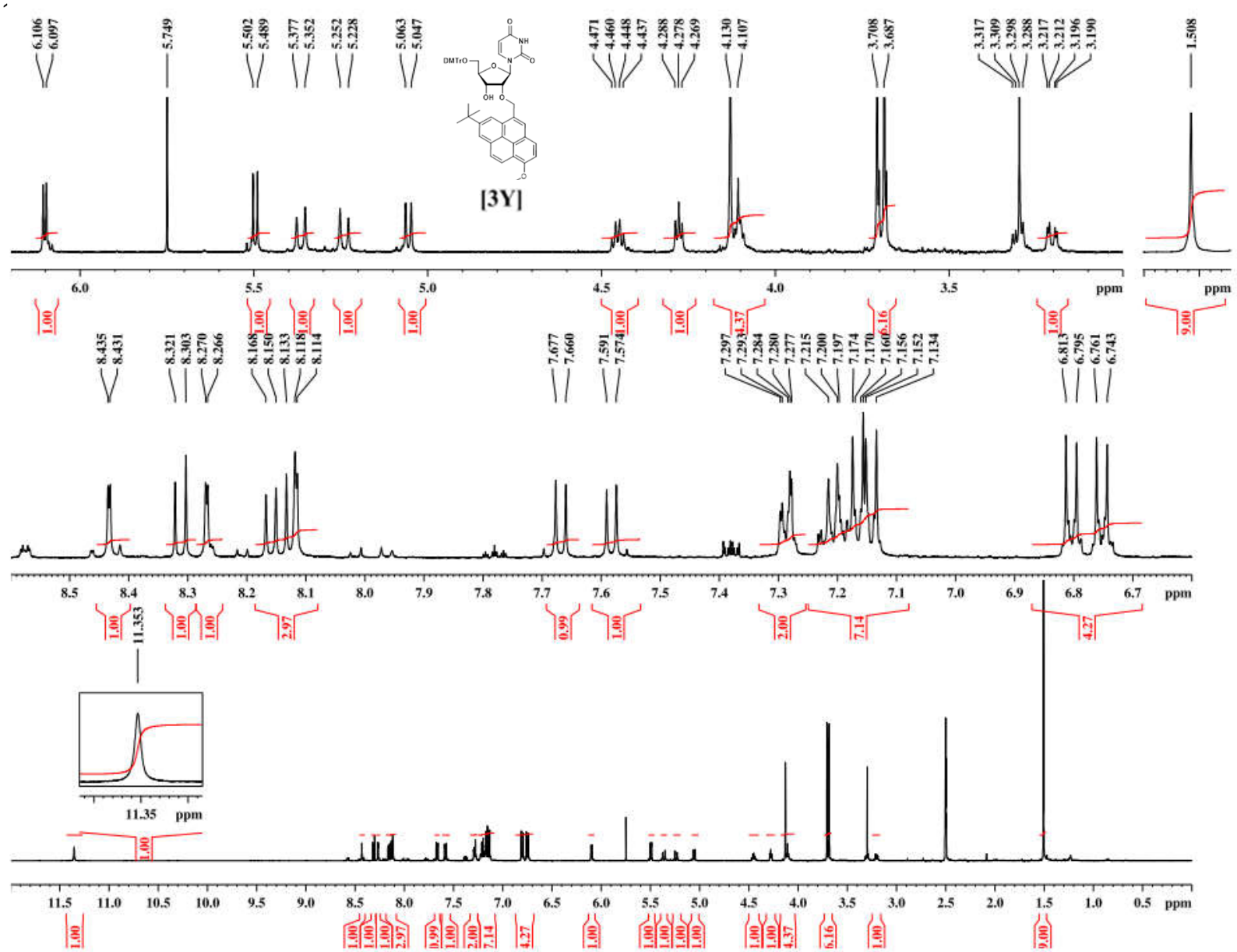
[3Y]

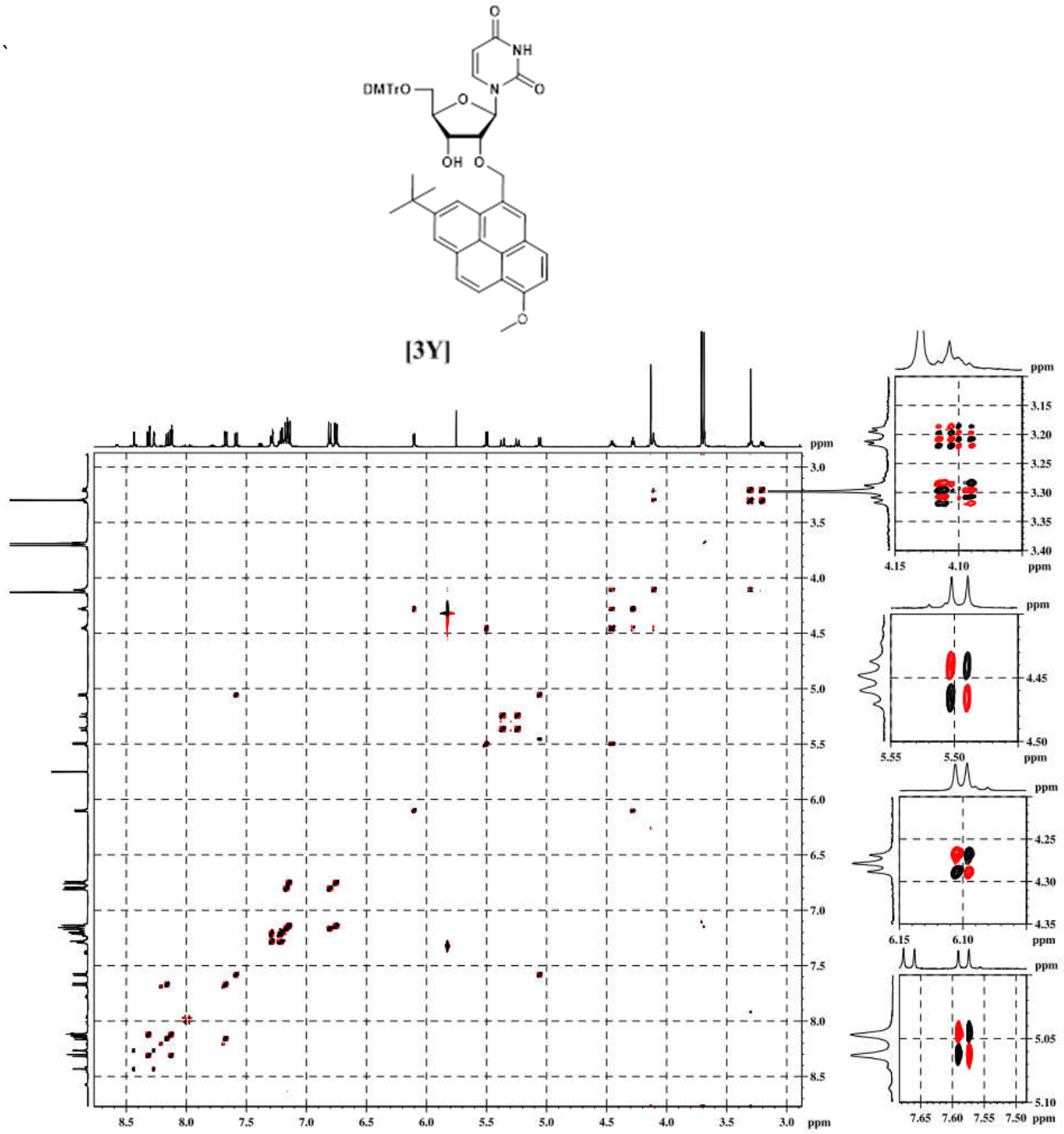
DMTrO
O
NH
N
O
OH
O
O
[3Y]
ppm
3.0
3.5
4.0
4.5
5.0
5.5
6.0
6.5
7.0
7.5
8.0
8.5
8.5 8.0 7.5 7.0 6.5 6.0 5.5 5.0 4.5 4.0 3.5 3.0 ppm
4.15 4.10 ppm
5.55 5.50 ppm
6.15 6.10 ppm
7.65 7.60 7.55 7.50 ppm

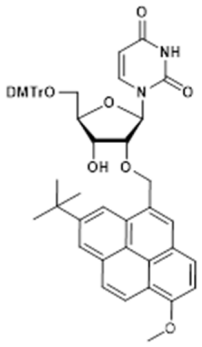
O
NH
DMTrO
N
O
O
OH
O
O

**[3Y]**

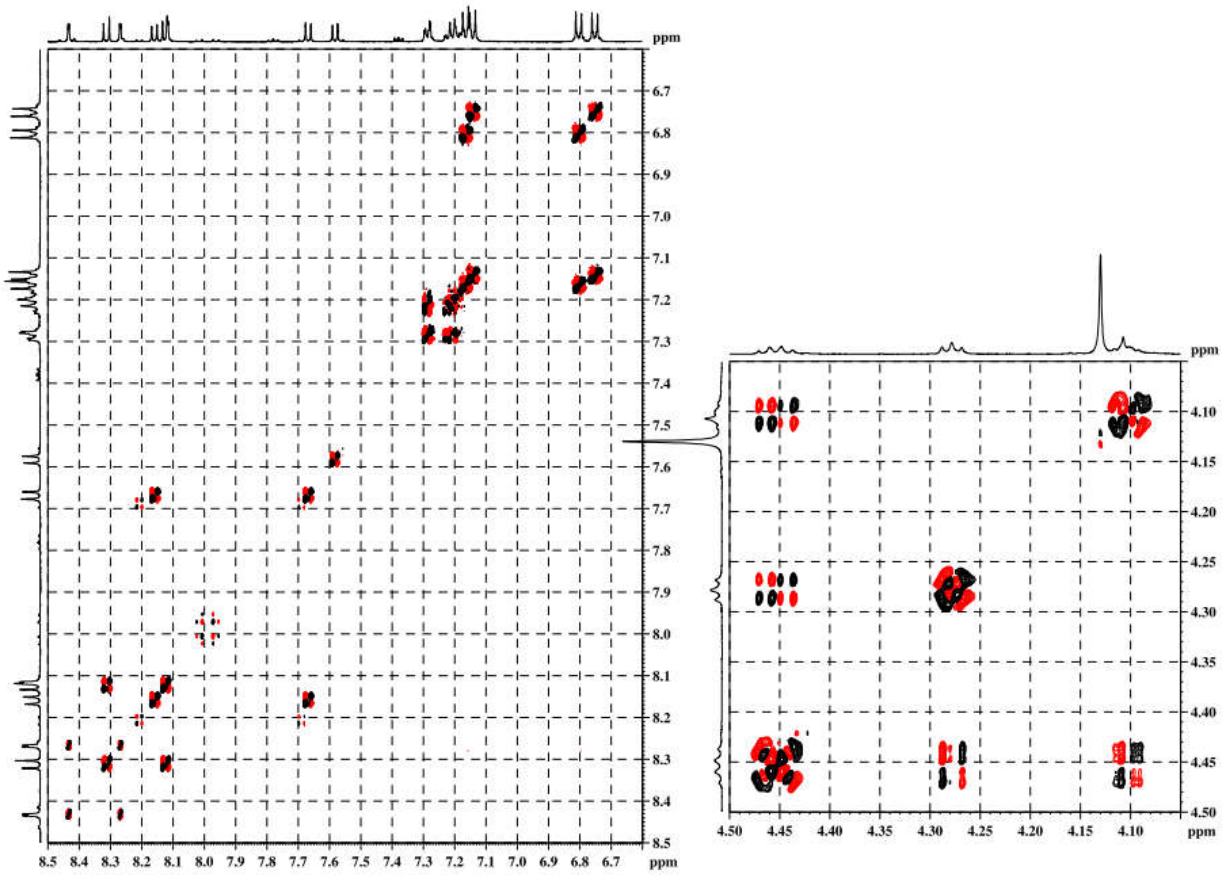
ppm
6.7
6.8
6.9
7.0
7.1
7.2
7.3
7.4
7.5
7.6
7.7
7.8
7.9
8.0
8.1
8.2
8.3
8.4
8.5
8.5 8.4 8.3 8.2 8.1 8.0 7.9 7.8 7.7 7.6 7.5 7.4 7.3 7.2 7.1 7.0 6.9 6.8 6.7
ppm
4.10
4.15
4.20
4.25
4.30
4.35
4.40
4.45
4.50
4.50 4.45 4.40 4.35 4.30 4.25 4.20 4.15 4.10
ppm

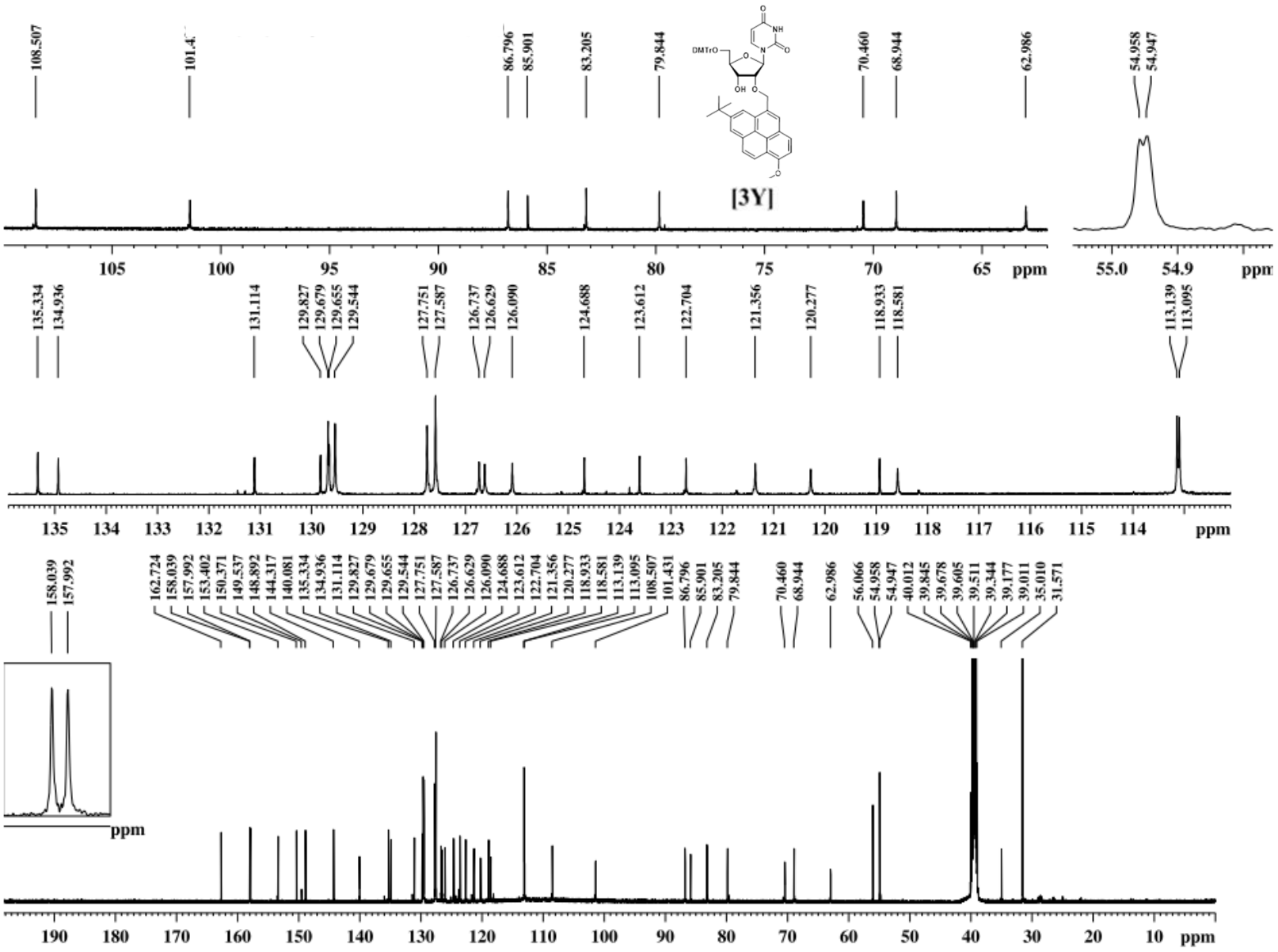
[3Y]
ppm

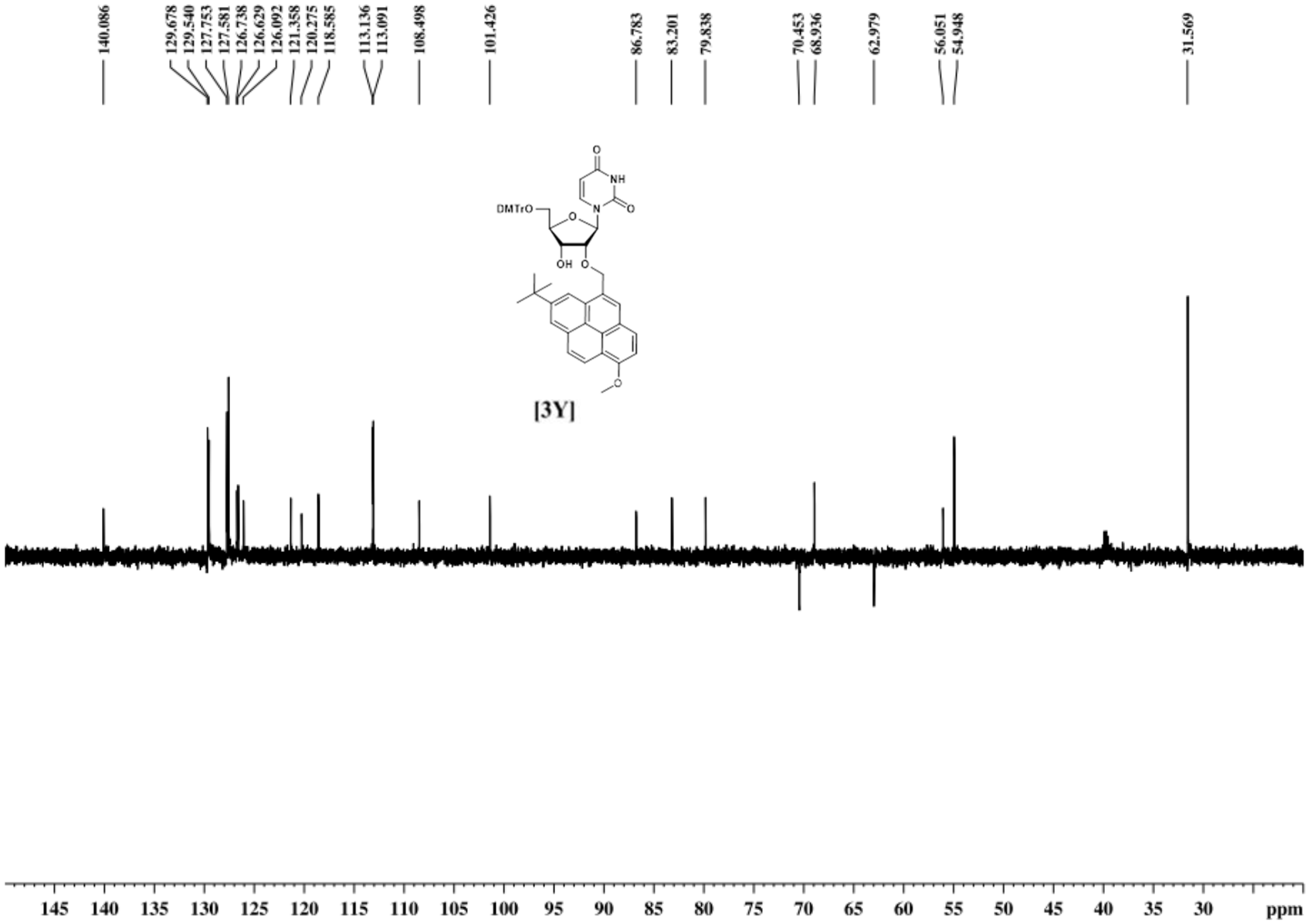
140.086
129.678
129.540
127.753
127.581
126.738
126.629
126.092
121.358
120.275
118.585
113.136
113.091
108.498
101.426
86.783
83.201
79.838
70.453
68.936
62.979
56.051
54.948
31.569
DMTrO
O
NH
N
O
OH
O
O
[3Y]
145 140 135 130 125 120 115 110 105 100 95 90 85 80 75 70 65 60 55 50 45 40 35 30 ppm

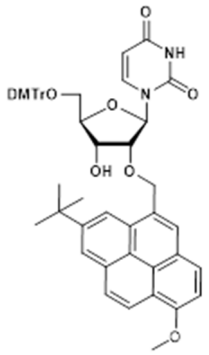
O
NH
DMTrO
N
O
O
OH
O
O

**[3Y]**

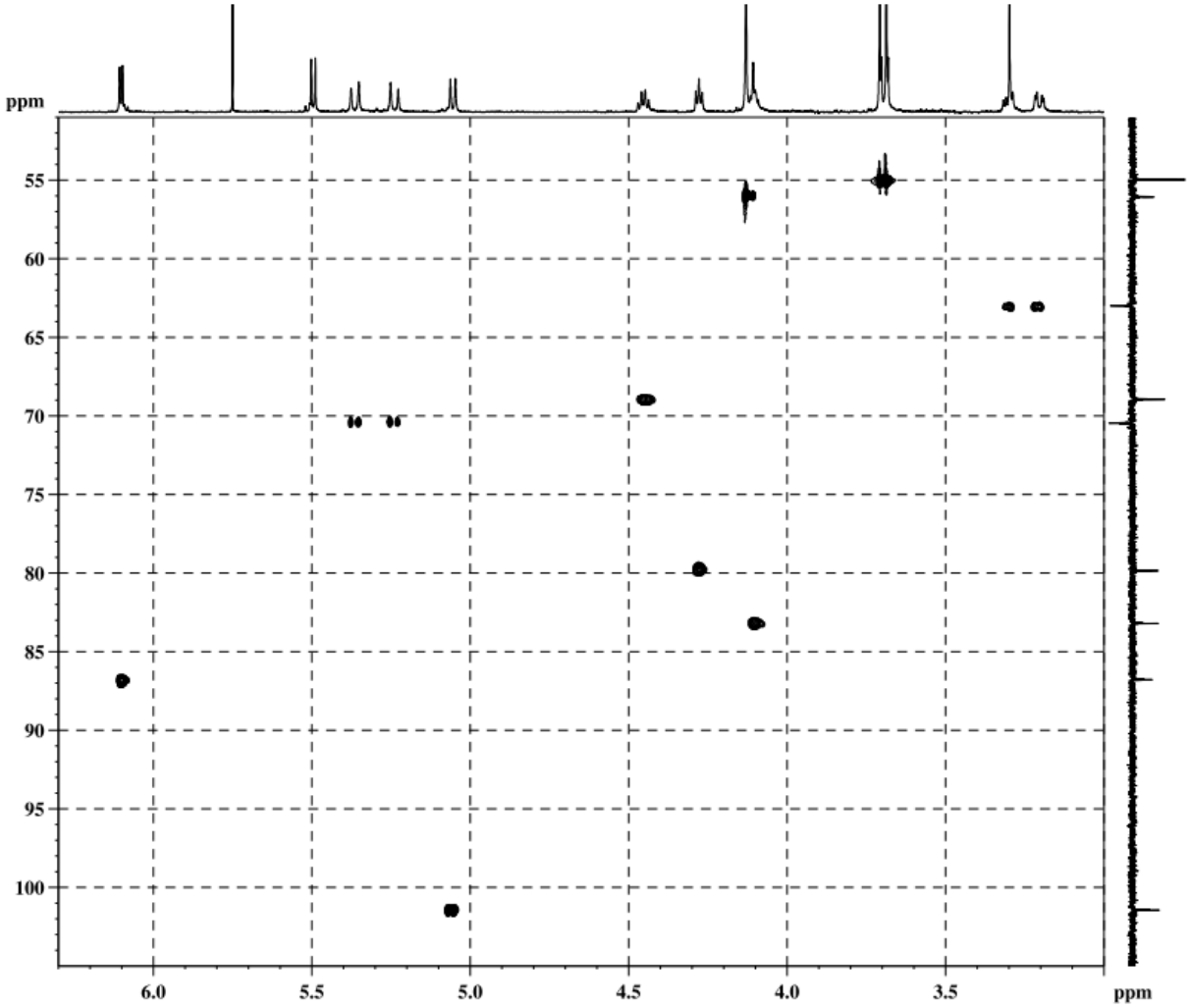
ppm
55
60
65
70
75
80
85
90
95
100
6.0
5.5
5.0
4.5
4.0
3.5
ppm

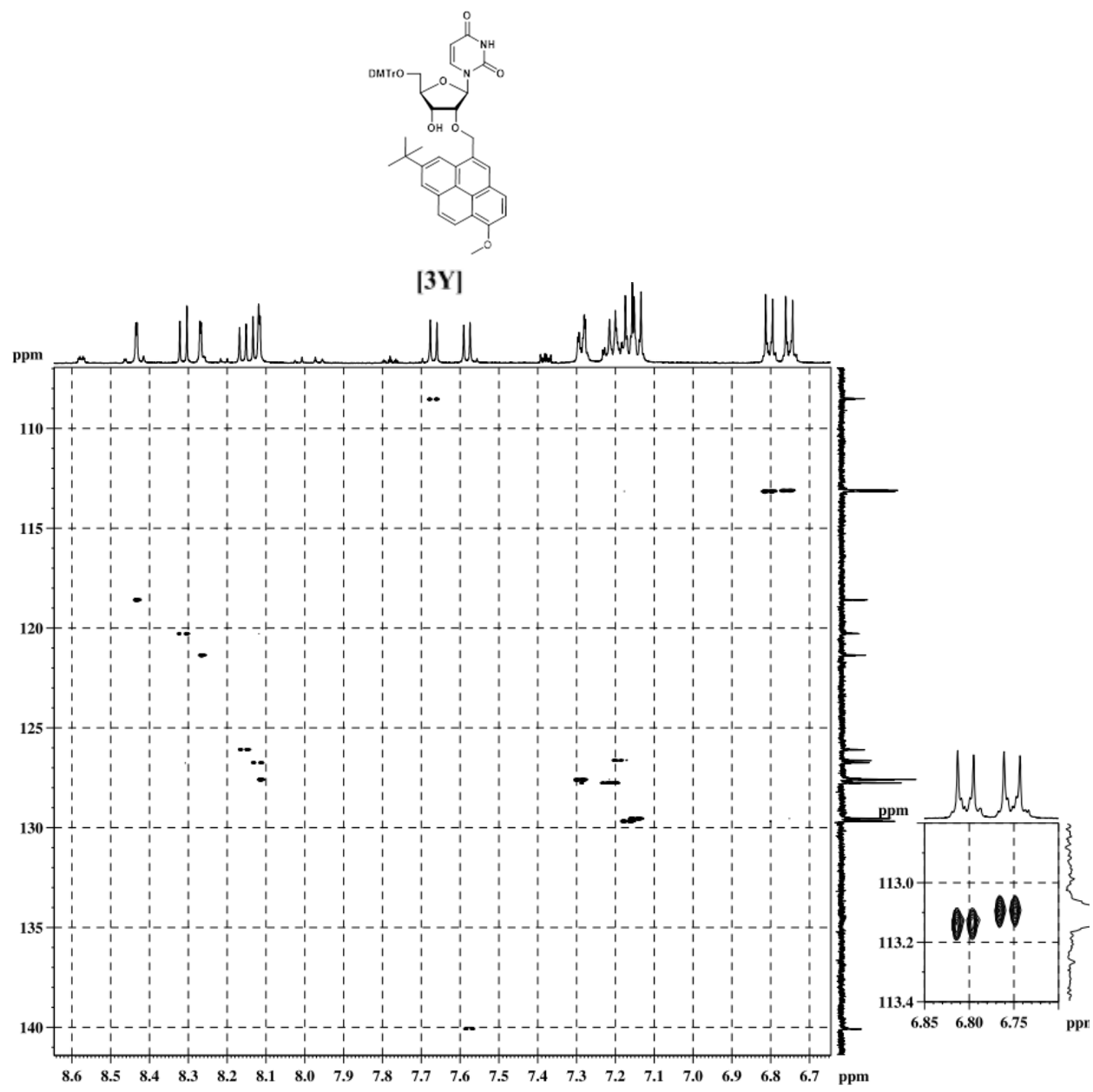
[3Y]
ppm
110
115
120
125
130
135
140
8.6 8.5 8.4 8.3 8.2 8.1 8.0 7.9 7.8 7.7 7.6 7.5 7.4 7.3 7.2 7.1 7.0 6.9 6.8 6.7 ppm
ppm
113.0
113.2
113.4
6.85 6.80 6.75

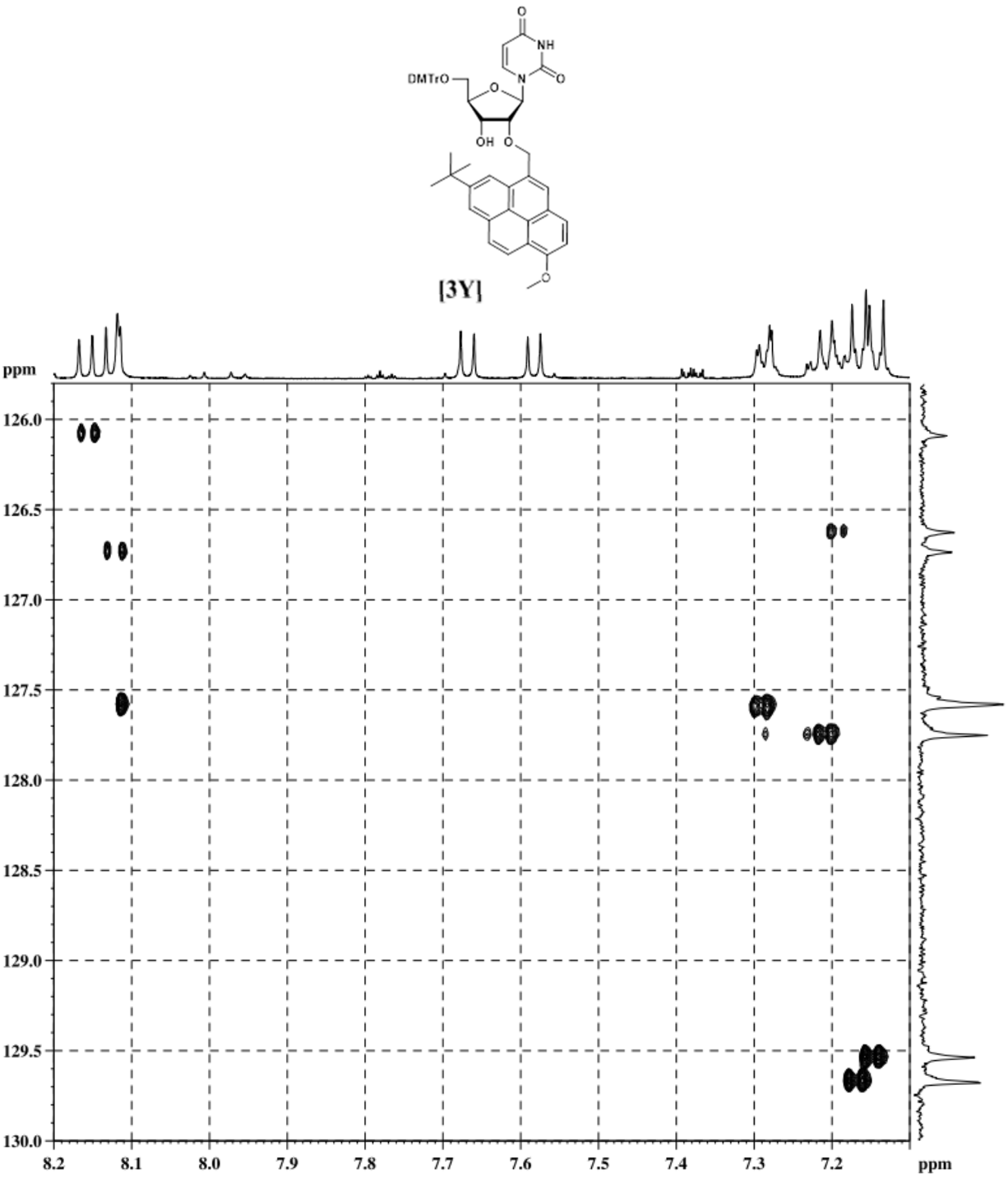
DMTrO
NH
O
N
O
OH
O
O
[3Y]
ppm
126.0
126.5
127.0
127.5
128.0
128.5
129.0
129.5
130.0
8.2
8.1
8.0
7.9
7.8
7.7
7.6
7.5
7.4
7.3
7.2
ppm

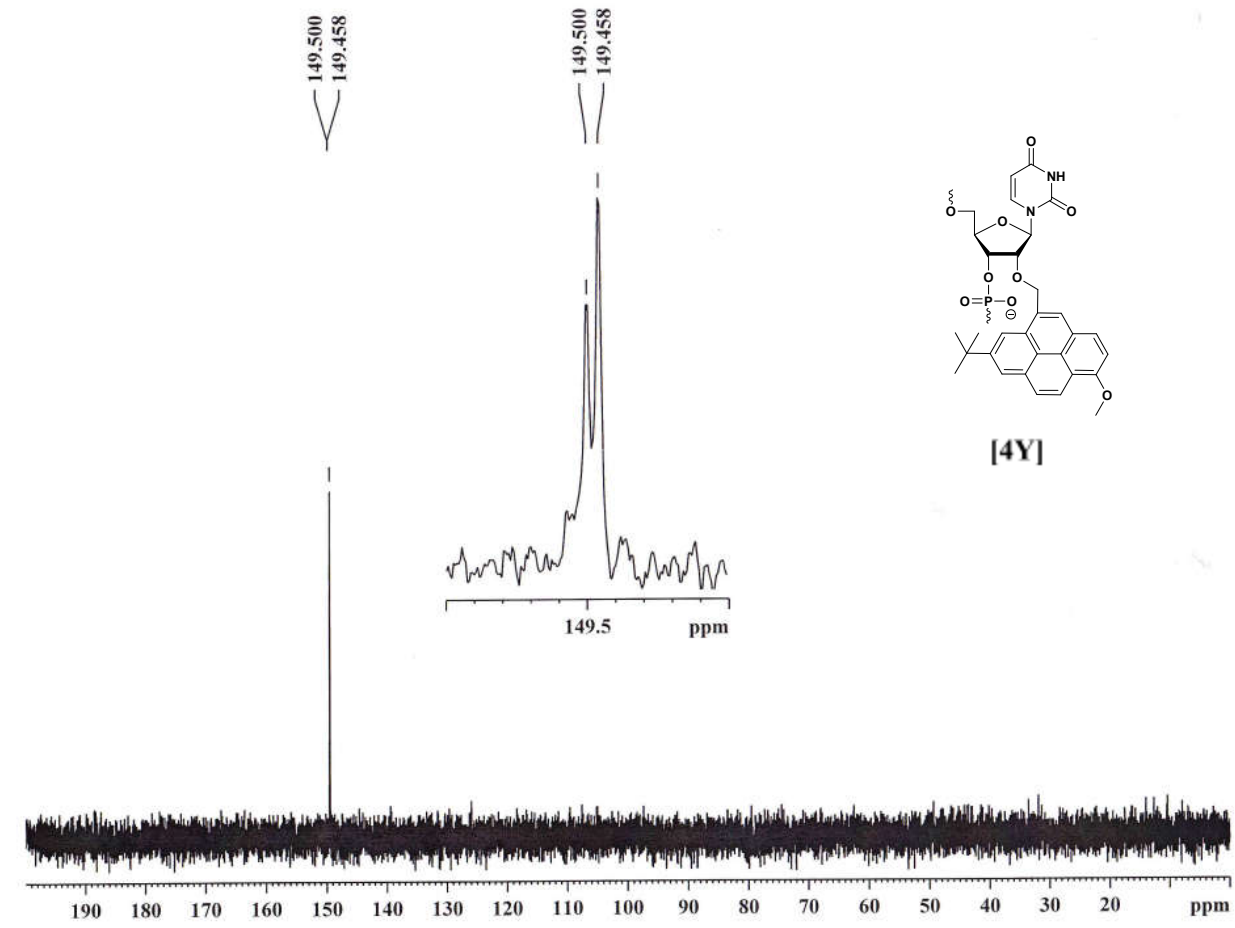
149.500
149.458
149.500
149.458
149.5
ppm
[4Y]
190 180 170 160 150 140 130 120 110 100 90 80 70 60 50 40 30 20 ppm